Stony Brook University

Regulation of Dimerization and Activation of the Thrombopoietin Receptor

A Dissertation Presented

by

Miki Itaya

to

The Graduate School

in Partial Fulfillment of the

Requirements

for the Degree of

Doctor of Philosophy

in

Biochemistry and Structural Biology

Stony Brook University

December 2012

Stony Brook University

The Graduate School

Miki Itaya

We, the dissertation committee for the above candidate for the

Doctor of Philosophy degree, hereby recommend

acceptance of this dissertation.

Steven O. Smith, Ph.D. - Dissertation Advisor
Professor, Department of Biochemistry and Cell Biology

Erwin London, Ph.D. - Chairperson of Defense
Professor, Department of Biochemistry and Cell Biology

Robert C. Rizzo, Ph.D.
Associate Professor, Department of Applied Mathematics and Statistics

Nancy Reich Marshall, Ph.D.
Professor, Department of Molecular Genetics and Microbiology

This dissertation is accepted by the Graduate School

Charles Taber
Interim Dean of the Graduate School

Abstract of the Dissertation

Regulation of Dimerization and Activation of the Thrombopoietin Receptor

by

Miki Itaya

Doctor of Philosophy

in

Biochemistry and Structural Biology

Stony Brook University

2012

The thrombopoietin receptor (TpoR) is an indispensable receptor that regulates megakaryocytopoiesis and platelet formation in response to its ligand, thrombopoietin (Tpo). Mutations in TpoR result in an increased or decreased number of platelets, leading to various platelet disorders, such as essential thrombocythemia (ET) and primary myelofibrosis (PMF). Most of the clinically relevant mutations of TpoR are found in the transmembrane (TM) domain and juxtamembrane (JM) region of the receptor, suggesting that the TM-JM region may play a critical role in regulation of TpoR activity. However, the precise molecular mechanism by which this region affects the TpoR conformation and the resultant receptor activity remains elusive. To better understand the role of the TM-JM region in activation of TpoR, we focused on a mutation at Ser505 (S505N) in the TM domain of the receptor and several mutations at Trp515 within the intracellular (IC) JM region. We chose these mutations because S505N, as well as diverse mutations at Trp515 such as W515K and W515L, are known to constitutively activate TpoR, causing myeloproliferative neoplasms in human. We analyzed how these mutations affect the structure of TpoR and its downstream signaling by various biophysical approaches. Using sedimentation equilibrium analytical ultracentrifugation and deuterium magic angle spinning NMR spectroscopy, we showed that peptides corresponding to the wild-type TpoR TM-JM

sequence do not dimerize strongly in detergent micelles or lipid bilayer membranes. On the other hand, TM-JM peptides containing the constitutively active S505N mutation undergo strong homodimerization, suggesting that TM-TM interactions may control a transition between the active and inactive states of TpoR. Consistent with these results, the S505N mutation enhanced the dimerization and activity of the full-length TpoR *in vivo*. Furthermore, we demonstrated that the W515 residue plays a critical role in maintaining of the inactive receptor state by inhibiting dimerization of the TpoR TM helix. Our polarized attenuated total reflection Fourier transform infrared (ATR-FTIR) experiments revealed that W515, which resides at the boundary between the TM and IC domains, acts to increase the helix tilt angle relative to the membrane bilayer normal, thereby preventing the formation of stable TM dimer contacts. In contrast, the W515K mutation reduced the TpoR TM helix tilt angle, leading to formation of a strong TM-TM interaction. The effect of these constitutively active mutations on the TM helix tilt angle was reversed by addition of a tryptophan residue at positions 514 or 516 (i.e., R514W and Q516W). Consistent with this observation, R514W and Q516W reverted the constitutively active phenotype of the W515K and W515L mutant receptors, restoring wild type-like ligand-induced downstream signaling. Based on these observations, we propose a novel receptor activation mechanism, in which a change in the tilt angle of the TpoR TM helix is induced by ligand binding and facilitates TM-TM interactions within a TpoR dimer. The TM-TM interactions, in turn, re-orient the receptor-associated kinase.

Table of Contents

List of Figures

List of Tables

List of Abbreviations

ATR, attenuated total reflection
AUC, analytical ultracentrifugation
BRET, bioluminescence resonance energy transfer
CAMT , congenital amegakaryocytic thrombocytopenia
CEL, chronic eosinophilic leukemia
CML, chronic myeloid leukemia
CMML, chronic myelomonocytic leukemia
Co-IP, co-immunoprecipitation
CR-D, cytokine receptor domain
CRM, cytokine receptor homology modules
β-OG, n-octyl-β-D-glucopyranoside
DDM, n-dodecyl-β-D-maltoside
DDT, dithiothrietol
DMPC, 1,2-dimyristoyl-sn-glycero-3-phosphocholine
DMPG, 1,2-dimyristoyl-sn-glycero-3-phosphoglycerol
DPC, dodecylphosphocholine
EC, extracellular
EDTA, ethylenediamine tetraacetic acid
FF, firefly luciferase reporter
EGF, epidermal growth factor
EGFR, epidermal growth factor receptor
Epo, erythropoietin
EpoR, erythropoietin receptor
ET, essential thrombocythemia
FBNIII, fibronectin TypeIII
FERM, Band-4.1, Ezrin, Radizin, Moesin
FGFR3, fibroblast growth factor receptor 3
FRET, fluorescence resonance energy transfer
FTIR, Fourier transform infrared
GHR, growth hormone receptor
HA, hemagglutinin
HER2, human epidermal growth factor receptor 2
HFIP, hexafluoroisopropanol
HPLC, high performance liquid chromatography

HSC, hematopoietic stem cell
IC, intracellular
IMF, idiopathic myelofibrosis
IR, infrared
IPTG, isopropyl β-D-1-thiogalactopyranoside
JAK2, Janus kinase 2
JM, juxtamembrane
LDLR, low-density lipoprotein receptor
MAS, magic angle spinning
MAPK, mitogen-activated protein kinase
MPN, myeloproliferative neoplasm
MW, molecular weight
NMR, nuclear magnetic resonance
PAGE- polyacrylamide gel electrophoresis
PI3K, phosphoinositol-3-kinase
PMF, primary myelofibrosis
PRLR, prolactin receptor
PV, polycythemia vera
RTK, receptor tyrosine kinase
RL, Renilla luciferase reporter
SE, sedimentation equilibrium
SH2, Src-homology 2
SM, systemic mastocytosis
STAT, Signal Transducer and Activator of Transcription
TM, transmembrane
Tpo, thrombopoietin
TpoR, thrombopoietin receptor
TCA, trichloroacetic acid
TFE, tetrafluoroethanol
UV-Vis, ultraviolet-visible
WT, wild-type

Acknowledgements

First of all, I sincerely thank my advisor, Dr. Steven O. Smith, for his intelligent and financial support during my Ph.D. study. He has always been my role model as a specialist of structural biology. Without his encouragement and his excellence in science, this dissertation could not have been accomplished.

Secondly, I thank my advisory committee members, Drs. Erwin London, Nancy Reich, Robert Rizzo, and Stuart McLaughlin for their invaluable comments and suggestions.

I also thank my current and previous lab mates for fruitful discussion and creating a lively atmosphere in the laboratory. My special thanks go to Drs. Ian Brett and Sato Takeshi for their preliminary work leading up to this dissertation.

During the course of this work, I was supported by many collaborators as well. I thank Drs. Stefan Constantinescu and Jean-Philippe Defour for dual luciferase assays and Drs. Vitalina Gryshkova and Christian Pecquet for split *Gaussia Princeps* luciferase reporter complementation assays.

Finally, I wish to thank my family and friends, who are always supportive and understanding of my career. My special thanks go to Dr. Shimpei Magori. He provided me with tremendous support in writing this thesis. In addition, I thank my best friend Dr. Yuka Furuya, MD for her moral support.

Chapter 1. Introduction

1.1 Thrombopoietin receptor (TpoR)

1.1.1 Biology of TpoR

Thrombopoietin receptor (TpoR) is a cytokine receptor that regulates megakaryocytopoiesis and platelet formation in response to its ligand, thrombopoietin (Tpo). This transmembrane protein is a polypeptide of 635 amino acids composed of an extracellular (EC) domain, a single transmembrane (TM) domain, and an intracellular (IC) domain (*1*) (**Figure 1.1**). TpoR belongs to the Type I cytokine receptor family, which is characterized by the presence of the cytokine receptor homology module (CRM) in the EC domain. The CRM contains conserved cysteine residues and a tryptophan-serine-*X*-tryptophan-serine (WS*X*WS) motif (*1-3*). The EC domain of TpoR possesses two CRMs, while the IC domain contains the Box 1 and Box 2 motifs, which serve as a docking site for the Janus Kinase 2 (JAK2) tyrosine kinase (*4-7*). Interaction of TpoR with JAK2 is essential for activation of downstream signaling because TpoR itself does not possess an intrinsic kinase domain.

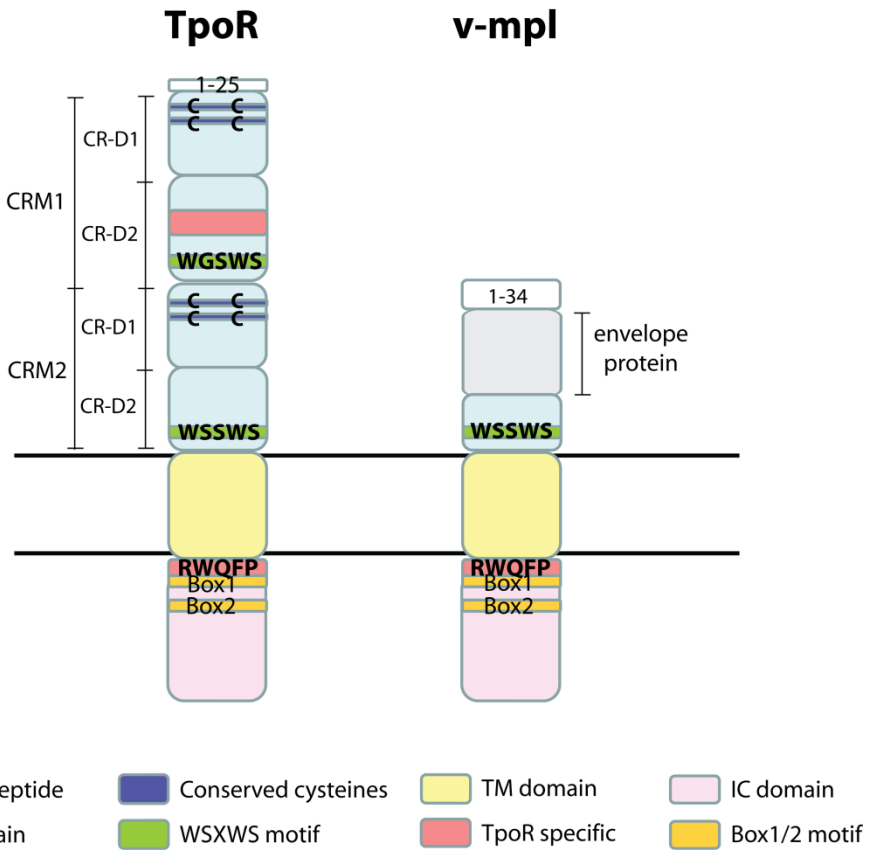

Figure 1.1: Schematic representation of the wild-type TpoR and the *v-mpl*-encoded mutant TpoR. The total length of TpoR (left) is 635 amino acids. The extracellular (EC), transmembrane (TM), and intracellular (IC) domains are composed of 465, 23, 122 amino acids, respectively. TpoR has two cytokine receptor homology modules (CRMs), each of which is composed of approximately 200 amino acids (*1*). This module is further divided into the N- and C-terminal cytokine receptor domains called CR-D1 and CR-D2, respectively. Each CR-D subdomain is comprised of two anti-parallel β-sheets, and closely related to the fibronectin Type III (FBNIII) domain (*8*). Each CRM has two pairs of conserved cysteine residues as well as a conserved C-terminal WSXWS (for tryptophan-serine-*X*-tryptophan-serine) motif. The TpoR IC domain contains Box 1 and Box 2 domains, which are highly conserved among cytokine receptors (*1*). TpoR has two unique motifs that are not found in other cytokine receptors: a 50-amino acid stretch in the EC domain (CRM1- CR-D2) and a 5-amino acid stretch (RWQFP) right below the TM domain. The total length of the *v-mpl*-encoded mutant TpoR (right) is 262 amino acids. Its EC, TM, and IC domains are composed of 99, 23, and 119 amino acids, respectively. The EC domain is composed of an envelope protein of the myeloproliferative leukemia virus and 43 amino acids derived from the TpoR EC domain. The TM and IC domains of v-mpl are the same as those of TpoR (*2*).

TpoR is encoded by the c-*mpl* (myeloproliferative leukemia virus) gene, the cellular homolog of the v-*mpl* oncogene. As its gene name suggests, TpoR was originally found through the studies of the myeloproliferative leukemia virus, an oncogenic retrovirus that induces overgrowth of hematopoietic cells (*2, 9, 10*). It has been demonstrated that this disease is caused

by the v-*mpl* gene of the myeloproliferative leukemia virus, which encodes a truncated form of TpoR (*2*). The v-*mpl*-encoded receptor lacks a large portion of the EC domain but retains the TM and IC domains, which exert a dominant-negative effect on TpoR-mediated megakaryocytopoiesis and platelet development. After this discovery, Tpo was identified as the ligand of TpoR (*11*) (**Figure 1.1**).

TpoR mainly functions in the hematopoietic cell lineage, including hematopoietic stem cells (HSCs), megakaryocytes and platelets (*12-16*) (**Figure 1.2**). Megakaryocytes originate from HSCs, which are mostly found in the bone marrow. During their maturation, megakaryocytes replicate their nuclear DNA without cytokinesis, developing into very large cells. Typically, a matured megakaryocyte is 50-100 μm in diameter, and contains DNA content of up to 64N (*17*). Ultimately, 1,000~1,500 platelets per megakaryocyte are produced by budding off from the matured megakaryocytes and circulate in the blood (*18*).

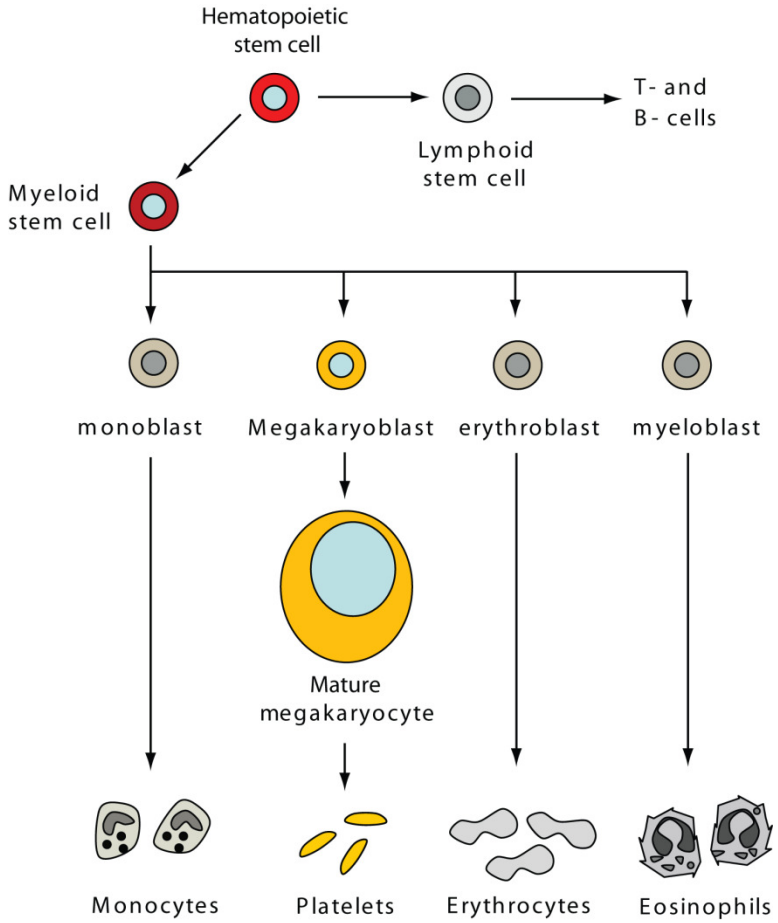

Figure 1.2: Overview of the hematopoietic lineage: Platelets formation from a hematopoietic stem cell (HSC). Platelets are differentiated from a hematopoietic stem cell (HSC) via a megakaryopoiesis pathway involving four major intermediate cell types: megakaryoblast, promegakaryocyte (not shown), granular megakaryocyte (not shown), and mature megakaryocyte (*19*).

Platelets, once referred to as "dust" particles in blood, drew little attention when they were discovered in blood more than 100 years ago (*20, 21*). However, the importance of platelets for human life is now unquestionable. The major function of platelets is to form blood clots and prevent bleeding from a ruptured blood vessel. A deficiency in platelets leads to an increased risk of hemorrhage, while overproduction of platelets restricts blood flow by forming clots in uninjured vessels. Thus, the development and number of platelets in blood needs to be tightly controlled. TpoR plays an essential role in platelet homeostasis by regulating platelet

development. Mutations in this receptor are known to cause a diverse array of blood disorders, depending on which domains or residues of TpoR are affected (summarized in **Table 1.1**). These TpoR-associated blood diseases are classified into two major groups: thrombocytopenia (low platelet count) and thrombocythemia (high platelet count). Thrombocytopenia is considered to be one of the most deleterious and most common hematologic disorders (*22*). Congenital amegakaryocytic thrombocytopenia (CAMT), a type of thrombocytopenia, is caused by different mutations in the c-*mpl* gene. CAMT patients are known to encode TpoR with various types of truncation or a point mutation in the EC domain (*23-26*). As a result, CAMT patients cannot properly respond to Tpo, manifesting thrombocytopenia symptoms (*27*). In addition, a recent study revealed a strong link between another type of thrombocytopenia, familial aplastic anemia (AA), and a proline-to-serine mutation at position 394 of TpoR (*28*). AA is characterized by a deficiency in all types of blood cells, including red blood cells, white blood cells, and platelets, due to the near-total absence of hematopoietic precursor cells (*22*).

Like thrombocytopenia, thrombocythemia is also a fundamental problem affecting many patients. Thrombocythemia, characterized by an increased platelet count, can be either a primary (essential) or secondary (reactive) effect of a certain disorder. Recent studies revealed that patients with myeloproliferative neoplasms (MPNs) possess various mutations in TpoR (*23, 29, 30*). The MPNs are a group of diseases characterized by abnormal myeloid proliferation, and classified into several categories, including chronic myeloid leukemia (CML), polycythemia vera (PV), essential thrombocythemia (ET), primary myelofibrosis (PMF), chronic eosinophilic leukemia (CEL), and chronic myelomonocytic leukemia (CMML), and systemic mastocytosis (SM) (*31*). Among them, at least 4.5% of ET and 5% of PMF patients

are known to possess mutations, most of which are found in the TM domain and the juxtamembrane (JM) region of TpoR (*29, 30, 32, 33*). The known mutations in the TpoR of ET and PMF patients include an amino acid substitution of serine for asparagine at position 505 (S505N) and a substitution of tryptophan for either leucine, lysine, alanine, or arginine at position 515 (W515L, W515K, W515A, and W515R) (*30, 32, 34*). These mutations are believed to cause overproduction of hematopoietic cells in the megakaryopoiesis lineage, including platelets (*35-38*). These TpoR mutations and the resulting disease symptoms further emphasize the importance of TpoR in platelet development. Furthermore, the characterized TpoR mutations can serve as great resources to understand the TpoR activation mechanism, which remains largely unknown.

Table 1.1: Clinically related TpoR mutations and disorders

A point mutation						
Domain	**Residue #**	**Mutation**	**# of patients**	**Diseases**	**Sub-category (# of patients)**	**References**
EC	102	R102P	9	Thrombocytopenias	CAMT	*(25, 39, 40)*
		R102C	2	Thrombocytopenias	CAMT	*(25, 40)*
	104	F104S	1	Thrombocytopenias	CAMT	*(40)*
	128	D128Y	1	Thrombocytopenias	CAMT	*(41)*
	136	P136H	1	Thrombocytopenias	CAMT	*(24)*
		P136L	1	Thrombocytopenias	CAMT	*(40)*
	154	W154R	2	Thrombocytopenias	CAMT	*(40, 42)*
	193	C193C	1	Thrombocytopenias	CAMT	*(43)*
	204	S204F	1	MPN	PMF	*(44)*
		S204P	1	MPN	IMF	*(45)*
	252	Y252H	1	MPN	ET	*(46)*
	394	P394S	1	Anemia	FAA	*(28)*
	487	T487A	1	MPN	AMKL	*(47)*
TM	505	S505N	8	MPN		*(34)*
					ET (5)	*(29)*
					PMF (1)	*(33)*
	506	A506T	2	MPN	PMF	*(33)*
	507	V507I	1	MPN		*(34)*
	510	L510P	1	MPN	PMF	*(33)*
JM	514	R514K	1	MPN		*(34)*
	515	W515L	163	MPN		*(30, 34, 48)*
					PMF (19)	*(33, 44, 49-53)*
					ET (89)	*(29, 49, 50-54)*
					CMML (1)	*(51)*
		W515K	45	MPN		*(30, 34, 48)*
					ET (33)	*(29, 49-55)*
					PMF (8)	*(33, 51-53)*
					IMP (1)	*(45)*
		W515A	11	MPN		*(34)*
					PMF (2)	*(33, 50)*
					ET (8)	*(49, 51, 52, 55)*
		W515R	8	MPN		*(34)*
					PMF (3)	*(50-52)*
					ET(1)	*(50)*
		W515S	2	MPN		*(34)*
		W515G	1	MPN		*(34)*

	519	A519V	1	MPN		*(34)*
		A519T	1	MPN	PMF	*(33)*
IC	545	D545G	1	MPN		*(34)*
		D545N	1	MPN		*(34)*
	614	G614V	1	Thrombocytopenias	CAMT	*(41)*
	635	P635L	1	Thrombocytopenias	CAMT	*(24)*
Double mutations						
Domain	**Residue #**	**Mutation**	**# of patients**	**Diseases**	**Sub-division (# of patients)**	**References**
TM/TM	501/505	V501L/ S505N	1	MPN		*(34)*
TM/JM	501/515	V501A/ W515R	1	MPN	ET	*(49)*
		V501A/ W515L	1		PMF	*(49)*
	505/515	S505C/ W515L	1	MPN	ET	*(49)*
		S505N/ W515L	1		ET	*(50)*
JM/JM	509/515	G509C/ W515L	1	MPN	ET	*(50)*
JM/IC	515/540	W515L/ G540S	1	MPN		*(34)*
Insertion-deletion mutations						
Domain	**Deletion -->**	**Insertion**	**# of patients**	**Diseases**	**Sub-division (# of patients)**	**References**
EC-TM	T469-A497	ALVI	1	MPN		*(34)*
JM	W515-P518	KT	2	MPN		*(34)*
					ET	*(55)*

#: numbers; CAMT: Congenital amegakaryocytic thrombocytopenia; MPN: myeloproliferative neoplasms; PMF: primary myelofibrosis; ET: essential thrombocythemia; AMKL: acute megakaryoblastic leukemia; IMF: idiopathic myelofibrosis; CMML: Chronic myelomonocytic leukemia; FAA: familial aplastic anemia; EC: extracellular; TM: transmembrane; JM: juxtamembrane; IC: intracellular

1.1.2 JAK2-STAT signaling pathway

Although the precise activation mechanism of TpoR remains to be determined, the consequence of the TpoR activation is relatively well understood; upon binding of Tpo, the TpoR activates the JAK2 - STAT (Signal Transducer and Activator of Transcription) signaling pathway (*56, 57*). JAK2 is a tyrosine kinase, and the STATs are transcription factors (*58*). Binding of Tpo to the EC domain of TpoR triggers the autophosphorylation of JAK2 (*59*), which is pre-associated with the TpoR IC domain. The phosphorylated JAK2 in turn phosphorylates several tyrosine residues of TpoR (*60, 61*). Subsequently, the phosphorylated TpoR recruits STATs to the TpoR/JAK2 complex, leading to JAK2-mediated phosphorylation of STATs (*58*). Finally, the phosphorylated STATs dimerize (*62*) and translocate into the cell nucleus, where they bind to the STAT-responsive promoters to initiate transcription of target genes.

JAK2 is a non-receptor tyrosine kinase that belongs to the JAK family. JAK2 is a relatively large protein of 130 kDa in molecular weight, composed of seven Janus homology domains (JH1 to 7) (**Figure 1.3**) (*63*). JH1 is a functional kinase domain that contains two conserved tyrosine residues (Y1007 and Y1008) in the activation loop. The JH1 domain is closely related to the kinase domain of the epidermal growth factor (EGF) receptor family (*64*). JH2 also shares considerable homology with the kinase domain of the EGF receptor family (*65*). However, unlike JH1, JH2 lacks several critical amino acids required for the kinase activity (*65*), indicating that JH2 represents a pseudokinase domain. The JH3, JH4, and JH5 domains constitute the Src-homology 2 (SH2)-like domain, the function of which remains unknown. The JH6 and JH7 domains serve as the FERM (Band-4.1, Ezrin, Radizin, Moesin) domain, through which JAK2 interacts with the Box 1 and Box 2 motifs of TpoR. Upon binding of Tpo to TpoR, two JAK2

molecules, each of which is pre-associated with one TpoR molecule within a TpoR dimer, induce auto/trans-phosphorylation of two tyrosine residues, Y1007 and Y1008, on the activation loop of the JH1 domain (*59*). In addition, JAK2 phosphorylates other tyrosine residues, such as Y221, Y570, and Y831 (*66, 67*).

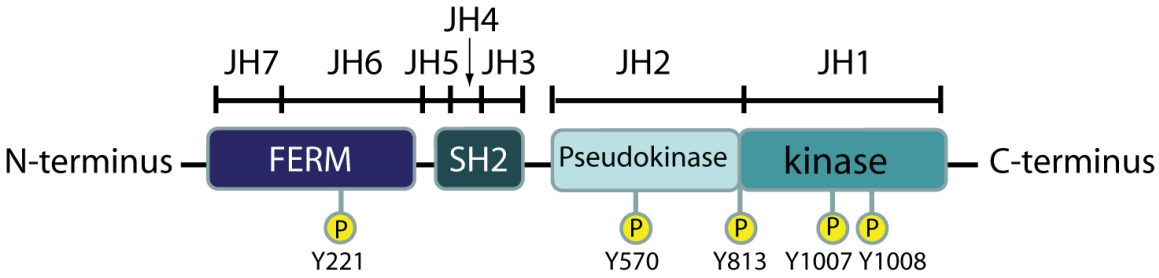

Figure 1.3: Schematic representation of the JAK2 structure. JAK2 is composed of FERM, SH2-like, pseudokinase, and kinase domains. Alternatively, the primary structure of JAK2 can be divided into seven Janus homology (JH) domains. JAK2 interacts with several cytokine receptors via the FERM domain. The kinase domain, in concert with the pseudokinase domain, catalyzes tyrosine phosphorylation of several cytokine receptors and their downstream signaling components. In addition, JAK2 autophosphorylates multiple tyrosine residues, including Y1007 and Y1008, both of which are found in the activation loop of the kinase domain (*63*). The schematic diagram is adapted from (*63*).

The activated JAK2 is known to phosphorylate at least Y78, Y112, and Y117 of TpoR. (*60, 61*). These phosphorylated tyrosine residues in TpoR serve as the docking sites of STATs, such as STAT3 and STAT5, and bring these transcription factors into close proximity of JAK2. In addition, many other molecules, including phosphoinositol-3-kinase (PI3K) and mitogen-activated protein kinases (MAPKs), are recruited to the TpoR/JAK2 complex, thereby modulating the JAK2-STAT signaling pathway.

The phosphorylated STAT molecules undergo homodimerization in the cytoplasm, and the STAT dimer then translocates to the cell nucleus. The nuclear STATs promote transcription of many genes critical for cell cycle regulation and cell survival control, such as cyclin D1, cyclin-dependent kinase inhibitor 1A (p21), cyclin-dependent kinase inhibitor 1B (p27KIP1), and

BCL2-like 1 (Bcl-XL) (*68, 69*). These STAT-induced dynamic gene expression changes orchestrate megakaryopoiesis and platelet development.

The Tpo/TpoR-induced signaling eventually needs to be terminated. Termination is mediated by at least four mechanisms: receptor internalization, dephosphorylation of JAK2, masking of the phosphorylated residues on the TpoR/JAK2 complex, and inhibition of the STAT activity. In the first mechanism, the activated TpoR is rapidly removed from the cell membrane by clathrin-dependent endocytosis (*70*). The second mechanism exploits tyrosine phosphatases, such as Src Homology Phosphatase 1 (SHP 1). These phosphatases are recruited to the TpoR/JAK2 complex and dephosphorylate the activated JAK2 (*68, 71*). The third mechanism involves the suppressor of cytokine signaling (SOCS) proteins, which are induced by cytokines (*72*). For instance, SOCS1, one of the SOCS proteins, directly binds to the phosphorylated JAK2, thereby masking the docking sites for the JAK2 target proteins (*73*). The fourth mechanism is mediated by transcriptional inhibitors that abrogate the DNA binding activity of STATs. For example, PIAS3 (for protein inhibitor of activated STAT3) has been shown to inhibit the transcriptional activity of STAT3 (*74*). Over the past few decades, a great deal has been learned about the complexity of the TpoR downstream signaling (**Figure 1.4**). However, the molecular mechanism underlying the TpoR-mediated JAK2 activation, the very first step of TpoR signaling, remains an enigma.

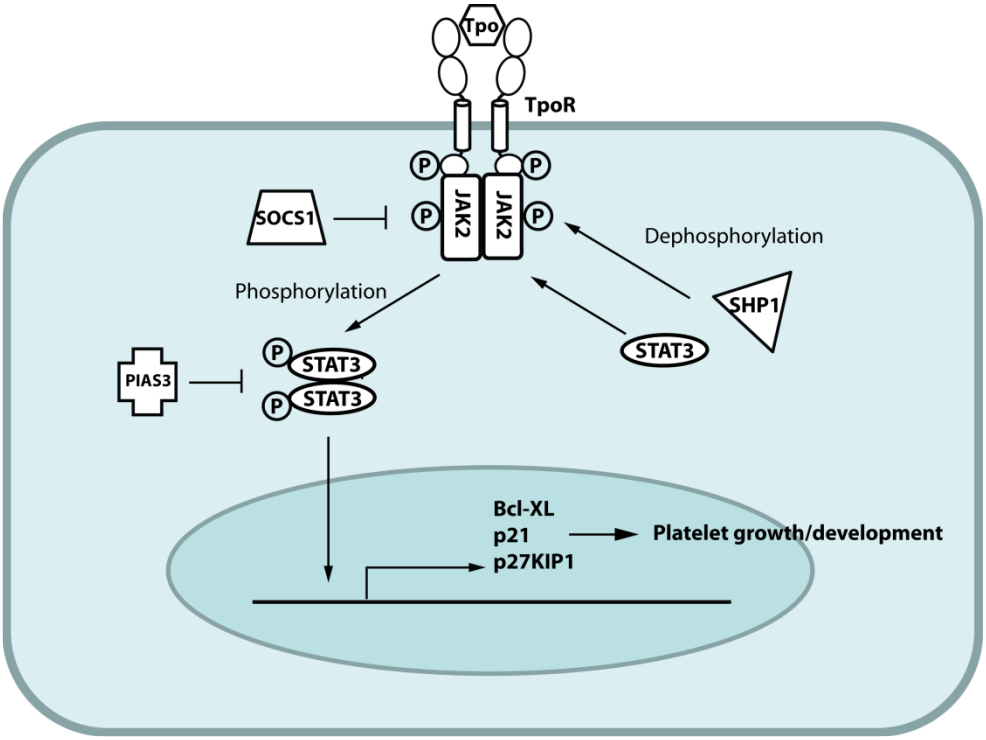

Figure 1.4: Schematic representation of the JAK2-STAT signaling pathway. Binding of Tpo to the TpoR EC domains induces the auto/trans-phosphorylation of JAK2. The phosphorylated JAK2 then phosphorylates the IC domains of TpoR. The phosphorylated residues on the TpoR/JAK2 complex serve as docking sites for the downstream signaling components, such as STAT3 and STAT5. The phosphorylated STATs undergo dimerization and enter the cell nucleus, in which they bind to the STAT-responsive promoters to initiate transcription of the target genes, such as Bcl-XL, p21, and p27KIP1. As a negative regulator of the JAK2-STAT signaling, SHP1 dephosphorylates JAK2. In addition, PIAS3 directly binds to STAT3 and inhibits its transcription activity. Furthermore, SOCS1 binds to the phosphorylated JAK2, thereby masking the docking sites for the JAK2 target proteins.

1.2 Type I-Group 1 cytokine receptors form ligand-independent dimers

The key to understanding the TpoR activation mechanism may lie in other Type I cytokine receptors that are structurally similar to TpoR. The Type I cytokine receptors can be further classified into five subgroups (i.e., Group 1 to 5) based on their sequence and structural homology as well as the type of cytokine ligands (*3*). TpoR belongs to Group 1, which is characterized by a relatively short IC domain and the absence of additional, functional modules, other than CRMs, in the EC domain (*3*) (**Figure 1.1**). Furthermore, the Type I-Group 1 cytokine receptors are known to form homodimers upon ligand binding (*75*). Group 1 is comprised of four

functional receptor members: TpoR, the erythropoietin receptor (EpoR), the growth hormone receptor (GHR), and the prolactin receptor (PRLR) (**Figure 1.5**). Increasing evidence suggests that these Type I-Group 1 cytokine receptors form homodimers even in the absence of the ligands (i.e., ligand-independent dimers or pre-formed dimers). For example, a study using antibody-mediated immunofluorescence co-patching showed that EpoR can oligomerize even without its ligand (*76*). In this study, the murine EpoR was fused to either the hemagglutinin (HA) or Myc tag, and their co-localization at the surface of live cells was detected by two fluorescently labeled antibodies. Consistent with this observation, a crystal structure of the EpoR EC domain showed that the EC domain interacts with each other in the absence of the ligand (*77*). Similarly, GHR also seems to form a ligand-independent dimer. Indeed, studies using various methods, such as co-immunoprecipitation (Co-IP), fluorescence resonance energy transfer (FRET), and bioluminescence resonance energy transfer (BRET), clearly demonstrated that GHR undergoes dimerization in the absence of the ligand binding (*78, 79*). Furthermore, studies using Co-IP and BRET experiments revealed the presence of ligand-independent dimers of PRLR (*80, 81*). By analogy, it is tempting to speculate that TpoR, another Type I-Group 1 cytokine receptor, also exists as a ligand-independent dimer.

EpoR, the closest relative of TpoR, is likely to form a ligand-independent dimer via the TM domain. A domain swapping study showed that at least the intact TM domain is necessary for EpoR dimerization and that the EpoR TM domain cannot be functionally replaced by the PRLR TM domain (*76*). The idea that the EpoR TM domain can associate was further augmented by two independent studies: one using analytical ultracentrifugation sedimentation equilibrium (SE-AUC) and another using the ToxR-transcriptional reporter assay (*82, 83*). The

SE-AUC analysis demonstrated that the TM domain of EpoR most likely interacts with each other at a 1:1 stoichiometric ratio in detergent micelles (*82*). Furthermore, the ToxR reporter system, in which dimerization of tested transmembrane proteins induces the homodimerization of the ToxR transcription factor and the resultant transcription activation, showed that the EpoR TM domain undergoes self-interaction within the *Escherichia coli* cell membrane.

In contrast to EpoR, the mechanism underlying the ligand-independent dimerization of GHR remains inconclusive. A study using Co-IP, FRET, and BRET assays suggests that the TM and JM regions of GHR mediate the receptor dimerization (*78*). This model was further supported by a more recent study using a cysteine cross-linking experiment and the ToxR bacterial reporter system (*84*). However, another study using the ToxR system failed to detect self-dimerization of the GHR TM domain (*83*). In addition, a chimeric GHR with its TM domain replaced by that of the human low-density lipoprotein receptor (LDLR) was still able to form a ligand-independent dimer, suggesting that the TM domain may not be involved in the GHR dimerization (*79*).

Similarly, it remains inconclusive how PRLR forms a ligand-independent dimer. It has been shown that deletion of either the EC or IC domain of PRLR does not affect the receptor dimerization, suggesting that the TM domain of PRLR is critical for dimerization of PRLR (*81*). However, replacement of the EC or IC domain of PRLR with the corresponding domain of EpoR abolished the ligand-independent dimerization of PRLR even though the chimeric PRLR retains the TM domain (*76*). Thus, unlike EpoR, the ligand-independent dimers of PRLR and GHR may be stabilized by a relatively complex mechanism.

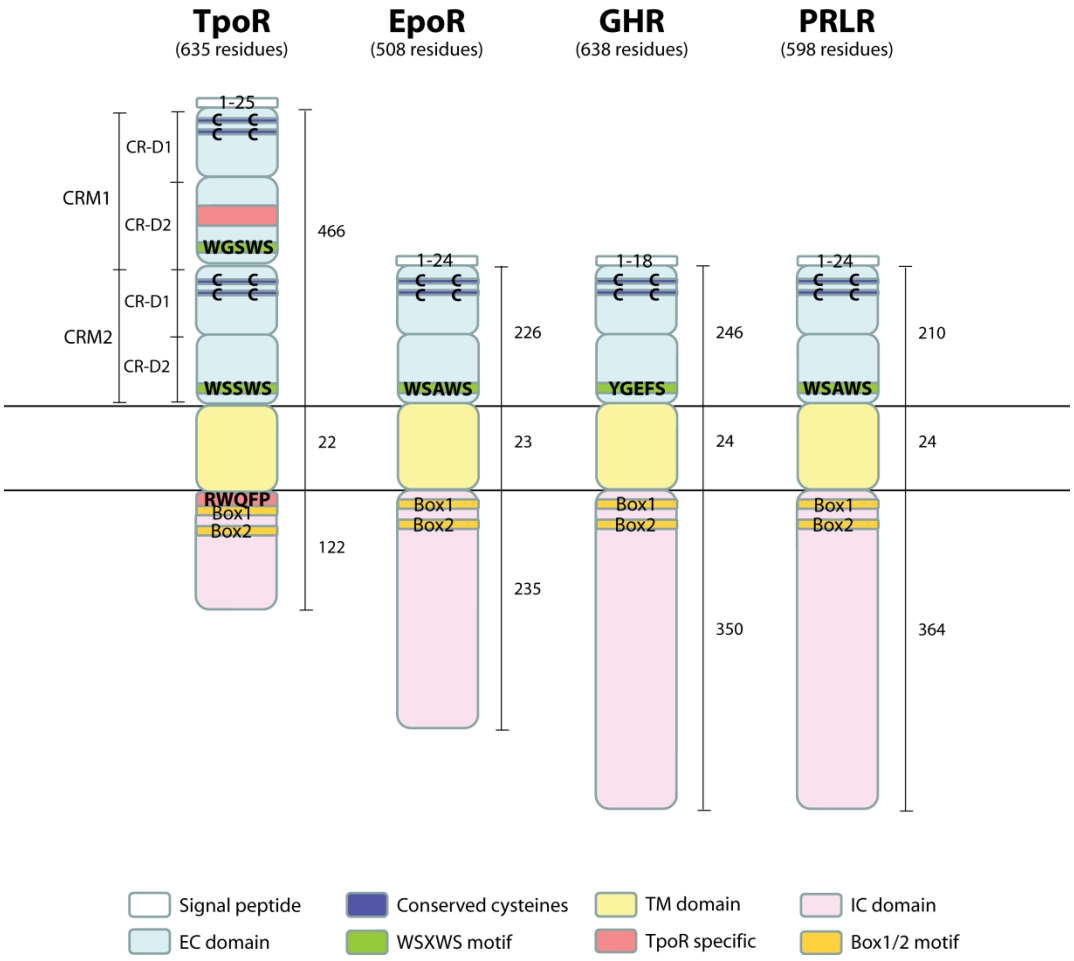

Figure 1.5: Schematic representations of the Type I-Group 1 cytokine receptor structures. The Type I-Group 1 cytokine receptor family is comprised of four members: TpoR, EpoR, GHR, and PRLR. The total length of these receptors is approximately 500-600 residues. TpoR possesses the largest extracellular (EC) domain with a unique 50-amino acid stretch, which is not found in the other receptors (*2*). The TpoR EC domain is composed of two cytokine receptor homology modules (CRMs), while the other receptors have only one CRM. The TpoR has the shortest intracellular (IC) domain with a unique motif of five amino acids (RWQFP). All the Type I-Group 1 cytokine receptors interact with JAK2 through their Box 1 and Box 2 domains. The number shown on the right side of each schematic receptor represents the number of amino acids in the corresponding region.

1.3 Type I-Group 1 cytokine receptors are activated by TM helix rotation

In conventional models, most transmembrane receptors are believed to be activated by dimerization upon ligand binding. However, several Type I-Group 1 cytokine receptors already

exist as dimers before ligand binding. Thus, the ligand-induced dimerization model cannot explain the activation mechanism of these Type I-Group 1 cytokine receptors. Instead, their activation may be mediated by an internal conformational change within the dimers, rather than the dimerization itself. Consistent with this notion, the crystal structure of the EC domain of EpoR suggests that EpoR undergoes "scissor-like rotation" within the dimer in response to Epo (**Figure 1.6**) (*77, 85*). This conformational change of the EpoR EC domain should affect the conformation or orientation of the TM and IC domains, which may be important for receptor activation.

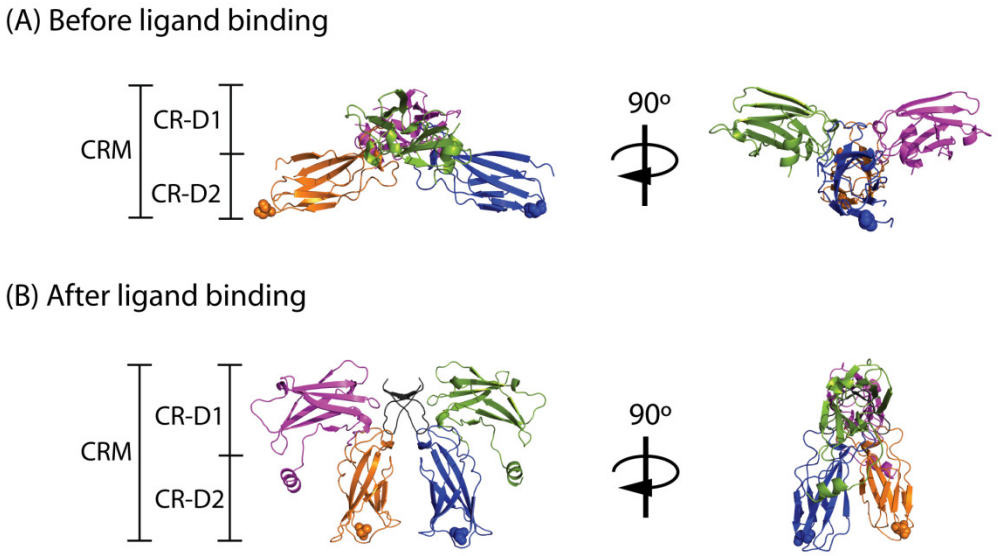

Figure 1.6: Comparison between the EC domain of the unliganded and liganded EpoR structures. (A) The EC domain of the unliganded EpoR (PDB ID: 1ERN) (*77*). (B) The EC domain of the EpoR with an Epo mimetic agonist (PDB ID: 1EBP) (*8*). Ligand binding induces the CR-D1 domain to position itself parallel to the membrane plane. At the same time, the CR-D2 domain rearranges its structure perpendicular to the membrane plane upon ligand binding. The CR-D1 and CR-D2 domains of one EpoR EC domain are shown in magenta and orange, respectively. The CR-D1 and CR-D2 of the other EpoR EC domain are shown in green and blue, respectively. The ligand is shown in black.

In addition, several studies suggest that a distinct set of residues lining the TM-TM interaction interface is critical for the EpoR activation (*83, 86-89*). It has been proposed that

binding of the ligand to EpoR induces rotation of the TM domain on its helical axis (α, α'), bringing a different set of amino acid residues into the dimerization interface (**Figure 1.7**).

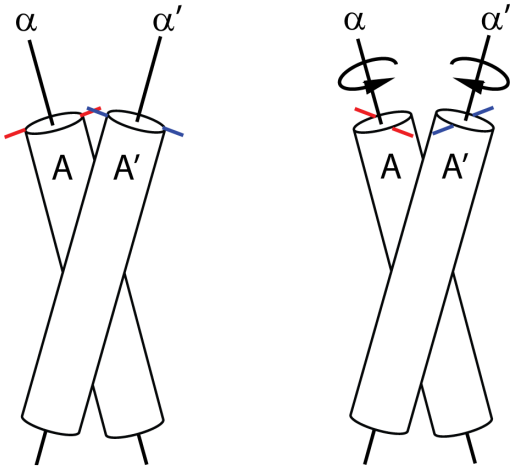

Figure 1.7: Ligand-induced rotation of TM helices within a pre-formed receptor dimer. Within a pre-formed dimer of a single-pass transmembrane receptor, such as EpoR, ligand binding may induce rotation of the TM domains on their helical axes (α, α'). This conformational change may bring a different set of amino acid residues into the dimerization interface, resulting in formation of the active receptor structure. The TM helices are represented as cylinders (A and A'). Red and blue bars highlight the relative orientation of the TM helices after ~100° rotation.

This model was supported by a study using the Put3 helix rotational tag (*86, 90*). In this study, an EpoR dimer lacking the EC domains was tethered to the extracellular Put3 dimer tag, and the TM domain of EpoR was artificially rotated on its helical axis by removing variable numbers of amino acids from the TM domain at the Put3-TM junction. Removal of one amino acid at the Put3-TM junction forces a rotation of the TM helix by ~100°. By sequentially removing up to seven amino acids from the Put3-TM junction, all possible TM-TM interfaces can be generated (*86*) (**Figure 1.8**). Out of seven possible helical orientations, only one activated the EpoR downstream signaling pathway, suggesting that a specific dimerization interface defines the active conformation of EpoR (*86*).

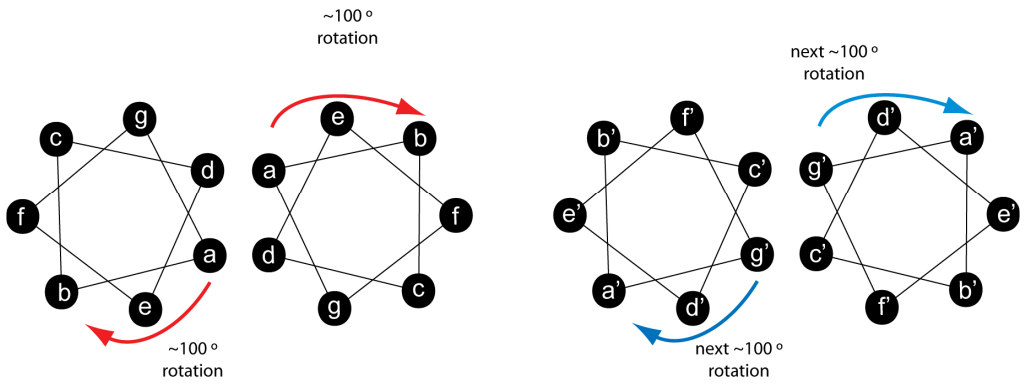

Figure 1.8: Helical-wheel diagram showing a coiled-coil structure composed of two TM helices. Within a pre-formed receptor dimer, two TM domains may form a coiled-coil structure, in which amino acids reside on seven different structural positions (*a*–*g*). These seven residues, called a heptad repeat, constitute exactly two helical turns in each helix. The diagrams show the top views of a TM helix dimer before (left) or after (right) ligand binding. Before ligand binding, the two TM helices may interact with each other at a specific interface (e.g., positions *a* and *d*) (left). Upon ligand binding to the receptor, the TM helices may rotate ~100° on their helical axes, bringing a different set of amino acids into the interaction surface (e.g., positions *c* and *g*) (right).

Similarly, another study also artificially rotated the TM helix of EpoR by inserting an alanine in the juxtamembrane (JM) region and found that a specific helical orientation is important for the downstream signaling (*87*). The helix rotation of a receptor TM domain may be indispensable for activation of not only EpoR, but also another Type I-Group 1 cytokine receptor, GHR. Indeed, a helix rotation study using alanine insertions suggests that a GHR dimer can be activated when a specific set of amino acids in the TM domain is brought to the dimerization interface by re-orientation of the TM helices (*78*).

To examine whether the TpoR activation is also mediated by the TM helix rotation, a recent study using the Put3 system changed the helical orientation of the TpoR TM domain. Unlike EpoR, six out of seven engineered helical orientations were able to activate the TpoR downstream signaling although their activation levels were variable (*91*). On the other hand, only one helical orientation rendered TpoR completely inactive (*91*). This result suggests that TpoR may adopt six different active states, each of which is determined by a distinct set of amino acid

residues lined up in the TM-TM interaction interface. However, it should be noted that this model was based on an assumption that the TM domain constitutes the interaction interface of a ligand-independent TpoR dimer. If this is not the case, we cannot rule out the possibility that the helical re-orientation of the TM domain may play only a minor role in the TpoR activation.

1.4 Clinically relavant mutations in TpoR

In addition to studies on other Type I-Group 1 cytokine receptors, clinically relevant mutations in TpoR are a useful resource to understand the molecular mechanism underlying TpoR activation. As shown in **Table 1.1**, a majority of the clinically relevant TpoR mutations are found in the TM domain and its adjacent region. Within this region, S505 and W515 are most frequently mutated, suggesting that these residues play a critical role in regulation of the TpoR activity.

1.4.1 Clinically relevant mutation at S505 of TpoR

The S505N mutation, which resides in the middle of the TpoR TM domain, is associated with familial ET (*34-36, 92*). It has been demonstrated that S505N constitutively activates the JAK2-STAT signaling pathway, resulting in an increased number of platelets (*35*). The TpoR mutant containing S505N can form a ligand-independent dimer (*38*). The dimerization and the resulting receptor activation of the mutant TpoR is not abrogated by deletion of its EC domain, suggesting that either the IC or TM domain is essential for the ligand-independent dimerization and the activation of the mutant receptor (*38*). Interestingly, amino acid substitution within the TM domain is known to cause constitutive activation of other single-pass transmembrane receptors.

For example, the human epidermal growth factor receptor 2 (HER2) is constitutively activated by substitution of valine for glutamic acid at position 664 (V664E), which is located in the middle of the TM domain (*93*). The V664E mutation was suggested to stabilize the dimer structure of HER2 by forming two hydrogen bonds: one with the backbone carbonyl of A661 and another with the side chain of T662 (*94*). Similarly, the fibroblast growth factor receptor 3 (FGFR3) is constitutively activated by substitution of alanine for glutamic acid at position 391 (A391E), a mutation in the TM domain. The E391 might form a hydrogen bond between two interacting TM helices, thereby stabilizing the active conformation of the FGFR3 dimer (*95*). By analogy, the S505N mutation may enhance the TpoR activity by stabilizing TM-TM interactions within a pre-formed TpoR dimer and/or rearranging the receptor dimer into the active conformation.

1.4.2 Clinically relevant mutation at W515 of TpoR

At least 4.5% of ET and 5% of PMF patients are known to possess a mutation of the tryptophan residue at position 515 (W515) of TpoR, which resides at the boundary between the TM domain and the intracellular side of the JM region (IC-JM) (*50*). At least six types of clinical mutations at this residue (W515K, W515L, W515R, W515A, W515S, and W515G) have been identified from ET and PMF patients (*34*). All of these mutations constitutively activate TpoR, resulting in an increased number of platelets (*34*). However, the molecular mechanism by which these mutations at W515 cause constitutive receptor activation remains largely unclear. Considering the high frequency of W515 mutations in TpoR, the ^{514}RWQFP motif surrounding W515 may play an essential role in regulation of the TpoR activity. Consistent with this notion, the RWQFP

motif in the IC-JM is highly conserved among the TpoR homologs from many other species (**Figure 1.9A**). On the other hand, the RWQFP motif is specific to TpoR, and not found in the other Type I-Group 1 cytokine receptors (**Figure 1.9B**). This suggests that the RWQFP possesses a TpoR-specific function in the control of receptor activation.

Figure 1.9: Sequence alignment of the TpoR TM-JM regions. (A) The amino acid sequence of the human TpoR TM-JM region including the Box 1 motif was aligned with the corresponding sequence of other primate TpoR receptors. The RWQFP motif, highlighted in red, is conserved throughout different species. (B) The human TpoR sequence was aligned with that of the other cytokine Type I-Group 1 receptors. Note that the RWQFP motif is unique to TpoR. Regions highlighted in blue and bold black indicate the predicted TM domains and the Box 1 motifs, respectively.

Furthermore, a study using the murine TpoR has demonstrated that deletion of the amphipathic motif (^{508}KWQFP), which corresponds to the human ^{514}RWQFP, constitutively activates TpoR (*96*). This constitutive activation resulted in activation of the JAK2-STAT signaling pathway, as well as induction of hematopoietic myeloid differentiation even in the absence of Tpo (*96*). Thus, these observations suggest that ^{514}RWQFP motif is required for maintaining the inactive state of the TpoR when the ligands are not bound to the receptor.

1.5 Models for the activation mechanism of TpoR

Increasing evidence suggests that several Type I-Group 1 cytokine receptors likely form ligand-independent dimers. By analogy, TpoR, another Type I-Group 1 cytokine receptor, may also

exist as a dimer in the absence of the ligand (**Figure 1.10**). The putative TpoR dimer may be stabilized by TM-TM interactions as is the case for EpoR, the closest relative of TpoR. Binding of Tpo to a TpoR dimer may alter the helical orientation of the two pre-associated TM domains, leading to a receptor conformation more favorable for JAK2 activation (**Figure 1.10**). The constitutively active TpoR mutants may force this TM helical orientation change in a ligand-independent manner, causing constitutive activation of the JAK2-STAT signaling pathway. For example, one of the clinical mutations in TpoR, S505N, might cause intermolecular hydrogen bonding between the associated TM domains, thereby mimicking the TM-TM orientation of the activated TpoR. However, we cannot exclude the possibility that, unlike EpoR, the TM domains do not interact with each other unless Tpo is bound to TpoR. If this is the case, the activation of TpoR may be mediated by a different mechanism. For instance, TpoR may exist as a monomer or form a dimer through a region other than the TM domain, and binding of Tpo to the EC domain of TpoR may promote the TM-TM interaction, resulting in the active receptor conformation. Based on this alternative model, we predict that several clinical mutations could constitutively activate the JAK2-STAT signaling by enhancing the ligand-independent TM-TM interaction.

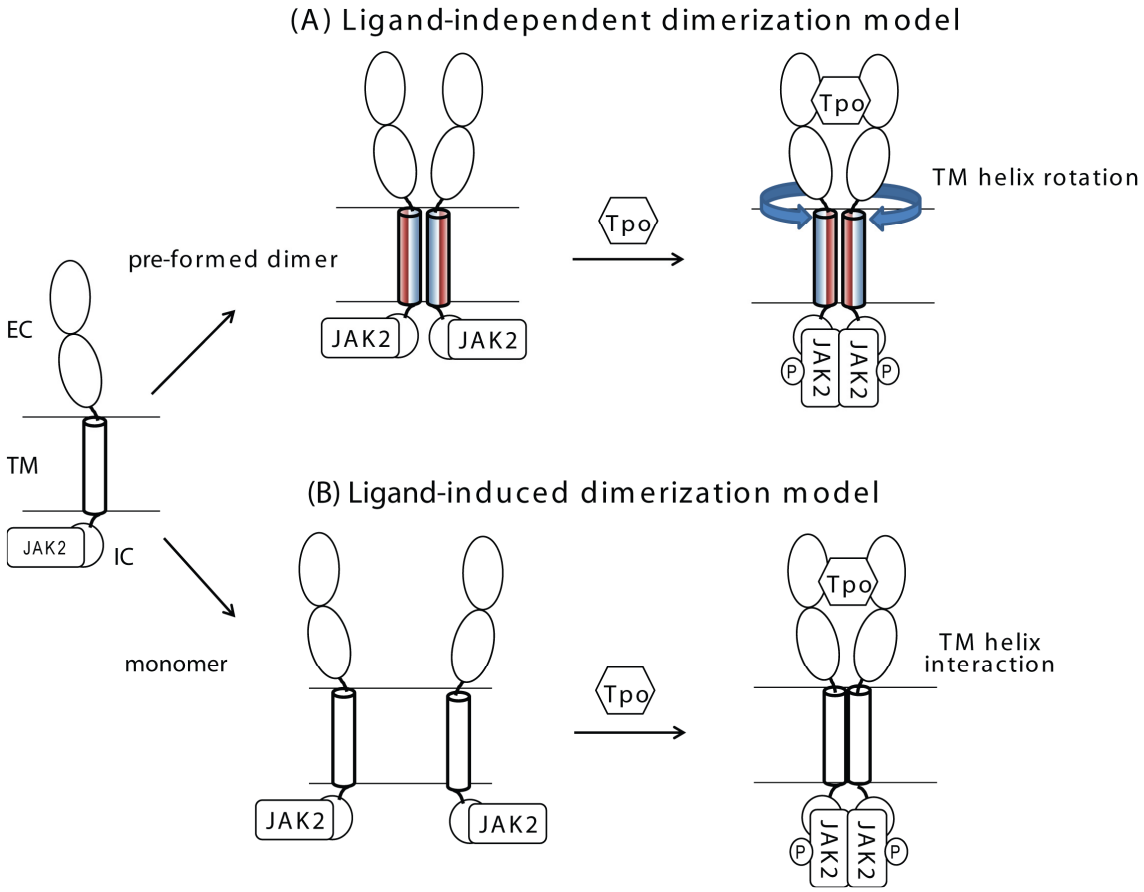

Figure 1.10: Potential models for the TpoR activation mechanism. (A) Ligand-independent dimerization of TpoR is mediated by TM-TM interaction, and inactive JAK2 kinases are associated with the intracellular (IC) domains of the receptor dimer (left). Once the ligand, Tpo, binds to the extracellular (EC) domains of the receptor dimer, the two TM helices are forced to rotate on their helical axes, bringing a distinct set of residues into the TM-TM interaction interface (right). This rotation of the TM helices rearranges the structure of the IC domain as well as the pre-associated JAK2 kinase. As a result, JAK2 becomes activated and promotes downstream signaling. An ellipse in the EC domain represents one cytokine receptor module (CRM). (B) In this model, the unliganded (inactive) receptor may exist as a monomer. The ligand binding mediates the dimerization of the receptor, leading to the activation of the receptor.

1.6 Summary and objectives

Despite the apparent importance of TpoR in megakaryocytopoiesis and platelet development, the molecular mechanism underlying the TpoR activation remains unclear. To better understand the

conformational change that TpoR undergoes upon the ligand binding, we ask the following questions:

- Like other Type I-Group 1 cytokine receptors, does TpoR dimerize in the absence of its ligand?
- Do the TM domain of TpoR and its adjacent JM region play a role in receptor dimerization and activation?
- How do mutations in the TM-JM domain of TpoR cause constitutive activation of the receptor?

Specifically, we focus on the TM-JM region of TpoR because many mutations in this region are known to constitutively activate the receptor. In addition, we examine the effect of several clinically relevant mutations on the dimerization and activity of the full-length receptor. The work on the full-length TpoR has been a collaborative effort with the research group of Prof. Stefan Constantinescu (Ludwig Institute for Cancer Research). The outline of the thesis is as follows.

Chapter 2 presents the methods used in this work.

The principal methods we used at Stony Brook University were as follows:

- Sedimentation equilibrium analytical ultracentrifugation (SE-AUC)

  This assay was used to measure the TpoR TM-TM helix interaction in detergent micelles. SE-AUC is a useful method particularly for determining membrane protein interactions because it allows for direct observation of protein self-association without considering the mass of micelles.
- Deuterium magic angle spinning (MAS) NMR spectroscopy

This assay was used to measure the TpoR TM-TM helix interaction in lipid bilayer membranes. The deuterium MAS NMR spectroscopy is beneficial for studying the TM-TM interaction of membrane proteins because this technique makes it possible to study membrane proteins in model cell membranes.

- Polarized infrared spectroscopy

  This assay was used to measure the secondary structure and helix orientation of the TpoR TM domain in lipid bilayer membranes.

The studies and approaches that were completed in the laboratory of Prof. Stefan Constantinescu were as follows:

- Split *Gaussia princeps* luciferase complementation assay – Dr. Vitalina Gryshkova

  This assay was used to measure the dimerization state of the full-length wild-type TpoR as well as its mutants in the absence of ligand. The luciferase complementation system is a highly sensitive analysis that does not require overexpression of the proteins to be tested. Thus, in this assay, proteins can be expressed at or near their endogenous levels, which should lower the risk of false positive protein interactions.

- Dual luciferase reporter assay – Dr. Jean-Philippe Defour

  This assay was routinely used to analyze the TpoR activity *in vivo*. We utilized the STAT-responsive promoter fused to the luciferase gene and determined the JAK2-STAT signaling activity in cells expressing various TpoR mutants.

In Chapter 3, we address the propensity of the wild-type TM domain to dimerize. It remains elusive whether TpoR undergoes ligand-independent dimerization via its TM domain. To address this question, we first use SE-AUC and deuterium NMR, and examine whether the TM-JM peptide of TpoR can self-associate. Our results show that, unlike EpoR, the TM-JM peptide of TpoR does not possess a strong propensity to dimerize in detergent micelles or lipid bilayer membranes. We then extend this study to the full-length receptor in collaboration with the laboratory of Stefan Constantinescu. Our split luciferase complementation assay shows that the

full-length TpoR can dimerize in a ligand-independent manner despite the lack of TM-TM interactions.

In Chapter 4, we extend the results presented in Chapter 3 on the wild-type TpoR to the S505N mutant receptor. The S505N mutation, which resides in the TM domain of TpoR, constitutively activates the receptor and its downstream signaling. Thus, this mutation is a useful tool to analyze the effect of the TM domain on the receptor conformation and the resultant activation. We first analyze the effects of the S505N mutation on self-interaction of the TpoR TM-JM peptide using SE-AUC and deuterium NMR. Then, we examine the effect of S505N on the dimerization and activation of the full-length TpoR in collaboration with the Constantinescu laboratory. Our results show that S505N is a gain-of-function mutation that enhances TM-TM interaction, receptor dimerization, and receptor activity.

In Chapter 5, we focus on W515, the mutations of which are known to constitutively activate TpoR. The W515 residue, which is part of a unique five-residue motif (RWQFP), is located at the intracellular TM-JM boundary. We first analyze the effects of various known mutations at W515 on the receptor activity as well as the receptor dimerization. Our data, which were obtained in collaboration with the Constantinescu laboratory, suggest that a tryptophan residue in the TpoR JM region is critical to maintain TpoR in an inactive conformation. We then utilize SE-AUC, deuterium NMR and polarized IR to examine in more detail how W515 stabilizes the inactive receptor conformation.

Finally, in Chapter 6, we discuss possible models of the TpoR activation mechanisms based on the results presented in Chapters 3-5.

Chapter 2. Materials and Methods

2.1 Synthetic TpoR transmembrane and juxtamembrane (TM-JM) peptides

2.1.1 Peptide synthesis

The wild-type human TpoR TM-JM peptide (E488 to W529) and the mutant peptides containing either S505N, W515K, W515K/Q516K, or R514A/W515A were synthesized using solid-phase methods at the W.M. Keck Peptide Synthesis Facility at Yale University (**Figure 2.1**). The mutant TpoR TM-JM peptide containing R514W/W515K was synthesized using the same method by Takeshi Sato at Osaka University (**Figure 2.1**). Three arginine residues were added at the N-terminus of human TpoR TM-JM peptides to increase the solubility of the peptides and to prevent protein aggregation, such as head-to-tail non-specific binding. Deuterated (5,5,5-d3) leucine and deuterium depleted water were obtained from Cambridge Isotope Laboratories. Solid-phase synthesis for hydrophobic peptides has been described previously (*97, 98*).

Figure 2.1: Synthetic TpoR TM-JM peptides used in this study. All synthesized peptides except W515A/Q516W cover the TpoR amino acid sequence from E488 to W529 and are fused to three arginine residues at their N-termini to increase peptide solubility. The W515A/Q516W mutant peptide contains the sequence from T481 to H520. Putative TM domains and the RWQFP motif are highlighted in blue and red, respectively. Mutated residues are highlighted in green.

2.1.2 Synthetic peptide purification

Crude peptides from solid-state synthesis were purified using reverse-phase HPLC, which is a widely-used technique for purifying hydrophobic peptides (*99*). Around 5 mg of crude peptides were dissolved in TFE and loaded onto a C4 reversed-phase semi-preparatory HPLC column (Higgins Analytical). The C4 reverse phase column was equilibrated with 30% solvent A (12% acetonitrile, 18% isopropanol, and 0.1% TFA) and 70% solvent B (40% acetonitrile, 60% isopropanol, and 0.1% TFA). Peptide was eluted using a linear concentration gradient of solvent B (from 95%) over 45 minutes at a flow rate of 2.5–3 mL/min. The HPLC trace was monitored by the optical absorbance at 220 nm and 280 nm. Peptide peaks were collected and checked by mass spectrometry for purity. Typically, the yield of pure peptides per crude peptide weight is ~10–20% with a C4 column (*97*). Pure peptides were lyophilized and stored at −80 ºC until further experiments, such as reconstitution into detergent micelles or lipid bilayers.

2.2 Recombinant TpoR TM-JM peptides

2.2.1 Peptide expression in bacteria

The DNA constructs for the wild-type and various mutants of the human and murine TpoR were provided by Dr. Stefan Constantinescu. The TM-JM region (i.e., T481 to H520) of the TpoR

sequence was PCR-amplified and inserted into the ligation-independent cloning (LIC) site of the His-MBP-TEV expression vector, which was obtained from Dr. Tim Cross (*100, 101*). Five TpoR TM-JM fusion constructs (wild-type, W515K, W515K/Q516K, R514W/W515K, and W515A/Q516W) were generated (**Figure 2.2**). All of the plasmid constructs were verified by sequencing.

```
Wild-type     481 TRVETATETAWISLVTALHLVLGLSAVLGLLLLRWQFPAH 520
W515K         481 TRVETATETAWISLVTALHLVLGLSAVLGLLLLRKQFPAH 520
W515K/Q516W   481 TRVETATETAWISLVTALHLVLGLSAVLGLLLLRKWFPAH 520
R514W/W515K   481 TRVETATETAWISLVTALHLVLGLSAVLGLLLLWKQFPAH 520
W515A/Q516W   481 TRVETATETAWISLVTALHLVLGLSAVLGLLLLRAWFPAH 520
```

Figure 2.2: Recombinant TpoR TM-JM peptides used in this study. All recombinant peptides cover the TpoR amino acid sequence from T481 to H520. Note that three non-native amino acid residues (SNA) derived from the linker sequence remain attached to the N-terminus of the recombinant peptide after cleavage of an N-terminal His-MBP (maltose binding protein) tag. Putative TM domains and the RWQFP motif are highlighted in blue and red, respectively. Mutated residues are highlighted in green.

The TpoR TM-JM fusion protein constructs were then introduced into chemically competent *Escherichia coli* BL21(DE3) cells. Transformed *E. coli* cells were incubated in 25 mL of LB broth containing 100 μg/ml ampicillin overnight at 37 °C. Cells were harvested by centrifugation at 6,000 x g for 20 minutes at 4 °C. Harvested cells were washed with M9 medium twice, and resuspended with 10 mL of M9 medium after the centrifugation. Resuspended cells were grown at 37 °C with shaking (200 rpm) for approximately 6 hrs until the optical absorbance at 600 nm (A_{600}) reached 0.5–0.6. Then, isopropyl β-D-1-thiogalactopyranoside (IPTG) was added into the cell culture to a final concentration of 0.4 mM, and the cells were grown overnight (12–16 hrs) at 23 °C to induce protein expression. Cells were harvested by centrifugation at 4,000 x g for 30 min at 4 °C. Cells were resuspended in 10 mL of binding buffer (20 mM Tris-HCl, 500 mM NaCl, 5 mM imidazole, pH 8.0) and frozen at – 20 °C until ready for extraction.

2.2.2 Recombinant peptide purification

Purification of the His-MBP TpoR TM-JM fusion protein was done using the Ni-NTA agarose method. Frozen resuspended cells were thawed by incubating in a water bath at 37 °C for 15 min and lysed using 2 µl benzonase (Novagen) and a French press. Lysates were centrifuged at 25,000 x g for 25 min at 4 °C and incubated with 200 mg of n-octyl-β -D-glucopyranosid (β-OG) (Sigma-Aldrich) for 5 min at room temperature. This lysate-detergent mixture and 20 mL of 50% Ni-NTA agarose slurry (10 mL bed volume), which was pre-equilibrated with 100 to 150 mL binding buffer, were loaded into a Ni-NTA agarose column (QIAGEN) and mixed by nutating overnight at 4 °C. After the flow-through was collected by gravity flow, 160 mL washing buffer (20 mM Tris-HCl, 500 mM NaCl, 50 mM imidazole, pH 8.0) was loaded onto the column (40 mL at a time) to remove non-specific binding proteins. Fusion proteins were eluted in 1 mL of elution buffer (20 mM Tris-HCl, 500 mM NaCl, 500 mM imidazole, pH8.0) several times until the A_{280} reached 0.05. Elution fractions with an A_{280} of > 0.1 were collected (50–60 mL total volume). Protein yields were typically 100–120 mg/L. The flow-through, all washes and eluted fractions were analyzed using 15 or 18% SDS-PAGE gels.

In the next step, the His-MBP tag was removed from the TpoR TM-JM fusion protein by the Tobacco Etch Virus (TEV) protease. Briefly, N-dodecyl-β-D-maltoside (DDM) (Sigma-Aldrich) was added to elutants to a final concentration of 0.2% (w/v). Approximately, 50–60 mL (~0.2 mg/mL) of His-tagged TEV protease was added to the elutants at a 1:1 (v/v) ratio and nutated for 32–40 hrs at room temperature to cleave the His-MBP off from the TpoR TM-JM peptide. The cleavage was verified using 15 or 18% SDS-PAGE gels. His-tagged TEV protease was expressed in BL21(DE3) and purified using the same purification steps as described for the

TpoR TM-JM peptide without any detergents. Elutants and sterilized glycerol were mixed in a 1:1 (v/v) ratio. In addition, dithiothrietol (DTT) and ethylenediamine tetraacetic acid (EDTA) were added to final concentrations of 5 mM and 1 mM, respectively. The yield for the TEV protease was typically 17–22 mg/L culture.

Further purification was done to remove the His-MBP tag and His-TEV as well as uncleaved His-MBP-TpoR TM-JM peptides. After the TEV protease cleavage, all proteins were precipitated by 6% (w/v) trichloroacetic acid (TCA). Precipitates were collected by centrifugation at 9,000 x g for 20 min at 4 °C. After two washes with ddH_2O, precipitates were lyophilized overnight.

As a final purification step, organic extraction was performed to extract only TpoR TM-JM peptide. Lyophilized proteins were rehydrated with 10 mL methanol-chloroform solution (9:1, v/v) for 2 hrs at room temperature with nutating. Supernatants were filtered through 0.2 μm PTEE syringe filter to remove TCA precipitates. The filtered sample was dialyzed against 2 changes of 2 L methanol-chroloform solution (9:1, v/v) to remove any residual glycerol and immidazole from TEV cleavage and TCA precipitation steps. The purity was verified by 18% SDS-PAGE gels and mass-spectrometry. Final peptide concentrations were calculated based on the A_{280} and the molar extinction coefficient using Beer's Law ($A=\varepsilon bc$). Typical yields of the TpoR TM-JM peptide were 1–2 mg/L.

2.3 Reconstitution of the TpoR TM-JM peptides

2.3.1 Reconstitution of peptides in detergent micelles

Membrane protein sample reconstitution in detergent micelles for sedimentation equilibrium analytical ultracentrifugation (SE-AUC) was based on the protocol provided in Kochendoerfer *et al.* and Sulistjo *et al.* (*102, 103*). Synthesized TpoR TM-JM peptides were dissolved in hexafluoroisopropanol (HFIP) or TFE. For the recombinant TM-JM peptides, samples that were subjected to organic extraction were purified using HPLC and lyophilized to obtain pure peptide powder. Then, pure peptides were dissolved in HFIP or TFE. Three different peptide concentrations were prepared based on the optical absorbance (A_{280} = ~0.3, ~0.5 and ~0.8). Dodecylphosphocholine (DPC) (Anatrace) was dissolved in 100 µl water to a final concentration of 15 mM and added drop-wise to 150 µl of peptide solutions. Additional 0.4–0.5 mL of water was added to the DPC-peptide mixture drop-wise while stirring the sample until the detergent bubbles do not immediately pop after sample agitation. Samples were frozen and lyophilized under the same conditions as the NMR sample preparation. Lyophilized samples were rehydrated with 150 µl of Tris buffer (50 mM Tris-HCl, 0.1 M NaCl pH 7.5) containing 52.5% D_2O, which achieves density match for accounting the buoyancy of DPC micelles (*103*). Sample concentrations were calculated based on the A_{280} and the molar extinction coefficient using Beer's Law ($A=\varepsilon bc$). Typically, the concentration ranged from ~15 µM to 100 µM.

2.3.2 Reconstitution of peptides in lipid bilayers

Two kinds of lipids, 1,2-Dimyristoyl-sn-glycero-3-phosphocholine (DMPC) and 1,2-Dimyristoyl-sn-glycero-3-phosphoglycerol (DMPG) (Avanti Polar Lipids), were mixed in 2 mL

of HFIP at a ratio of 10:3 (w/w). Then, a detergent, β-OG, was added to a final concentration of 5–10% (v/w) in the lipid mixture. Lipid-detergent mixture was frozen by liquid nitrogen and lyophilized overnight. Dried samples were rehydrated by 1 mL of water. Approximately, 5 mg (~1–2 μmol) pure synthesized peptides were dissolved in 1 mL of HFIP or TFE. Lipid-detergent solution was added to the peptide solution at a lipid/peptide molar ratio of 50:1. In addition, typically, 2–3 mL of water was added to lipid-detergent-peptide solution while stirring until bubbles form. Protein-lipid mixtures were frozen and further lyophilized. Lyophilized samples were rehydrated with 4 mL of phosphate buffer (10 mM phosphate, 50 mM NaCl pH7.0). Rehydrated samples were dialyzed ~5–8 times against 2 L of phosphate buffer over 48 hrs (*104*). A fraction of the dialyzed samples (100 μl, ~200–400 μM) was analyzed by Fourier transform infrared (FTIR) spectroscopy. The rest of the dialyzed samples were centrifuged at 228,556 x g for 1 hr at 4 °C. Pellets were lyophilized and rehydrated with 50% weight deuterium depleted water (Cambridge Isotope Laboratories) overnight at 37 °C.

2.4 Sedimentation equilibrium a nalytical ultracentrifugation (SE-AUC)

SE-AUC experiments were performed using a Beckman XL-I analytical ultracentrifuge. Absorbance at 280 nm was measured radially across the centrifuge cell. Data points were collected in radial increments of 0.001 cm, with each data point representing the average of 10 replicates. Three different peptide concentrations (ranging from ~15 μM to 100 μM) were used to improve the quality of the data. Each peptide sample was separated into its potential oligomeric states by centrifugation at 35k, 40k, or 48k rpm for 20–24 hrs. All the data were

analyzed by non-linear least-squares global curve fitting using the *UltraScanII* (version 9.9) data analysis software developed by B. Demeler (http://www.ultrascan.uthscsa.edu/). The analysis software can fit the experimental data to different functional models, such as a single component fit (**Figure 2.3A**) and a monomer-dimer equilibrium fit (**Figure 2.3B**), to calculate thermodynamic properties of peptide samples. The analysis uses the solvent density $\rho = 1.0580$ and the partial specific volume of the wild-type TpoR (0.7645 cm^3/g) and mutants at 20 °C as calculated by SEDNTERP software for input (*105*).

Single component model

$$= exp\left[\left(\ln(A)+M\omega^2(1-vbarD)\frac{(X^2-X_r^2)}{(2RT)}\right)\right]+B$$

Monomer − Dimer equilibrium model

$$= exp\left[\left(\ln(A)+M\omega^2(1-vbarD)\frac{(X^2-X_r^2)}{(2RT)}\right)\right]$$
$$+ exp\left[\left(2\ln(A)+\ln\left(\frac{2}{el}\right)+\ln(K1,2)+2M\omega^2(1-vbarD)\frac{(X^2-X_r^2)}{(2RT)}\right)\right]+B$$

Figure 2.3: Single component and monomer-dimer equilibrium models for SE-AUC analyses. Two exponential functions were used to analyze the experimental data. X = radius, Xr = reference radius, A = amplitude, e = extinction coefficient, M = molecular weight, l = path length, K1 = monomer-dimer equilibrium constant, D = density, R = gas constant, T = temperature, B = baseline

2.5 Polarized attenuated total reflection (ATR) Fourier transform infrared (FTIR) analysis

ATR-FTIR spectroscopy was used to monitor two properties of the reconstituted peptide: 1) the secondary structure and 2) the TM orientation (*106*). Parallel and perpendicular polarized light is absorbed in the region of amide I vibration (1600–1690 cm^{-1}) (*107*). The amide I vibration frequency is especially sensitive to the global secondary structure of protein and the orientation of the helix relative to the plane of the membrane (*107*). Frequencies in the 1660-1650 cm^{-1}

region are assigned to α-helices, 1640–1620 cm^{-1} to β-sheets, and 1695-1660 cm^{-1} to β-sheets and β-turns (*107*). Random coil is assigned to broad bands centered at ~1650 cm^{-1} (*107*).

One hundred microliters of the TpoR TM-JM peptides (~200–400 μM) reconstituted in DMPC/DMPG were layered on a germanium internal reflection element using a slow flow of air directed at an oblique angle to the IR plate to form an oriented multilamellar lipid-peptide film. Spectra were obtained using both parallel and perpendicular polarized light. For each polarization, 1000 scans were acquired and averaged at a resolution of 4 cm^{-1}. Typically, a range between ~1695 and 1610 cm^{-1} (α-helix amide I region) was integrated using Bruker OPUS software (version 5.0). The dichroic ratio (R^{ATR}) was obtained as the ratio of the absorption of parallel ($A_{\parallel}$) to that of perpendicular ($A_{\perp}$) polarized light. The TM helix tilt angle was determined by the dichroic ratio and the following equations (**Figure 2.4**). It should be noted that the measurement of the dichroic ratio is also a useful, rapid approach to confirm that TM peptides are properly inserted into the lipid bilayers (*107, 108*).

Solve for θ (helix tilt angle)

$$S_{means} = \frac{E_x^2 - R^{ATR}E_y^2 + E_z^2}{E_x^2 - R^{ATR}E_y^2 - 2E_z^2}$$

$$S_{means} = S_{membrane}\, S_{helix}\, S_{dipole} = S_{membrane} \left[\frac{3\cos^2\theta - 1}{2}\right] S_{dipole}$$

Dicroic ratio

$$R^{ATR} = \frac{A_{||}}{A_{\perp}}$$

Electric field amplitudes

$$E_x^2 = 1.399, \quad E_y^2 = 1.514, \quad E_z^2 = 1.621$$

Order parameters

$$S_{membrane} = 0.9, \quad S_{dipole} = 0.33$$

$$S_{helix} = S_{helix\ angle}\, S_{helix\ order} = \left[\frac{3\cos^2\theta - 1}{2}\right]$$

$$S_{helix\ order} = 1$$

$$S_{helix\ angle} = \left[\frac{3\cos^2\theta - 1}{2}\right]$$

Figure 2.4: Equations to determine a TM helix tilt angle. The dichroic ratio is obtained experimentally. The values used for electric field amplitudes and order parameters are previously described in (*108-110*).

2.6 Deuterium magic angle spinning (MAS) nuclear magnetic resonance (NMR) spectroscopy

The reconstituted peptide samples were packed into 4 mm NMR rotors for solid-state NMR structural analysis. Deuterium MAS NMR was done to obtain structural information of the wild-type TpoR TM-JM and its mutants.

Deuterium MAS NMR spectroscopy can be used to characterize the dynamic properties of membrane proteins (*111, 112*). Combining MAS NMR with selective deuterium isotopic labeling at specific amino acids allows us to probe amino acid side chain motions of

reconstituted proteins in membranes (*113*). Liu *et al.* (*114*) demonstrated in detail how deuterium MAS NMR spectra are correlated with side chain motions in different surfaces of TM helices in membranes. Typically, the methyl groups of aliphatic amino acids (valine, methionine, leucine or isoleucine) were deuterated during sample preparation. With this labeling scheme, amino acids in the dimer interface show a broader lineshape relative to those oriented towards lipids.

Deuterium MAS NMR spectra were obtained at a ^{2}H frequency of 55.26 MHz on 360 MHz or 500 MHz using a Bruker AVANCE spectrometer with a MAS frequency of 3 kHz. A 3–7.5 μsec single 90° pulse was applied, and the data were collected after 4.5 μsec delay. The repetition delay was set to 0.25 sec. A 100 Hz exponential line broadening function was used to process each spectrum, which was averaged of the 600,000–1,500,000 transients. Spectra were acquired at 25 °C.

2.7 Computational simulations

CHI is a computational search program for determining low-energy conformations of helix dimers with improved packing interactions between helices (*115*). Computational searches were carried out on the TpoR TM (I492 to L513) and TpoR TM-JM (I492 to P518) sequences. Input parameters, such as the peptide sequence, the separation between helices, and sampling step size, were defined, and two canonical helices were generated. Each helix was rotated relative to one another from 0° to 360° with a sampling step size of 45° at helix separations of 9.0 Å to 10.5 Å to find low energy conformations of helix dimers. Both right-handed and left-handed conformations were searched. The crossing angles and rotations were variable. Energy minimized conformations were first placed on an initial grid. When there were more than five

structures with a root mean square deviation of 1 Å or less, these conformations can form a "cluster" and the individual minimized structures in each low energy cluster were averaged and re-minimized. The computational search was done under vacuum conditions (dielectric constant ε=1) to mimic the low dielectric environment within the hydrophobic core of bilayer membranes.

2.8 In vivo analyses of the TpoR activation mechanism

2.8.1 Plasmids

Construction of the retroviral vectors pMX-JAK2-IRES-CD4 and pMX-HA-TpoR-IRES-GFP, which harbor the human JAK2 (accession No. O60674) and the human TpoR (accession No. P40238), respectively, has been described (*91, 116*). Retroviral vectors containing a mutant TpoR coding DNA sequence (CDS) were generated by the Quickchange site-directed mutagenesis kit (Stratagene) using pMX-HA-TpoR-IRES-GFP as a template. For dual luciferase reporter assays, the pGRR5-Luc vector (*117*), which expresses the firefly luciferase reporter under the control of the STAT-responsive promoter, was used. This promoter contains five copies of the STAT-responsive element, which is found in the IFN-γ-responsive region (GRR) of the FcγRI gene promoter (*117*). As an internal control, pRL-TK (Promega), which constitutively expresses the *Renilla* luciferase reporter under the control of the thymidine kinase (TK) promoter, was used. For split *Gaussia princeps* luciferase complementation assays, the human TpoR CDS was PCR-amplified and cloned in frame at its C-terminus, eliminating the stop codon, with either the N-terminal half (hGluc1) or C-terminal half (hGluc2) of the *G. princeps* luciferase into the *NotI-ClaI* sites of pcDNA3.1/Zeo vector (Invitrogen), resulting in pcDNA3.1/Zeo-TpoR-hGluc1 and pcDNA3.1/Zeo-TpoR-hGluc2, respectively (*118*). Mutant TpoR CDSs were generated by

the Quickchange site-directed mutagenesis kit (Stratagene) using pcDNA3.1/Zeo-TpoR-hGluc1/2 as a template.

2.8.2 Cell lines

To generate TpoR-expressing stable cell lines, the retroviral vector pMX-HA-TpoR-IRES-GFP (wild-type or mutant) was transfected into the BOSC packaging cell (*119*). The resulting virus supernatants were harvested and used to infect γ-2A cells after 24 hrs of transfection. The γ-2A cell line corresponds to JAK2-deficient human fibrosarcoma cells (*120*). The host cells were co-infected with the pMX-JAK2-IRES-CD4 virus, which was produced in the BOSC packaging cell. Cells that stably express TpoR were selected based on expression levels of the GFP marker by fluorescence-activated cell sorting (FACS). Expression of HA-TpoR was also confirmed by Western blotting with anti-HA antibodies. All of the γ-2A-derived cells were cultured in Dulbecco's modified Eagle medium supplemented with 10% fetal bovine serum and appropriate antibiotics.

2.8.3 Dual luciferase reporter assay

Reporter vectors, pGRR5-Luc and pRL-TK, were transiently co-transfected into TpoR-expressing γ-2A cells using Lipofectamine (Invitrogen) (*116*). Bioluminescence from the firefly luciferase reporter (FF) and the *Renilla* luciferase reporter (RL) were detected by the Victor X light analyzer (Perkin-Elmer) 24 hrs after transfection. The signal intensity of FF was normalized to that of RR.

2.8.4 Split Gaussia princeps luciferase complementation assay

A pair of split luciferase constructs, pcDNA3.1/Zeo-TpoR-hGluc1 and pcDNA3.1/Zeo-TpoR-hGluc2, were transiently co-transfected into HEK293 cells at a 1:1 ratio (1 μg of DNA for each construct) using Lipofectamine (Invitrogen). After 48 hrs of transfection, cells were harvested by centrifugation at 4 ºC for 1 min and lysed by freeze-thaw. Bioluminescence derived from luciferase reconstitution was analyzed using the Victor X light analyzer (Perkin-Elmer).

Chapter 3. Oligomerization status of wild-type TpoR in the absence of the ligand

3.1 Introduction

The key to understanding the TpoR activation mechanism may lie in other Type I-Group 1 cytokine receptors, such as the erythropoietin receptor (EpoR), the growth hormone receptor (GHR), and the prolactin receptor (PRLR). As discussed in detail in Chapter 1.2, studies using various methods, such as Co-IP, FRET, and BRET, demonstrated that GHR, PRLR, and EpoR exist as dimers even in the absence of the ligand binding (i.e., ligand-independent dimers or pre-formed dimers) (*76, 78, 80*). The EpoR, the closest relative of TpoR, has a strong propensity to dimerize through its TM domain (*76, 82, 83*). Similarly, we speculate that the TM domain of TpoR has a propensity to undergo self-interaction. Our analytical ultracentrifugation analysis and deuterium MAS NMR spectroscopy using the TpoR TM-JM peptide showed that, unlike EpoR, the TM domain of the TpoR did not interact with each other in a 1:1 stoichiometric ratio. Furthermore, to analyze the oligomerization state of the full-length TpoR in the absence of Tpo, we performed a *Gaussia princeps* luciferase complementation assay in collaboration with the

laboratory of Stefan Constantinescu. This analysis revealed that, like other Type I-group 1 cytokine receptors, at least some fraction of the full-length TpoR undergoes ligand-independent homodimerization. Together, our data suggest that TpoR may possess a unique dimerization mechanism among the Type I-group 1 cytokine receptor family.

3.2 Results

3.2.1 The TpoR TM-JM peptide does not dimerize in detergent micelles

At least two cytokine Type I-Group 1 receptors, EpoR and GHR, are known to dimerize via their TM-JM domains (*76, 78*). Similarly, the TM-JM domain of TpoR may also contribute to the homodimerization of TpoR. To test this hypothesis, we utilized two approaches: sedimentation equilibrium analytical ultracentrifugation (SE-AUC) and deuterium magic angle spinning (MAS) NMR spectroscopy. For an SE-AUC analysis, we used recombinant or synthetic TM-JM peptides of TpoR (**Figure 3.1**). As a positive control, we used the EpoR TM-JM region, which is known to interact with each other and stabilize the EpoR dimer (*76, 82, 121-123*).

```
Recombinant TM+Box1 481 TRVETATETAWISLVTALHLVLGLSAVLGLLLLRWQFPAHYRRLRHALWPSLPDLHRVLGQY 542
Synthesized         488        ETAWISLVTALHLVLGLSAVLGLLLLRWQFPAHYRRLRHALW                529
```

Figure 3.1: Recombinant and synthetic wild-type TpoR TM-JM peptides used for SE-AUC and deuterium MAS NMR spectroscopy. For the recombinant peptide, the TpoR TM-JM region containing the Box 1 motif was fused to an N-terminal His-MBP (maltose binding protein) tag. The recombinant peptide was expressed in *Escherichia coli* cells and purified using Ni-NTA agarose. After cleavage of the His-MBP tag, the TM-JM peptides were further purified by organic extraction and the subsequent HPLC. Note that three non-native amino acid residues (SNA) derived from the linker sequence remain attached to the N-terminus of the recombinant peptide. For the synthetic peptide, the TpoR TM-JM region (from E488 to W529) was conjugated to an N-terminal tag of three arginine residues to prevent protein aggregation. Putative TM domains and the RWQFP motif are highlighted in blue and red, respectively. The Box 1 motif is indicated in bold black.

The EpoR TM-JM peptides were dissolved in dodecylphosphocholine (DPC) detergent micelles at three different peptide concentrations, and were analyzed by SE-AUC using three

different centrifugation speeds (for details, see Methods). The SE-AUC analysis on the EpoR TM-JM peptide resulted in two kinds of graphs (top and bottom) (**Figure 3.2**). In the bottom graph, the x-axis is a radius across the centrifuge cell and the y-axis is optical density at A_{280}. In the top graph, the x-axis corresponds to the radius across the centrifuge cell and the y-axis shows the distribution of residuals, which indicate how well the experimental data fit to a functional model (evenly distributed residuals around the zero line across the x-axis indicates that the experimental results are consistent with a given functional model). The experimental data of the EpoR TM-JM peptide were analyzed using a monomer-dimer equilibrium model (**Figure 3.2**). The calculated molecular weight (MW) of the EpoR peptide oligomer is 11680 Da, while the MW of the peptide monomer is 5922 Da (**Table 3.1**). This result shows that the TM-JM peptide of EpoR exists as a homodimer in micelles as previously reported (*82*), indicating that our SE-AUC analysis is reliable for detecting TM-TM association.

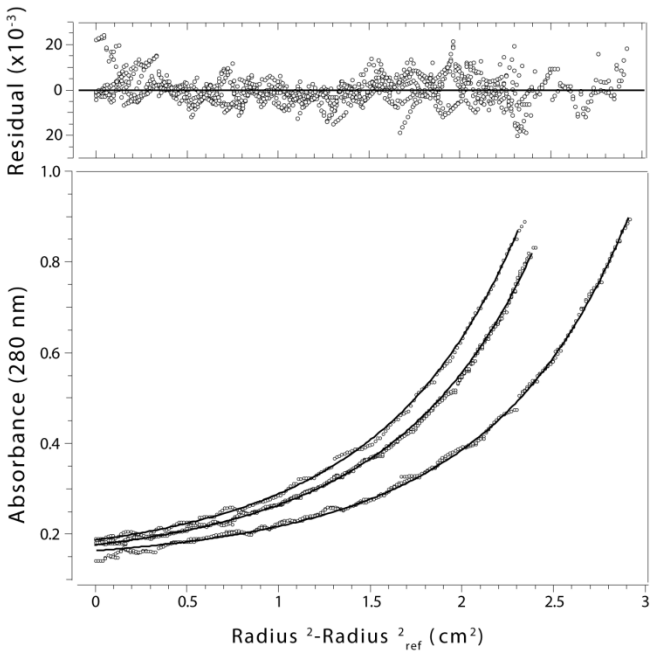

Figure 3.2: The EpoR TM-JM peptide forms homodimers. The bottom graph shows the absorbance profiles at 280 nm when the samples were centrifuged at 40k rpm. Plots derived from three different peptide concentrations (60 μM, 70 μM, and 180 μM) are shown as representative data. DPC detergent (15 mM) was used to solubilize the peptide. The experimental data were analyzed using a monomer-dimer equilibrium model, and the top graph shows how well the experimental data fit the model.

Using the same SE-AUC assay, we analyzed the oligomeric state of the synthetic TpoR TM-JM peptide lacking the Box 1 motif (**Figure 3.1**) in DPC micelles. The experimental data of the synthetic TpoR TM-JM peptide were analyzed using a single component model (**Figure 3.3**). Based on this model and the obtained SE-AUC spectrum, the MW of the predominant form of the peptide was calculated to be 6,960 Da (**Figure 3.3**, **Table 3.1**). Considering that the MWs of the monomeric and dimeric TpoR TM-JM peptides are 5,360 Da and 10,720 Da, respectively, our result indicate that the TM-JM domain of TpoR does not have a strong propensity to undergo dimerization.

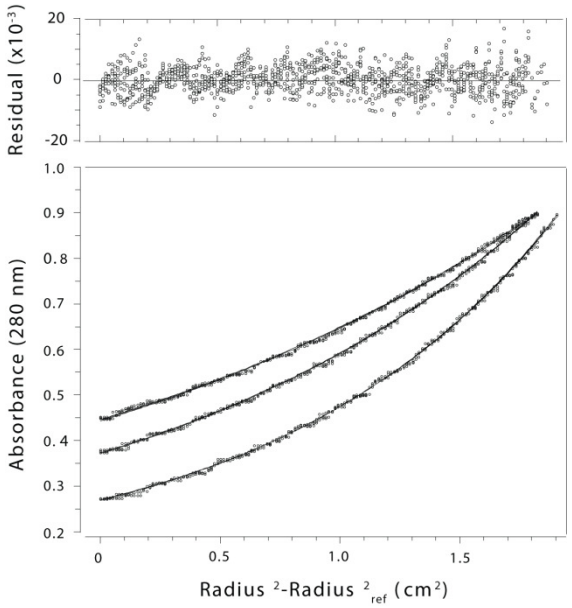

Figure 3.3: The TpoR TM-JM peptide lacking the Box 1 motif does not form a homodimer in DPC micelles. The bottom graph shows the absorbance profiles at 280 nm when the samples were centrifuged at 35k, 40k, and 48k rpm. Plots derived from one peptide concentration (35 μM) are shown as representative data. DPC detergent (15 mM) was used to solubilize the peptide. The experimental data were analyzed using a single component model, and the top graph shows how well the experimental data fit the model.

Similarly, the single component model predicted that the recombinant TM-JM peptide containing the Box 1 motif (**Figure 3.1**) does not interact with each other (**Figure 3.4**). After centrifugation, the TpoR TM-JM peptides were found mostly in a fraction with an estimated MW of 7,500 Da, which is very close to the MW of the peptide monomer (7,400 Da) (**Table 3.1**). Together, our data suggest that, unlike EpoR, TpoR does not form ligand-independent TM-TM interactions.

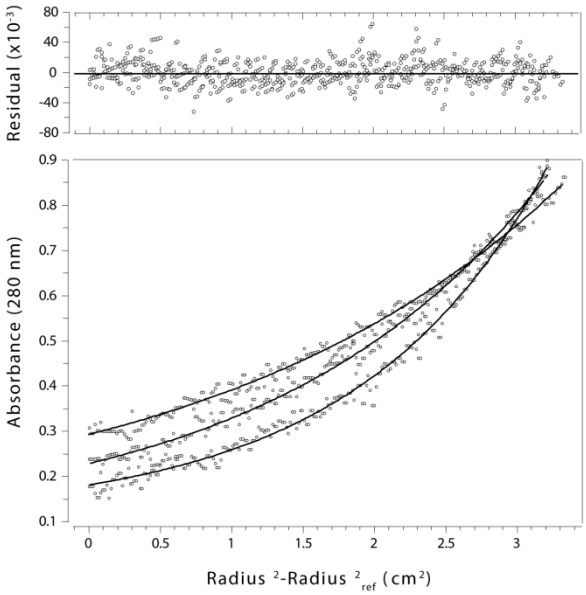

Figure 3.4: The TpoR TM-JM peptide containing the Box 1 motif does not form a homodimer in DPC micelles. The bottom graph shows the absorbance profiles at 280 nm when the samples were centrifuged at 35k and 40k rpm. Plots derived from one peptide concentration (48 μM) are shown as representative data. Fifteen mM DPC detergent was used to solubilize the peptide. The experimental data were analyzed using a single component model, and the top graph shows how well the experimental data fit the model.

Table 3.1: Summary of SE-AUC analysis.

	MW	MW (fit)
EpoR TM-JM	5922	11680
TpoR TM-JM	5360	6960
TpoR TM-Box1	7400	7519

3.2.2 The TpoR TM-JM peptide does not dimerize in lipid bilayers

The SE-AUC analyses demonstrated that the TM-JM peptide of TpoR favors a monomeric state. However, we cannot exclude the possibility that the DPC micelles used in this assay may hinder stable TM-TM dimerization. Thus, we next utilized deuterium MAS NMR spectroscopy and examined the oligomerization status of the TpoR TM-JM domain within synthetic lipid bilayer membranes, which more closely mimic natural cell membranes. In this analysis, we deuterated the methyl group of the leucine residue at positions 510, 511, 512 or 513 of the synthetic TpoR

TM-JM peptide. As a control, we also deuterated the methyl group of the leucine residue at positions 239, 240, or 241 of the synthetic EpoR TM-JM peptide. Each deuterated peptide was reconstituted into 1,2-dimyristoyl-*sn*-glycero-3-phosphocholine (DMPC), 1,2-dimyristoyl-*sn*-glycero-3-[phospho-rac-(1-glycerol)] (DMPG) lipid bilayers at a lipid/peptide molar ratio of 50:1. We chose this molar ratio because this ratio has been experimentally shown to prevent non-specific peptide aggregation (*106*). Then, the potential oligomeric states of each TM peptide were determined by deuterium MAS NMR spectroscopy. Deuterium MAS NMR has been a useful method for characterizing dynamic properties of membrane proteins (*113*). The basis of this method is that the methyl groups of aliphatic amino acids (i.e., valine, methionine, leucine, and isoleucine) are sensitive to molecular motion. Deuteration of such methyl groups and the following NMR analysis result in a deuterium line shape that reflects the molecular motion of the peptide sample. In general, any local environmental changes around the deuterated methyl group affect the resultant deuterium line shape. For instance, when a TM-JM peptide forms a homodimer, the motion of the site-specific methyl-deuterated leucine in the peptide is restricted, giving rise to an increase in the overall width of the deuterium MAS side band pattern. **Figure 3.5** shows the deuterium MAS NMR spectra of the wild-type TpoR TM-JM peptide and the EpoR TM-JM peptide. The x-axis is the frequency between 20 kHz to -20 kHz, where the quadruple splitting of rapid methyl rotation can be observed. An intense peak at zero frequency is residual water (HDO) peak. Consistent with the SE-AUC result, the EpoR TM-JM peptide gave rise to characteristic deuterium line shapes with a rotational side band pattern, the indication of TM-TM association (**Figure 3.5B**). On the other hand, we did not detect the rotational side band pattern from the TpoR TM-JM peptide (**Figure 3.5C**). This complete

absence of the rotational side band pattern is unusual. One possible explanation for this phenomenon is that the rotational motion of the peptide occurs on the time scale of MAS, and thus interferes with averaging by MAS. To test this idea, it is possible to slow the rotational motion of the peptide by lowering the temperature of the sample. As **Figure 3.6** shows, a distinctive pattern of rotational side bands appeared in the NMR spectra of the TpoR TM-JM peptide when the experiments were done at low temperatures (288K and 273K) that reduce the mobility of the surrounding lipids and, hence, the embedded TM peptide. Thus, the absence of the MAS side bands in the TpoR sample (**Figure 3.5C**) demonstrates that the TpoR TM-JM peptide does not undergo dimerization in lipid bilayers.

(A) EpoR: 221-RDLDP**LILTLSLILVLIS**LLL**TVLALL**SHRRTLQQKIWPC-260
TpoR: 488-ETA**WISLVTALHLVLGLSAVLG**LLLL**R**WQFPAHYRRLRHALW-529

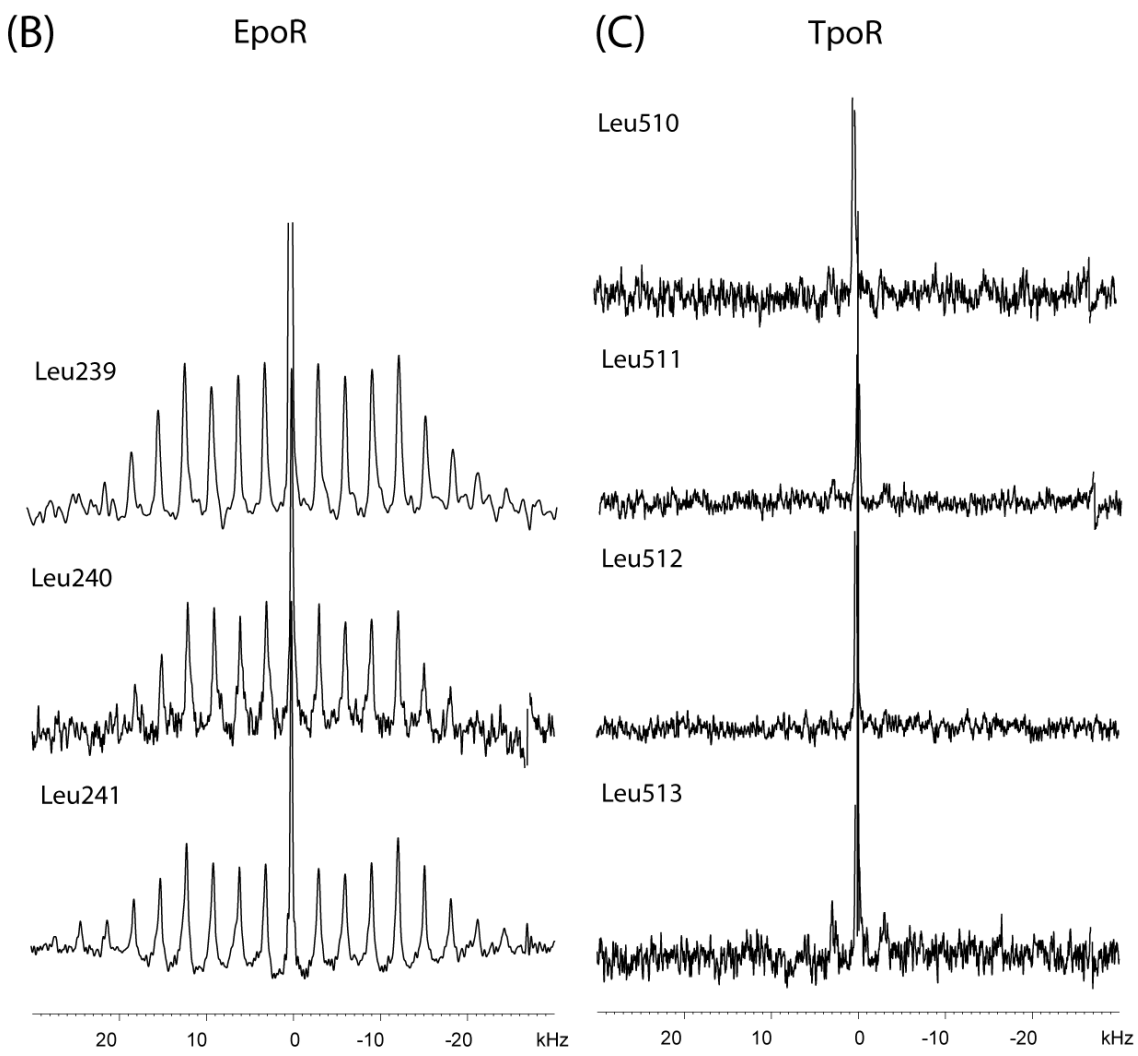

Figure 3.5: Deuterium MAS NMR of TpoR and EpoR. (A) The wild-type EpoR and TpoR TM-JM peptides used in deuterium MAS NMR spectroscopy. The predicted TM domains are highlighted in blue. Leucine residues deuterated in this study are underlined. The TM-JM peptides of TpoR and EpoR were reconstituted in DMPC:DMPG and DMPC lipid bilayer membranes, respectively. The NMR spectra were obtained using single pulse excitation at a deuterium frequency of 55.26 MHz with a spinning speed of 3 kHz. Each spectrum represents the average of the 600,000-1,500,000 transients. Spectra were obtained at 25 °C. The sharp peak at 0 frequency is residual deuterated water in the sample. (B) Deuterium MAS NMR spectra of the EpoR TM-JM peptide. (C) Deuterium MAS NMR spectra of the TpoR TM-JM peptide.

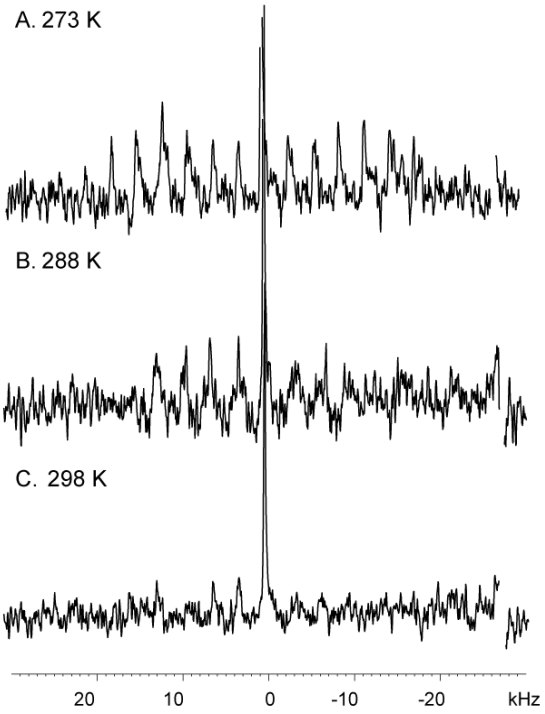

Figure 3.6: Lowering temperature of the sample restricted the rapid methyl rotational motion. Deuterium MAS NMR was performed on the TpoR TM-JM peptide in which the methyl group of the leucine residue at position 512 was deuterated. A series of different temperatures, 298K, 288K, and 273K were used to modulate the lipid rigidity. As the temperature decreased, spinning side bands appeared, suggesting that the rotational motion was exactly at the time scale of MAS at 298K.

3.2.3 The full-length wild-type TpoR forms a pre-formed dimer in vivo

To investigate whether the full-length TpoR can also dimerize *in vivo*, we used a split *Gaussia princeps* luciferase complementation assay. In this assay, the full-length TpoR was fused to either the N-terminal (hGluc1) or C- terminal (hGluc2) fragment of the *G. princeps* luciferase (**Figure 3.7A**). Interaction between TpoR-hGluc1 and TpoR-hGluc2 in HEK293 cells is expected to bring the two luciferase fragments within proximity and reconstitute the luciferase reporter.

As shown in **Figure 3.7B**, co-expression of TpoR-hGluc1 and TpoR-hGluc2 in HEK293 cells led to reconstitution of the luciferase even in the absence of Tpo, giving rise to bioluminescence. On the other hand, almost no luminescence was detected when only TpoR-hGluc-1 or TpoR-hGluc-2 alone was expressed. Thus, as is the case for other cytokine Type I-Group 1 receptors, at least some fraction of the wild-type TpoR is likely to form a pre-formed dimer.

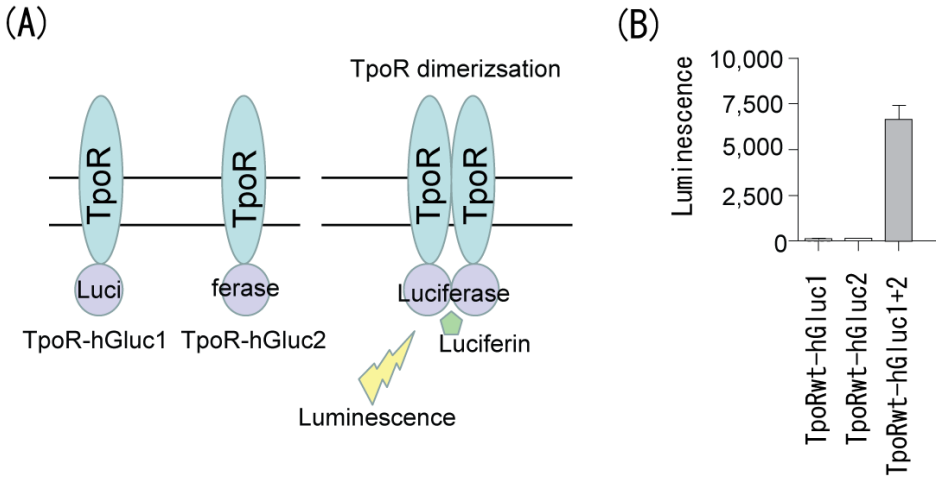

Figure 3.7: The full-length TpoR can form a dimer in the absence of the ligand. (A) Schematic diagram of the split *Gaussia princeps* luciferase complementation assay. The N-terminal half (hGluc1) or C-terminal half (hGluc2) of the *G. princeps* luciferase was fused to the C-terminus of TpoR. The resultant TpoR-hGluc1 and TpoR-hGluc2 were co-expressed in HEK293 cells, and the dimerization was detected by bioluminescence derived from the chemical reaction mediated by the reconstituted luciferase and its substrate, luciferin. (B) The full-length TpoR can dimerize in *vivo*. Co-expression of TpoR-hGluc1 and TpoR-hGluc2 resulted in emission of bioluminescence. Expression of TpoR-hGluc1 or TpoR-hGluc2 alone was used as a negative control. This experiment was carried out by Dr. Vitalina Gryshkova.

3.3 Discussion

Type I-Group 1 cytokine receptors, such as EpoR, GHR, and PRLR, form ligand-independent dimers. In the case of EpoR, receptor dimerization is mediated by its TM domain. However, our SE-AUC and deuterium MAS NMR analyses revealed that the TM domain of TpoR cannot interact with each other. Using the *G. princeps* luciferase complementation assay, we showed that the full-length wild-type TpoR can undergo dimerization in a ligand-independent manner *in*

vivo (**Figure 3.7**). However, it should be noted that this ligand-independent dimerization of TpoR was relatively weak compared with that of EpoR (approximately 2.5-3 fold weaker, unpublished observations). This weak dimerization may be due to the lack of a TM-TM interaction in the TpoR dimer.

Based on these observations, we refine the ligand-independent receptor dimerization model, one of the two proposed models for the TpoR activation mechanism (**Figure 1.10A**). In the refined model (**Figure 3.8A**), at least some fraction of TpoR forms a ligand-independent dimer, the dimerization of which may be mediated by the EC or IC domain instead of the TM domain. A TM-TM interaction within a TpoR dimer does not occur in the absence of Tpo. However, binding of Tpo to TpoR induces an internal conformational change in the receptor dimer, leading to a TM-TM interaction. This specific receptor conformation in turn reorients the TpoR-associated kinase JAK2 into an active position, resulting in activation of the JAK2-STAT signaling pathway (**Figure 3.8**). Our model predicts that the TpoR TM domain plays a critical role not only in the receptor activation, but also in maintenance of the inactive receptor state.

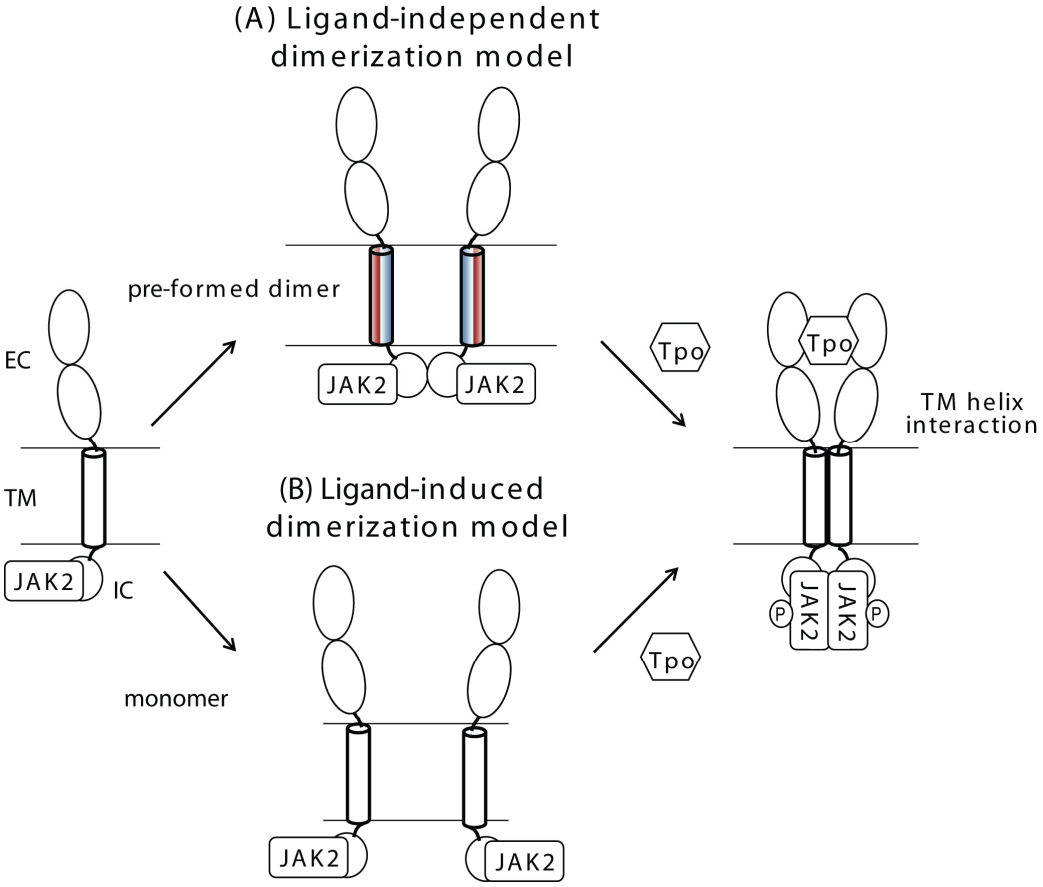

Figure 3.8: Revised models for the TpoR activation mechanisms. (A) Ligand-independent dimerization of TpoR may be mediated by an interaction between two extracellular (EC) domains or between two intracellular (IC) domains. In this pre-formed dimer, the TM domains do not interact with each other. In this schematic model, the IC domain-mediated dimerization is shown as an example. (B) Ligand-induced dimerization model, which was explained in **Figure 1.10**, is still valid because this model does not require the TM-TM interaction. In either ligand-independent dimerization (A) or ligand-induced dimerization (B) models, binding of the ligand, Tpo, to the EC domains induces an internal structural rearrangement in the receptor dimer, leading to a TM-TM interaction. This specific receptor conformation in turn reorients the JAK2 into an active position, resulting in activation of the JAK2-STAT signaling transduction.

The question is, however, how the pre-formed TpoR dimer can be stabilized. Because the TpoR TM domain does not seem to be involved in the dimer stabilization, either the EC or IC domain should fulfill this role. Although the IC domains have never been implicated for dimerization of any Type I-Group 1 cytokine receptor, several studies on the epidermal growth factor receptor (EGFR), a single-pass transmembrane receptor, revealed the importance of the IC domain for ligand-independent EGFR dimerization (*124-126*). For example, Co-IP experiments

showed that a truncated EGFR lacking its EC domain can still form a dimer with a full-length EGFR (*125*). Furthermore, a chimeric EGFR with its IC domain replaced by that of EpoR was unable to undergo self-interaction in the absence of the ligand, suggesting that the intact IC domain is necessary for the EGFR dimerization. Consistent with this notion, a crystal structure of an inactive EGFR dimer showed that the two IC domains interact with each other in a symmetric manner within an EGFR dimer (*126*). Similarly, TpoR may dimerize via its IC domain, resulting in a pre-formed dimer.

However, we cannot exclude the possibility that ligand-independent dimerization of TpoR is mediated by its EC domain. A study using Co-IP revealed that the wild-type GHR as well as a chimeric GHR with its TM domain replaced by that of the low-density lipoprotein receptor (LDLR) can interact with the GHR mutant lacking its IC domain, suggesting that neither the TM domain nor the IC domain is required for the GHR dimerization (*79*). Another study using a series of truncated EC domains of the vascular endothelial growth factor receptor FLT-1 (VEGFR-1) showed that the fourth immunoglobulin-like loop in the EC domain is critical for mediating the receptor dimerization (*127*). By analogy, the EC domain might play a role in the TpoR dimer formation. It is also possible that both the EC and IC domains cooperatively facilitate the ligand-independent TpoR dimerization. To examine these possibilities, further analyses, such as a domain-swapping study, will be needed.

Our data revealed a striking difference between TpoR and EpoR in terms of the dimerization mechanism even though these two receptors share the highest sequence homology among the Type I-Group 1 cytokine receptor family (*3*). It is well known that the TM domain of EpoR possesses a strong propensity for self-interaction (*82*). Within a pre-formed EpoR dimer,

two TM α helices most likely form a left-handed coiled coil (LHCC) **(Figure 3.9)** (*86, 128-130*). Although the canonical pitch of a standard α helix is 3.6 residues per turn, the number of residues per turn in the helical region that constitutes the interaction interface of a LHCC structure is reduced to 3.5. As a result, the pattern of side chain interactions between the two intertwined helices repeats exactly every seven residues. This repetitive sequence with a period of seven residues is called a heptad repeat, and is usually labeled as "*a*–*g*". In such a dimerization interface, two residues that are separated by three residues (e.g., positions *a* and *d*) are always located at the same molecular surface of the α helix (**Figure 3.9**) (*131*). In the case of the TM helices in a EpoR dimer, such a LHCC structure positions small amino acid residues (serine, alanine, and threonine) at the same molecular surface of each α helix (**Figure 3.9**). These small amino acids may be essential for a stable TM-TM interaction within a pre-formed EpoR dimer because at least serine and threonine residues are known to contribute to the tight packing of LHCC dimers (*132*). Consistent with this notion, the study using the Put3 system predicted that the TM surface comprised of those small residues is favored as the TM-TM interaction interface of the inactive EpoR dimer (*86*). More recently, a study using solution NMR spectroscopy showed that the TM dimer interface of the murine EpoR is comprised of S231, V235, S238, T242, and A245 (Brett et al., unpublished data).

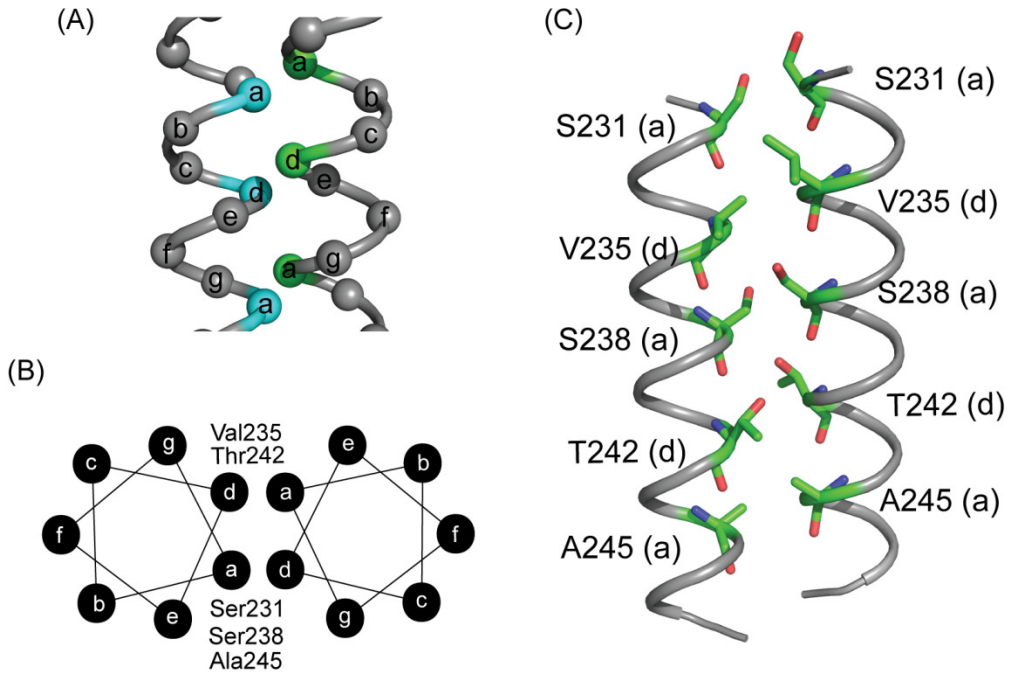

Figure 3.9: Schematic overview of a LHCC structure comprised of two TM helices of EpoR. (A) Side view of the interaction interface of a LHCC structure. Amino acid residues that constitute heptad repeats are labeled as "*a*–*g*". In this figure, residues at positions *a* and *d* are located within the dimerization interface. (B) Helical-wheel diagram of the LHCC comprised of two EpoR TM helices. Ser231, Ser238, and Ala245 are located at position *a*, while Val235 and Thr242 are located at position *d*. (C) The lowest energy structure of an EpoR TM dimer based on a CHI simulation. The simulation suggests that small residues, such as alanine, serine, and threonine, line the TM-TM interaction interface.

On the other hand, our SE-AUC and deuterium MAS NMR analyses suggest that the TM domain of TpoR is not likely to interact with each other. Why does not the TpoR TM domain undergo self-interaction? A possible explanation is that the amino acid sequence of the TpoR TM helix may not be suitable for formation of a TM-TM interaction interface. A comparison between the predicted TM sequence of EpoR and that of TpoR shows that the TpoR TM domain contains not only small amino acids, but also long-side chain amino acids, such as leucine (**Figure 3.10**). As a result, at least two long-side chain amino acids are always located at any possible TM dimer interface (i.e., positions *a*–*d*).

EpoR	226	227	228	229	230	231	232	233	234	235	236	237	238	239	240	241	242	243	244	245	246	247
	LEU	ILE	LEU	THR	LEU	**SER**	LEU	ILE	LEU	**VAL**	LEU	ILE	**SER**	LEU	LEU	LEU	**THR**	VAL	LEU	**ALA**	LEU	LEU
TpoR	492	493	494	495	496	497	498	499	500	501	502	503	504	505	506	507	508	509	510	511	512	513
	ILE	SER	LEU	VAL	THR	**ALA**	LEU	HIS	LEU	**VAL**	VAL	GLY	**GLY**	SER	ALA	VAL	**LEU**	GLY	LEU	**LEU**	LEU	LEU

Figure 3.10: Side-by-side sequence comparison between the EpoR and TpoR TM domains. Residues highlighted in red represent one of the potential TM dimer interfaces. Note that a TpoR TM dimer interface contains leucine (long-side chain amino acid), which may inhibit TM-TM interaction.

Furthermore, a computational simulation predicted a hypothetical LHCC composed of two TpoR TM helices in their the lowest energy state and revealed that its interaction surface contains bulky and long side chain residues, such as histidine and leucine (**Figure 3.11**) (*91*). The molecular nature of this potential interaction surface, which is certainly not small residue-rich, may be the reason why the TpoR TM domains do not possess a strong affinity for self-interaction.

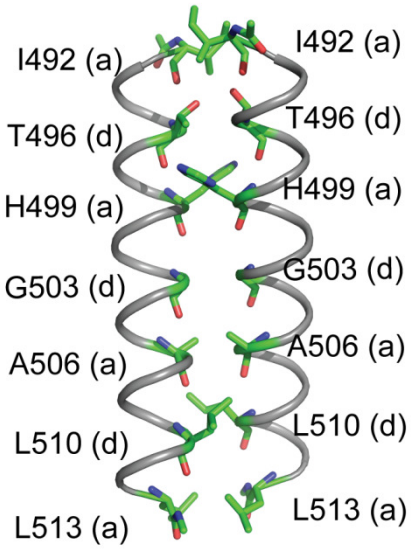

Figure 3.11: The TpoR TM dimer interface predicted by a CHI simulation. A computational search for the lowest energy dimer structures of the TpoR TM region (Ile492 to Leu513) was performed using with variable distances between two TM helices (9.5 Å to 10.5 Å). Regardless of the interface distance used in the simulation, the lowest energy TpoR TM dimer structure was the same, and this structure locates long and bulky side chain amino acids, such as leucine and histidine, in the dimer interface. The residues in the dimer interface are indicated as (a) and (d).

Alternatively, the RWQFP motif (KWQFP in murine), which resides just below the TM domain of TpoR, may play a critical role in inhibition of a TM-TM interaction. It has been shown that deletion of this TpoR-specific motif induces activation of downstream signaling by possibly stabilizing the TM-TM association in the receptor dimer (*91, 96, 133*) Thus, the RWQFP motif may function as a "gimmick" that keeps the two TM helices apart in a TpoR dimer. We will further discuss the roles of the RWQFP motif in Chapter 5.

Most single-pass transmembrane receptors have long been thought to undergo dimerization upon ligand perception (*134, 135*). However, this ligand-induced dimerization model cannot fully explain the activation mechanism of several receptors. For example, Type I-Group 1 cytokine receptors, including EpoR, GHR, and PRLR, already exist as pre-formed dimers even in the absence of ligand binding (*76, 78, 80*). Thus, another type of regulation, rather than ligand-induced dimerization, is required to modulate the activity of these receptors. Is this ligand-independent receptor dimerization only unique to certain receptors, or more general among single-pass transmembrane receptors? Although the ligand-independent dimerization of TpoR was relatively weak, this receptor may serve as a good model to decipher the complexity of the receptor activation mechanisms. In the following chapters, we will focus on several clinically relevant mutations of TpoR and discuss a more detailed molecular mechanism underlying the TpoR activation.

3.4 Conclusion

- TpoR can form a ligand-independent dimer.
- Unlike EpoR, the TM domain of TpoR does not have a strong propensity to self-interact.
- The role of the TpoR TM domain in the receptor activity control is different from that of the EpoR TM domain.

Chapter 4. TM-TM interaction regulates the TpoR activity

4.1 Introduction

Increasing evidence indicates that EpoR, the closest relative of TpoR, forms a ligand-independent dimer (i.e., pre-formed dimer) (*76, 77*). Within a pre-formed EpoR dimer, two TM domains interact with each other, thereby stabilizing the receptor dimer (*76, 82, 83*). It has been proposed that ligand binding to a pre-formed EpoR dimer induces rotation of each TM helix on its helical axis, bringing a distinct set of amino acids into the TM-TM interaction interface (**Figure 3.9**) (*86*). This switching of the TM-TM interaction surface has been suggested to regulate EpoR activity (*86*). However, the same scenario may not be applicable to TpoR. Unlike EpoR, the TpoR dimerization does not seem to be mediated by the TM domain. Indeed, our SE-AUC and deuterium MAS NMR analyses showed that the TM domain of TpoR does not dimerize strongly as compared with that of EpoR. Thus, despite their sequence similarity, TpoR

and EpoR may control their dimerization and activation by different molecular mechanisms. To better understand the mechanism of receptor activation, we now focus on several constitutively active mutants of TpoR. These constitutively active receptors supposedly mimic the active state of TpoR, more specifically, the active dimer. We reason that a comparison between the wild-type TpoR and such constitutively active mutants should provide us with useful information on how TpoR undergoes the transition between the inactive and active conformations. In this chapter, we specifically focus on an amino acid substitution of serine for asparagine at position 505 (S505N), which renders TpoR constitutively active.

The S505N mutation has been found in some patients with familial essential thrombocythemia (ET) (*34-36, 92*). Familial ET is a rare hereditary chronic myeloproliferative disorder that causes excessive proliferation of megakaryocytes and platelets in the bone marrow (*22, 35*). Considering that S505 is located in the middle of the TpoR TM domain (**Figure 2.1**), the TM domain may play a critical role in the regulation of the TpoR activity. The importance of a TM domain for receptor activation has been implicated in several single-pass transmembrane receptors. For instance, the TM domain of the human epidermal growth factor receptor 2 (HER2) is known to be critical for its activation control. Substitution of valine for glutamic acid at position 664 (V664E), a mutation in the middle of the HER2 TM domain, has been shown to constitutively activate the receptor (*93*). This observation suggests that V664 of HER2 is necessary to maintain the inactive receptor conformation. On the other hand, the V664E mutation has been proposed to stabilize the active HER2 dimer conformation by forming hydrogen bonds between two TM domains of the receptor dimer (*94*).

In addition to HER2, the activity of the fibroblast growth factor receptor 3 (FGFR3) may also be controlled by its TM domain. Substitution of alanine for glutamic acid at position 391 (A391E), which resides in the TM domain, leads to constitutive activation of FGFR3, resulting in a skeletal disorder called Crouzon syndrome (*136*). Like the V664E mutation of HER2, A391E might stabilize the active FGFR3 dimer structure by forming a hydrogen bond between two associated TM helices (*95*). It is tempting to speculate that a similar mechanism may be involved in the S505N-induced constitutive activation of TpoR.

To elucidate the effect of the TpoR TM domain on the receptor conformation and activity, we utilized the TpoR TM-JM peptides containing the S505N mutation and analyzed the effect of the mutation on TM association. Our sedimentation equilibrium analytical ultracentrifugation (SE-AUC) and deuterium magic angle spinning (MAS) NMR spectroscopy analyses demonstrated that unlike the wild-type TpoR, the TM domain containing S505N can form a stable TM dimer in both detergent micelles and lipid bilayer membranes. We also analyzed the effect of S505N on JAK2-STAT signaling activity using a dual luciferase reporter assay in collaboration with the laboratory of Stefan Constantinescu. As expected, S505N was found to upregulate JAK2-STAT signaling even in the absence of Tpo. Finally, we asked if S505N mediates full-length TpoR dimerization using a split *G. princeps* luciferase reporter assay. We found that the S505N mutant receptor exhibited a stronger propensity to undergo ligand-independent dimerization than the wild-type receptor. This enhanced dimerization and constitutive activation may be due to the increased self-interaction of the S505N-containing TM domain. Together, our data suggest that incorporation of a polar residue, such as asparagine, into

the TpoR TM domain stabilizes the active dimer conformation by facilitating TM-TM interaction, which does not occur in the wild-type TpoR.

4.2 Results

4.2.1 The S505N TM-JM peptide forms a homodimer in detergent micelles

It is plausible that the S505N-containing TM domain has a strong tendency to associate with each other. To examine this possibility, we utilized a synthetic peptide covering the TM domain and its juxtamembrane region (i.e., TM-JM peptide; **Figure 2.1**) of S505N TpoR and analyzed homodimerization of the TM-JM peptide by two approaches: SE-AUC and deuterium MAS NMR spectroscopy.

We first examined the molecular nature of the S505N TM-JM peptide (**Figure 2.1**) using SE-AUC. To this end, three different samples were prepared by dissolving the S505N TM-JM peptide in n-dodecylphosphocholine (DPC) micelles (for details, see Methods). The oligomeric states of the peptides were determined by measuring absorbance at 280 nm (A_{280}). The data obtained were further analyzed by AUC software, *UltraScanII* (*137*). The analysis revealed that, unlike the wild-type TpoR TM domain, the S505N TM-JM peptide exists as a dimer (**Figure 4.1**). The majority of the mutant peptides were accumulated in a fraction with an estimated molecular weight (MW) of 11850 Da, which is close to 10783 Da, the expected MW of the TM-JM peptide homodimer (**Figure 4.1**). This result suggests that the S505N mutation stabilizes a TM-TM interaction within a TpoR dimer.

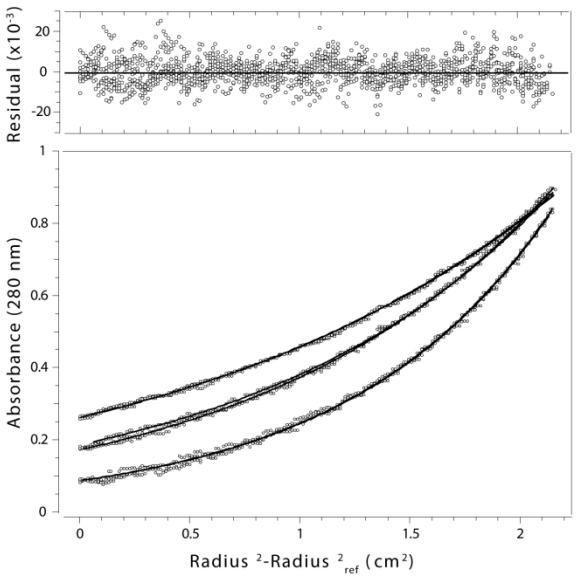

Figure 4.1: The TpoR TM-JM peptide containing the S505N mutation undergoes homodimerization. The bottom graph shows the absorbance profiles at 280 nm when the samples were centrifuged at 35k, 40k, and 48k rpm. Plots derived from one peptide concentration (30 μM) are shown as representative data. DPC detergent (15 mM) was used to solubilize the peptide. The data were analyzed using a single component equilibrium model, and the top graph shows how well the experimental data fit the model. The calculated MW of the predominant peptide based on this SE-AUC analysis was 11850 Da, while the MW of the peptide monomer is 5391 Da.

4.2.2 The S505N TM-JM peptide forms a homodimer in lipid bilayers

The SE-AUC analysis revealed that the TM-JM peptide of S505N TpoR favors the dimeric state in contrast to the wild-type, which favors the monomeric state. However, we cannot exclude the possibility that the S505N-induced TM association might be an artifact caused by the DPC micelles used in this assay. Thus, we next utilized deuterium MAS NMR spectroscopy and examined the multimeric states of the S505N TM-JM peptide within synthetic lipid bilayer membranes, which more closely mimic the natural cell membranes. In this analysis, we deuterated the methyl group of the leucine residue at position 510, 511, 512, or 513 of the synthetic TpoR TM-JM peptide. Each deuterated peptide was reconstituted into 1,2-dimyristoyl-*sn*-glycero-3-phosphocholine (DMPC), 1,2-dimyristoyl-*sn*-glycero-3-[phospho-rac-(1-glycerol)] (DMPG) lipid bilayers at a lipid/peptide molar ratio of 50:1. As described in Chapter 3, the

deuterium MAS NMR spectrum exhibits a characteristic deuterium line shape when formation of the TM-TM homodimer restricts the fast rotational motion of deuterated methyl groups (**Figure 3.5**). Compared with the wild-type TM-JM peptide (**Figure 4.2B**), the S505N TM-JM peptide gave rise to an intense deuterium line shape (**Figure 4.2C**), suggesting that the TM helices associate. It should be noted that the spectrum obtained from deuteration of L513 in the S505N TM-JM peptide showed a lower side-band intensity between -20 kHz and 20 kHz as compared with the spectra obtained from deuteration of L510, L511 and L512. This low intensity may be due to a greater flexibility at the lipid membrane boundary where L513 is likely to reside.

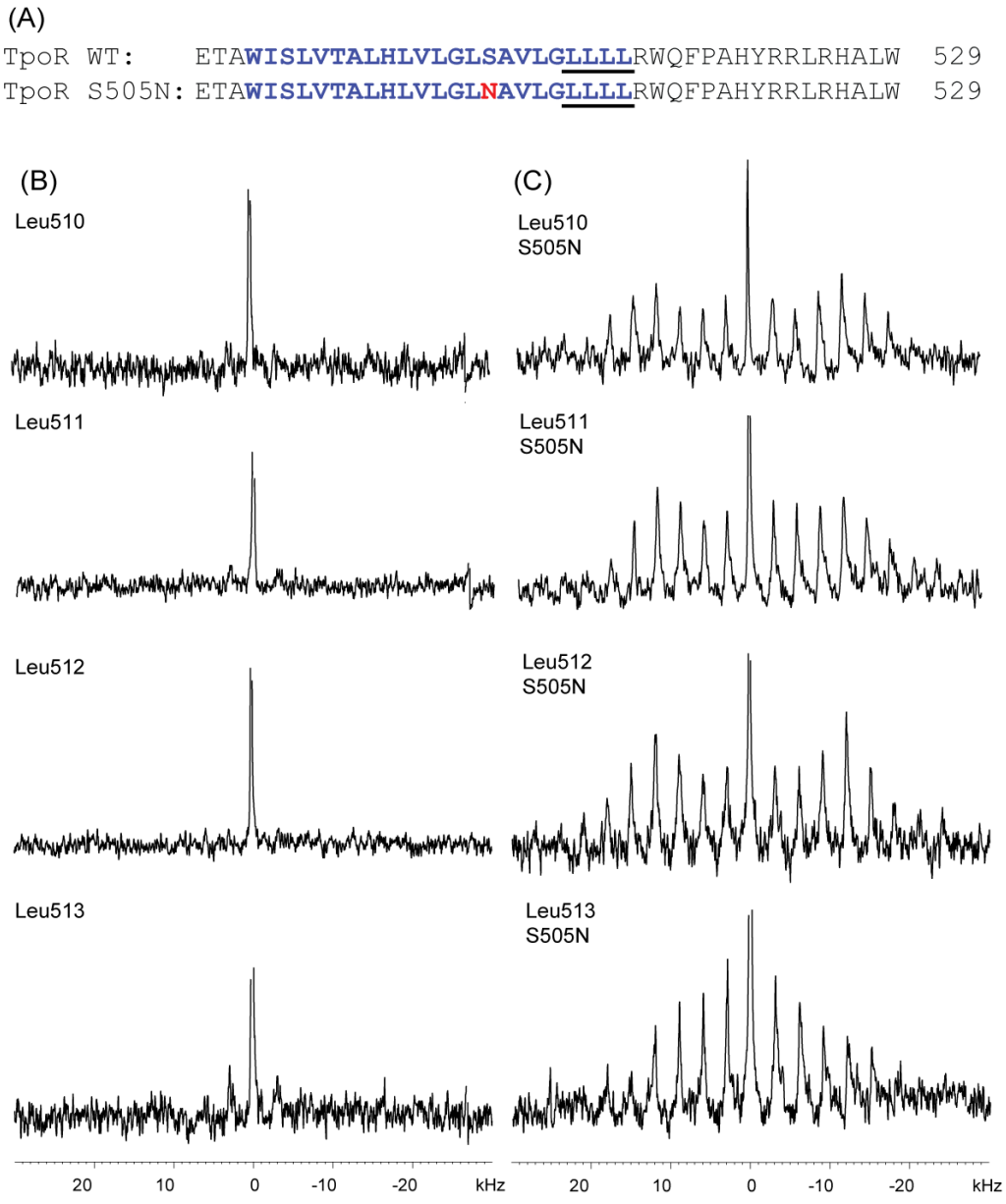

Figure 4.2: Deuterium MAS NMR of the S505N TpoR. (A) The wild-type and mutant TpoR TM-JM peptides used in deuterium MAS NMR spectroscopy. The S505N mutation, a substitution of Ser505 for Asn, is highlighted in red. The predicted TM domains are highlighted in blue. Leucine residues deuterated in this study (Leu510-513) are underlined. (B, C) The TM-JM peptides of the wild-type (B) or S505N (C) TpoR were reconstituted in DMPC:DMPG lipid bilayer membranes. The NMR spectra were obtained using single pulse excitation at a deuterium frequency of 55.26 MHz with a spinning speed of 3 kHz. Each spectrum represents the average of 600,000-1,500,000 transients. Spectra were obtained at 25 °C. The sharp peak at 0 frequency is residual deuterated water in the sample. The MAS NMR spectra derived from the wild-type peptide showed no rotational side band pattern, suggesting that the wild-type TM-JM peptide exists as a monomer. On the other hand, the MAS NMR spectra derived from the S505N mutant peptide showed characteristic deuterium line shapes with a rotational side band pattern, an indication of the peptide homodimerization.

4.2.3 The S505N mutation enhances ligand-independent receptor dimerization

To confirm the effect of the S505N mutation on the TpoR downstream signaling, we examined activation of the JAK2-STAT pathway using a dual luciferase reporter assay. In this assay, the firefly luciferase reporter gene was fused to the STAT-responsive elements found in the promoter of the FcγRI gene, a known target of STAT3/5. As an internal control, the *Renilla* luciferase gene was incorporated downstream of the thymidine kinase gene promoter in a separate vector. We first prepared the γ-2A cells that stably express the wild-type or S505N mutant TpoR. Then, these cells were transfected with the dual luciferase reporter system, and the luminescence derived from the firefly luciferase (FF) and the *Renilla* luciferase (RL) was determined. Compared with wild-type TpoR, the S505N mutant receptor was found to upregulate STAT-mediated gene expression by about three-fold even in the absence of Tpo (**Figure 4.3**). This high activity of the JAK2-STAT signaling was not significantly altered by addition of Tpo to the cell culture (**Figure 4.3**). These results clearly indicate that the S505N mutation indeed causes constitutive activation of TpoR in our experimental system.

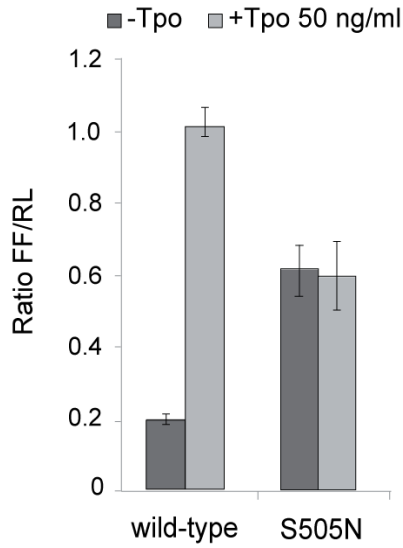

Figure 4.3: The S505N mutation constitutively activates the JAK2-STAT signaling pathway. The wild-type or S505N mutant TpoR was expressed in γ-2A cells. The JAK2-STAT signaling activity was determined based on the firefly luciferase (FF) reporter fused to the STAT-responsive promoter. As an internal control, the *Renilla* luciferase (RL) reporter was expressed under the control of the thymidine kinase gene promoter. The FF bioluminescence was normalized to the RL bioluminescence (Ratio FF/RL). All quantified data are means ± SD (n = 3 independent experiments). This experiment was carried out by Dr. Jean-Philippe Defour.

We next asked whether the S505N mutation affects ligand-independent dimerization of TpoR using the split *Gaussia princeps* luciferase complementation assay. As expected, the full-length TpoR containing the S505N mutation was also able to form a dimer in a ligand-independent manner (**Figure 4.4**). Interestingly, the S505N mutant receptor gave rise to approximately two-fold higher luminescence compared with the wild-type TpoR (**Figure 4.4**), indicating that the S505N mutation enhances TpoR dimerization in living cells.

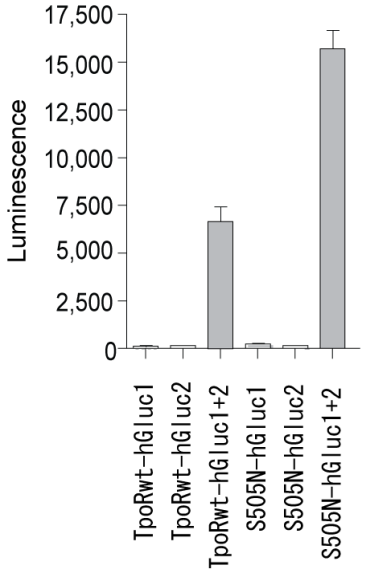

Figure 4.4: The S505N enhanced ligand-independent dimerization in the absence of the ligand. The effect of the S505N mutation on the receptor dimerization was determined by a split *Gaussia princeps* luciferase complementation assay. The N-terminal half (hGluc1) or the C-terminal half (hGluc2) of the *G. princeps* luciferase was fused to the C-terminus of TpoR. The resultant TpoR-hGluc1 and TpoR-hGluc2 constructs were co-expressed in HEK293 cells, and the dimerization was detected by bioluminescence derived from the chemical reaction mediated by the reconstituted luciferase and its substrate, luciferin. S505N enhanced ligand-independent dimerization of TpoR by more than two-fold based on the luminescence level. This experiment was carried out by Dr. Vitalina Gryshkova.

4.3 Discussion

Consistent with previous reports (*35, 138*), our dual luciferase reporter assay showed that the S505N mutation activates the JAK2-STAT signaling pathway in a ligand-independent manner. This constitutive activation of TpoR and its downstream signaling is likely to be a major cause of the S505N-associated familial ET, a disease characterized by abnormal platelet proliferation (*34, 36, 92*). The *G. princeps* luciferase complementation assay revealed that the S505N mutation in the TpoR TM domain enhanced ligand-independent dimerization of TpoR (**Figure 4.4**). This enhanced dimerization is likely due to the strong propensity of the S505N-containing TM helix to undergo self-interaction. Indeed, our SE-AUC and deuterium MAS NMR experiments indicated that the S505N TM domain preferably exists as a dimer rather than a monomer. These

observations support our TpoR activation model, in which the TM-TM association/dissociation regulates receptor activity (**Figure 3.8**).

It is well known that asparagine can serve as a hydrogen bond acceptor/donor. Thus, the S505N mutation may stabilize the active dimer conformation by forming hydrogen bonds between two TM helices (**Figure 4.5**). The stabilizing effect of an asparagine residue on TM-TM interaction has also been implicated by several studies using artificial TM peptides (*139-142*). For example, using artificial TM peptides, Degrado and his co-workers showed that the presence of asparagine, but not valine, on the potential TM-TM interaction surface augments homodimerization (*141*). This observation suggests that asparagine can provide a strong driving force (most likely hydrogen bonds) for boosting a TM-TM helix interaction within a receptor dimer.

A similar model has been proposed for a glutamate mutation in the TM domain of HER2, a single-pass transmembrane receptor. An amino acid substitution of valine for glutamic acid at position 664, which is located in the middle of the TM domain, is known to constitutively activate HER2 and its downstream signaling, leading to oncogenic tumor formation in the rat model (*93, 143*). It has been suggested that this glutamic acid residue stabilizes the active HER dimer via inter-helical hydrogen bonding between two TM helices (*94, 144*). Furthermore, a glutamic acid mutation in the TM domain of another single-pass transmembrane receptor, FGFR3, has been shown to activate in a ligand-independent manner (*144*). In a fashion similar to the V664E mutation in HER2, the substitution of alanine for glutamate at position 391 of FGFR3 is likely to stabilize a TM-TM interaction within an FGFR3 dimer via hydrogen bonding (*95*). These results suggest that not only asparagine but also other polar residues in any receptor TM

domain can enhance TM-TM interaction within a receptor dimer. Thus, theoretically, substitutions of the TpoR S505 for other polar residues, such as glutamate, should also stabilize the active dimer state. To examine this possibility, it will be interesting to see whether replacement of S505 to any other polar residue affects the TpoR activity as well as the active receptor conformation.

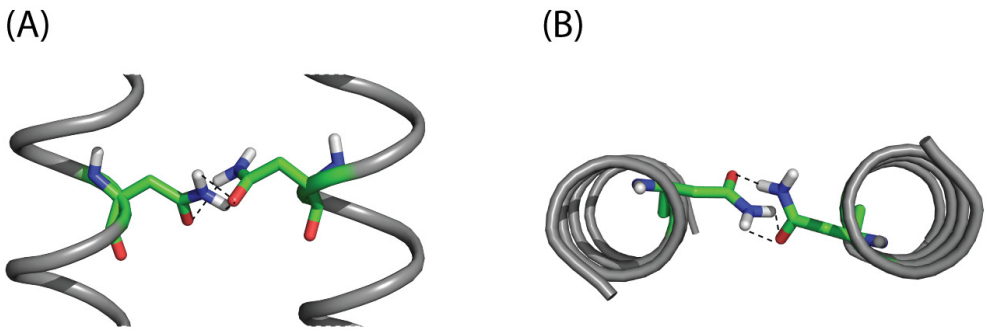

Figure 4.5: Asparagine mediates the TM interaction by forming hydrogen bonds. The side view (A) and top view (B) of the dimerization interface of two TM helices. The dotted line represents a potential hydrogen bond between two asparagine residues.

Although the role of asparagine in the TpoR TM domain is now clear, it remains an open question whether the specific location of an asparagine mutation is relevant for stabilization of the receptor dimer. Among known clinically related mutations in the TpoR TM domain, such an asparagine mutation only occurs at position 505 (**Table 1.1**). Is this just a coincidence, or do asparagine substitutions in other positions within the TM domain also cause constitutive activation of TpoR? One possibility is that position 505 is located on the TM-TM interaction surface of a TpoR dimer. In this scenario, only asparagine mutations at specific positions in the TM sequence will be able to stabilize the active receptor conformation. To test this hypothesis, asparagine-scanning mutagenesis in the TpoR TM domain will be needed.

Our data highlights the importance of the TpoR TM domain for receptor activation. In addition, we provide the potential molecular mechanism by which the S505N mutation constitutively activates the TpoR dimer. However, it is not likely that S505 is the only essential residue that controls TM-TM interaction and the resultant receptor activation. Indeed, other motifs or regions in TpoR have been suggested to play a critical role in the receptor activity modulation. In the next chapter, we will focus on other clinically relevant mutations and discuss a more detailed molecular mechanism underlying TpoR activation.

4.4 Conclusions

- The S505N TpoR mutant constitutively activates the JAK2-STAT downstream signaling.
- S505N enhances ligand-independent dimerization of TpoR.
- The S505N-containing TM domain has a strong propensity for self-interaction.
- The S505N mutation may constitutively activate TpoR by forming hydrogen bonds between two TM helices within a pre-formed TpoR dimer.

Chapter 5. W515 in the RWQFP motif of TpoR maintains the receptor inactive state by inhibiting the TM-TM interaction

5.1 Introduction

In the previous chapters, we elucidated both common features and differences between TpoR and its close relative, EpoR, in terms of their control of receptor activity. We found that, like EpoR, some, but not all, TpoR molecules can undergo ligand-independent dimerization (Chapter 3). However, unlike EpoR, the two TM domains do not appear to interact with each other (Chapter 3). Thus, the TM helix rotation model, which has been suggested for the EpoR activation mechanism, does not apply to TpoR because this model requires a ligand-independent TM-TM interaction. Instead, we proposed that TpoR is activated at least partly by ligand-induced TM-TM interaction within the dimer (Chapter 3). Consistent with this model, the S505N mutation was shown to stabilize a TM-TM interaction, thereby constitutively activating TpoR and its downstream signaling (Chapter 4). This observation suggests that the TM domain and/or its surrounding region play an indispensable role in the regulation of the TpoR activity. To further

investigate the function of the TpoR TM domain, we next focus on a series of mutations of tryptophan at position 515 (W515), which is located at the boundary between the TM domain and its intracellular juxtamembrane (IC-JM) region of TpoR.

Mutations at W515 have been found in 4.5% and 5% of essential thrombocythemia (ET) and primary myelofibrosis (PMF) patients, respectively (*50*). Both ET and PMF disorders are characterized by abnormal proliferation of megakaryocytes and platelets in the bone marrow (*145*). At least six different amino acid substitutions of W515 (W515K, W515L, W515R, W515A, W515S, and W515G) have been identified from patients with myeloproliferative neoplasms (MPNs), including ET and PMF (*34*) (**Table 1.1**). All of these clinically related mutations are thought to constitutively activate TpoR (*34*). However, the precise effects exerted by these mutations on the TpoR conformation remain largely unknown.

It should be noted that W515 resides within the ^{514}RWQFP motif, an amino acid sequence that is unique to TpoR and not found in the other Type I-Group 1 cytokine receptors (**Figure 1.9B**). This TpoR-specific region seems to be critical for the control of receptor activity as an insertion-deletion mutation in this motif (RWQFP to RKT) causes a MPN disorder (*34, 55*). Moreover, a study using the murine TpoR has shown that deletion of the corresponding motif (^{508}KWQFP) leads to constitutive activation of TpoR (*96*). Considering the relatively high mutation frequency at W515 in TpoR-related MPN patients (**Table 1.1**), this specific residue may be the key regulator that controls receptor dimerization and activation.

To better understand the role of W515 and the RWQFP motif, we first examined JAK2-STAT signaling in cells expressing the W515-related mutant receptors by a dual luciferase reporter assay. As expected, all of the clinically relevant mutants (W515K, W515L, W515R,

W515A, W515S, and W515G) activated STAT-mediated gene expression even in the absence of Tpo, suggesting that these mutations force the dimerization and the resultant activation of TpoR. This constitutive activation phenotype was reverted by incorporation of a tryptophan residue at position 514 or 516, suggesting that the presence of tryptophan in the IC-JM region is critical for maintaining the inactive receptor state. Our sedimentation equilibrium analytical ultracentrifugation (SE-AUC) as well as deuterium magic angle spinning (MAS) NMR analyses demonstrated that the TM domain containing a revertant mutation (R514W/W515K or W515K/Q516W) does not undergo self-interaction. On the other hand, the TM domain containing the constitutively active mutation (W515K) strongly interacted with each other. Furthermore, polarized attenuated total reflection Fourier transform infrared (ATR-FTIR) spectroscopy showed that the constitutively active receptor mutants have a smaller tilt angle with respect to the bilayer normal than the wild-type and the revertant mutants. These observations suggest that the tryptophan residue in the RWQFP region controls the tilt angle of the TM helix, thereby inhibiting TM-TM interactions in the unliganded, inactive receptor.

5.2 Results

5.2.1 Clinically relevant mutants at W515 constitutively activate the JAK2-STAT signaling pathway

To analyze the *in vivo* activity of the clinically known TpoR mutants (W515K, W515L, W515R, W515A, W515G, and W515S), we first examined the activation level of JAK2-STAT signaling by a dual luciferase reporter assay in γ-2A cells that stably express the wild-type or mutant TpoR. In this assay, the firefly luciferase (FF) reporter gene was fused to the STAT-responsive

elements. As an internal control, the *Renilla* luciferase (RL) gene was incorporated downstream of the thymidine kinase gene promoter in a separate vector. These dual reporter vectors were co-transfected into the TpoR-expressing γ-2A cells, and JAK2-STAT activity was determined based on the luminescence derived from the luciferase. Compared with the wild-type TpoR, all of the tested clinical TpoR mutants led to strong activation of the JAK2-STAT pathway even in the absence of Tpo (**Figure 5.1**). This ligand-independent JAK2-STAT activation was slightly enhanced by addition of Tpo in all mutants except W515A. Our data indicate that an amino acid substitution at W515 of TpoR modulates the receptor activity.

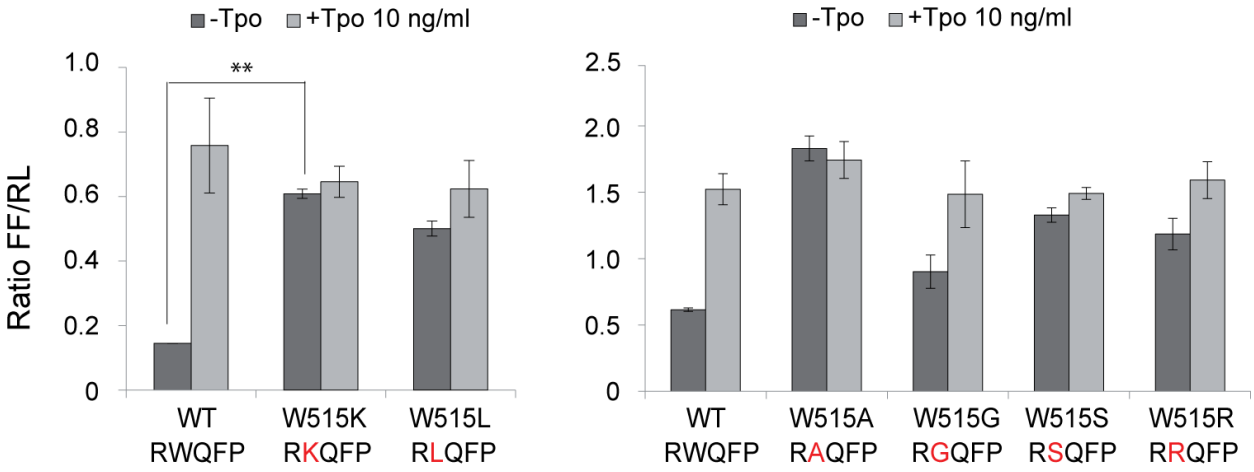

Figure 5.1: Clinically relevant mutations at W515 cause constitutive activation of JAK2-STAT signaling. TpoR variants containing clinically relevant mutations at W515 were expressed in γ-2A cells. Mutated residues in the RWQFP motif are highlighted in red. The JAK2-STAT signaling activity was determined based on the firefly luciferase (FF) reporter fused to the STAT-responsive promoter. As an internal control, the *Renilla* luciferase (RL) reporter was expressed under the control of the thymidine kinase gene promoter. The FF bioluminescence was normalized to the RL bioluminescence (ratio FF/RL). All quantified data are means ± SD (n = 3 independent experiments). ** P<0.01 (Student's t-test). This experiment was carried out by Dr. Jean-Philippe Defour.

5.2.2 Replacement of W515 with an aromatic residue is not sufficient to maintain the TpoR inactive state

The six known amino acid substitutions at W515 (i.e., K, L, A, G, S and R) do not share a common chemical property in their amino acid side chains. Thus, the constitutively active

mutations at W515 may be loss-of-function mutations that abrogate the ability to maintain the inactive receptor state. To examine this possibility, we next asked whether the role of W515 can be replaced by other aromatic residues. To this end, we substituted W515 of TpoR with another aromatic residue, either tyrosine or phenylalanine (i.e., W515Y or W515F), and examined the effect of these mutations on JAK2-STAT activity using the dual luciferase reporter assay.

Compared with the wild-type TpoR, both the W515Y and W515F mutants led to higher activity of JAK2-STAT signaling in the absence of Tpo (**Figure 5.2**). This result suggests that the role of W515 in maintenance of the TpoR inactive state cannot be fully replaced by other aromatic amino acids. However, addition of Tpo to cells expressing either W515Y or W515F increased the JAK2-STAT activity almost two-fold (**Figure 5.2**). Thus, unlike the constitutively active TpoR mutants, which only marginally enhanced the JAK2-STAT activity upon addition of Tpo (**Figure 5.1**), W515Y and W515F can at least partly control the TpoR activity in a ligand-responsive manner (**Figure 5.2**). Together, these results suggest that an aromatic residue at position 515 is necessary, but not sufficient, to fully maintain the inactive TpoR state.

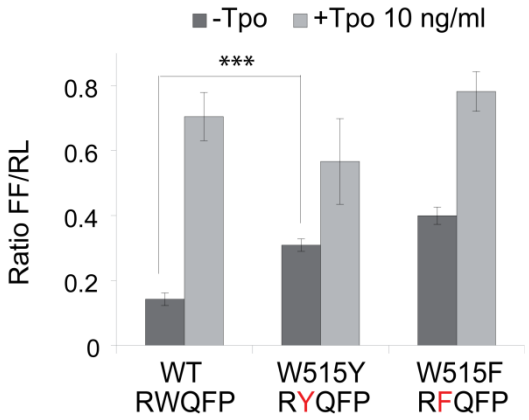

Figure 5.2: W515Y and W515F mutants can activate the JAK2-STAT signaling in response to Tpo. TpoR variants containing the W515Y or W515F mutation were expressed in γ-2A cells. Mutated residues in the RWQFP motif are highlighted in red. The JAK2-STAT signaling activity was determined based on the firefly luciferase (FF) reporter fused to the STAT-responsive promoter. As an internal control, the *Renilla* luciferase (RL) reporter was expressed under the control of the thymidine kinase gene promoter. The FF bioluminescence was normalized to the RL bioluminescence (Ratio FF/RL). All quantified data are means ± SD (n = 3 independent experiments). *** P<0.001 (Student's t-test). This experiment was carried out by Dr. Jean-Philippe Defour.

5.2.3 Incorporation of a tryptophan residue at position 514 or 516 reverts the constitutive activation phenotype of W515K, W515L and W515A mutants

That phenylalanine or tyrosine could not fully replace the role of W515 suggests that tryptophan *per se*, rather than just its aromaticity, is important for TpoR. This notion prompted us to ask whether incorporation of a tryptophan residue in the RWQFP region can reverse the constitutively active phenotype of the W515-related mutant receptors. To examine this possibility, we substituted R514 or Q516 for tryptophan in three constitutively active mutants (W515K, W515L, and W515A), resulting in six different double mutants: R514W/W515K, W515K/Q516W, R514W/W515L, W515L/Q516W, R514W/W515A, and W515A/Q516W. The W515K and W515L mutants were selected because these mutations occur at a high frequency in TpoR-associated MPN patients (**Table 1.1**). The W515A mutation is relatively rare among the

MPN patients, but we included this mutant in our assays because W515A led to the strongest activation of JAK2-STAT signaling (**Figure 5.1**).

All of the double mutants were independently expressed in γ-2A cells and their effect on JAK2-STAT signaling was analyzed by the dual luciferase reporter assay. In the absence of Tpo, the receptor activity of all the double mutants except W515A/Q516W was almost indistinguishable from that of the wild-type TpoR, and only basal levels of the reporter expression were observed in these mutants (**Figure 5.3**). In cells expressing these revertant mutants, JAK2-STAT activity was enhanced upon addition of Tpo, as was the case for the wild-type TpoR (**Figure 5.3**). For example, addition of Tpo increased JAK2-STAT activity about 2-3 fold in R514W/W515K and W515K/Q516W, while the original mutant, W515K, showed little increase (< 1.1-fold) in signaling activity in the presence of Tpo (**Figure 5.3**). These observations suggest that a tryptophan residue at position 514 or 516 can functionally mimic W515 and inhibit constitutive receptor activation.

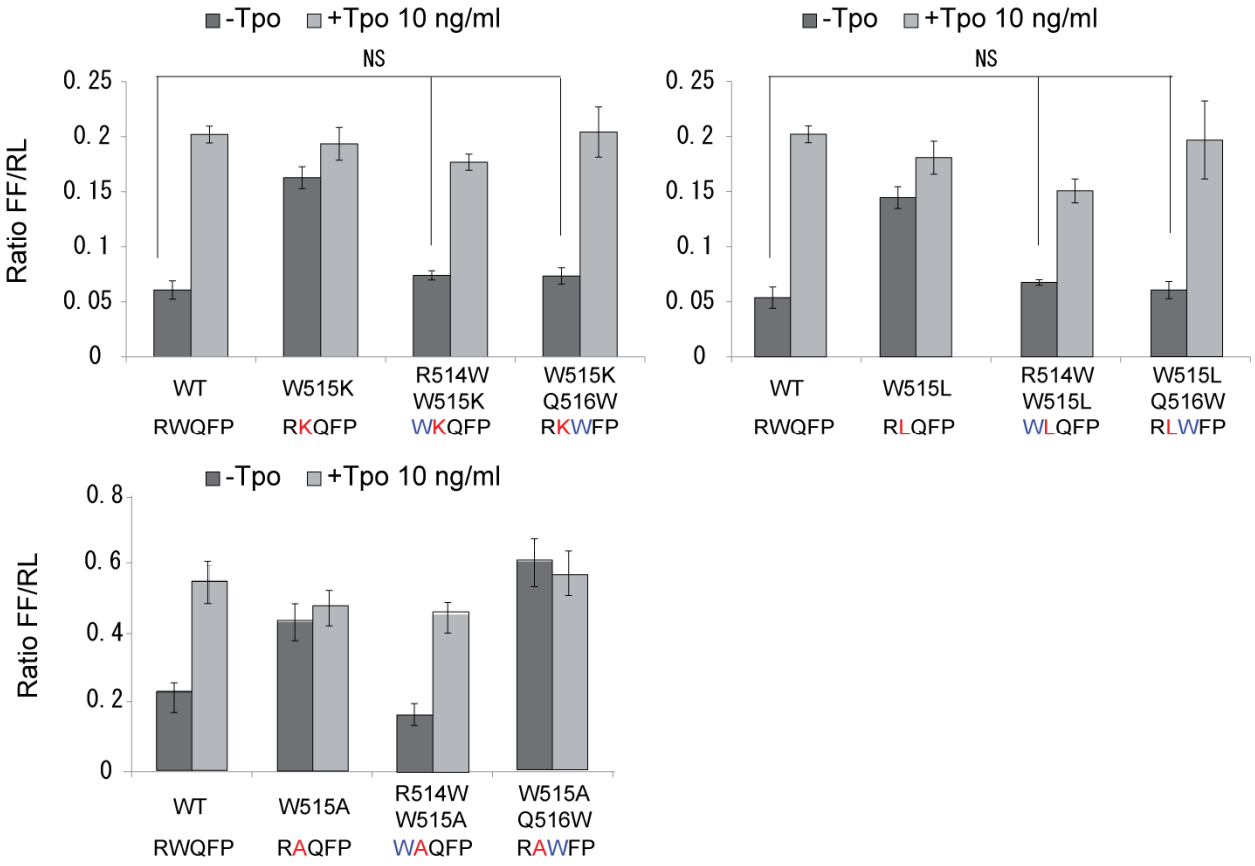

Figure 5.3: Incorporation of tryptophan at position 514 or 516 reverts the effect of the constitutively active mutations on the TpoR activity. TpoR variants containing a constitutively active mutation and a revertant mutation were expressed in γ-2A cells. The constitutively active mutations and second-site mutations in the RWQFP motif are highlighted in red and blue, respectively. JAK2-STAT signaling activity was determined based on the firefly luciferase (FF) reporter fused to the STAT-responsive promoter. As an internal control, the *Renilla* luciferase (RL) reporter was expressed under the control of the thymidine kinase gene promoter. The FF bioluminescence was normalized to the RL bioluminescence (ratio FF/RL). All quantified data are means ± SD (n = 3 independent experiments). NS: not significant (Student's t-test). This experiment was carried out by Dr. Jean-Philippe Defour.

5.2.4 Mutations in the RWQFP motif affect the dimerization of full-length TpoR

We next asked whether the constitutively active mutation (W515K) and the revertant mutation (W515K/W516Q) affect ligand-independent dimerization of TpoR using the split *Gaussia princeps* luciferase complementation assay. As expected, the full-length TpoR containing the W515K mutation was able to form a dimer in a ligand-independent manner (**Figure 5.4**). As

observed in the S505N mutant receptor (**Figure 4.4**), W515K gave rise to approximately two-fold higher luminescence compared with the wild-type TpoR (**Figure 5.4**). The double mutant receptor, W515K/W516Q, also formed a ligand-independent dimer. However, like the wild-type TpoR, the dimerization affinity of this double mutant was relatively weak (**Figure 5.4**), further indicating that Q516W is a revertant mutation of W515K. Together, our observations suggest that a tryptophan residue in the TpoR JM region plays a critical role in stabilization of the inactive receptor state by controlling the dimerization strength.

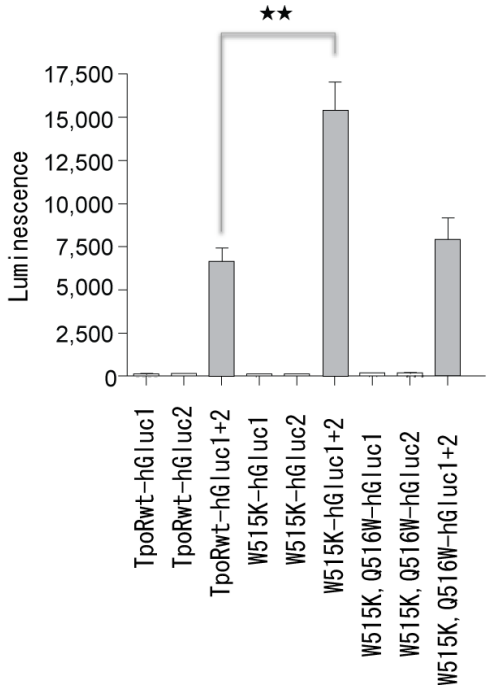

Figure 5.4: Ligand-independent dimerization of the W515K and W515K/Q516W TpoR mutants. The full-length wild-type and mutant TpoR were fused to either the N-terminal half (hGluc1) or C-terminal half (hGluc2) of the *Gaussia princeps* luciferase. The hGluc1- and hGluc2-tagged TpoR were co-expressed in HEK293 cells. The levels of TpoR ligand-independent dimerization were measured by the bioluminescence derived from the luciferase reconstitution. The W515K mutant enhanced the ligand-independent dimerization. However, the double mutant (W515K/W516W) restored the dimerization level back to the wild-type level. All quantified data are means ± SD (n = 3 independent experiments). $^{**}P < 0.001$ (one-way analysis of variance). This experiment was carried out by Dr. Vitalina Gryshkova.

5.2.5 W515 and its surrounding region modulate TM-TM interaction in detergent micelles

To further investigate the role of W515 in the TpoR activity control, we next asked whether a tryptophan residue in the TpoR JM region affects TM-TM interaction within a TpoR dimer. To this end, we prepared synthetic TM-JM peptides containing various W515-related mutations (**Figure 2.1**). These peptides include W515K (constitutively active), W515K/Q516W (revertant), R514W/W515K (revertant), and W515A/Q516W (constitutively active). We also generated a TM-JM peptide lacking the RWQFP motif (ΔRWQFP), the deletion of which is known to cause constitutive activation of the murine TpoR (*96*). The generated TM-JM peptides were solubilized in n-dodecylphosphocholine (DPC) micelles at three different peptide concentrations, and were analyzed by SE-AUC using three different centrifugation speeds (for details, see Methods). The oligomeric states of the peptides were determined by measuring absorbance at 280 nm (A_{280}). The resultant spectra were further analyzed by an AUC software, *UltraScanII* (*137*), using a single component or monomer-dimer equilibrium model (for details, see Methods). The results are summarized in the **Table 5.1**. As expected, both the single component model and the monomer-dimer equilibrium model predicted that the TM-JM domains of the constitutively active TpoR mutants (W515K, ΔRWQFP, and W515A/Q516W) preferably exist as a dimer (**Table 5.1**). Indeed, the majority of the constitutively active mutant peptides were accumulated in a fraction with an expected molecular weight (MW) at least twice as large as that of the corresponding peptide monomer (**Table 5.1**). These results suggest that the constitutively active mutations enhance ligand-independent dimerization of TpoR by stabilizing a TM-TM interaction within the receptor dimer.

Table 5.1: **Potential oligomeric states of the wild-type and mutant TM-JM peptides of TpoR determined by SE-AUC.**

	MW	MW (100% dimer)	MW (AUC: S)	MW (AUC: M-D)
wild-type: RWQFP	5360	10720	6960	4737
ΔRWQFP	4650	9300	12760	8532
W515K (RKQFP)	5306	10612	10630	8182
R514W/W515K (WKQFP)	5364	10728	8303	6629
W515K/Q516W (RKWFP)	5365	10730	7535	5962
W515A/Q516W (RAWFP)	3989	7978	8558	7967

S: single component model; M-D: monomer-dimer equilibrium model. Note that our SE-AUC data from all of the TpoR TM-JM peptides, except the wild-type and ΔRWQFP peptides, equally fit both the single component model and the monomer-dimer equilibrium model. The SE-AUC data from the wild-type TM-JM peptides better fit the single component model, as manifested by a more even distribution of the data residuals (data not shown). On the other hand, the SE-AUC data from the constitutively active mutant, ΔRWQFP, better fit the monomer-dimer equilibrium model (data not shown).

On the other hand, the TM-JM peptides containing a revertant mutation (W515K/Q516W and R514W/W515K) did not possess a strong propensity to undergo self-interaction, as was the case for the wild-type TM-JM peptide (**Table 5.1**). This suggests that R514W and Q516W reversed the effect of W515K on the TpoR activity by inhibiting a TM-TM interaction.

5.2.6 W515 and its surrounding region modulate TM-TM interaction in lipid bilayers

The SE-AUC analysis revealed that the TpoR TM-JM peptides with the constitutively active mutations favor a dimeric state while the wild-type and revertant mutant peptides favor a monomeric state. However, we cannot exclude the possibility that the observed dimerization might be an artifact caused by the micelles used in the SE-AUC experiment. Thus, as a parallel approach, we also utilized a deuterium MAS NMR spectroscopy to assess the oligomeric states of the mutant TpoR TM-JM peptides in a synthetic lipid bilayer membrane, which more closely

reflects the characteristics of the biological cell membranes. In this analysis, we deuterated the methyl group of the leucine residue at position 512 of the five different synthetic TpoR TM-JM peptides (W515K, W515K/Q516W, ΔRWQFP, R514W/W515K, and W515A/Q516W). Each peptide was reconstituted into 1,2-dimyristoyl-*sn*-glycero-3-phosphocholine (DMPC), 1,2-dimyristoyl-*sn*-glycero-3-[phospho-rac-(1-glycerol)] (DMPG) lipid bilayers at a lipid/peptide molar ratio of 50:1. Dimerization of the TM-JM peptides was detected by deuterium MAS NMR (*114, 146*). Compared with the wild-type peptide, the constitutively active mutants (W515K, ΔRWQFP, and W515A/Q516W) showed intense rotational side bands that appeared at intervals of 3 kHz NMR frequency (**Figure 5.5**). On the other hand, the revertant mutants (W515K/Q516W and R514W/W515K) did not give rise to such an NMR spectrum with a rotational side-band pattern. This result indicates a great mobility of the deuterated methyl groups in the revertant mutant peptides, hence, the absence of the peptide homodimerization. Thus, we can conclude that the revertant mutant TM-JM peptide behaves like the wild-type peptide and does not interact with each other strongly.

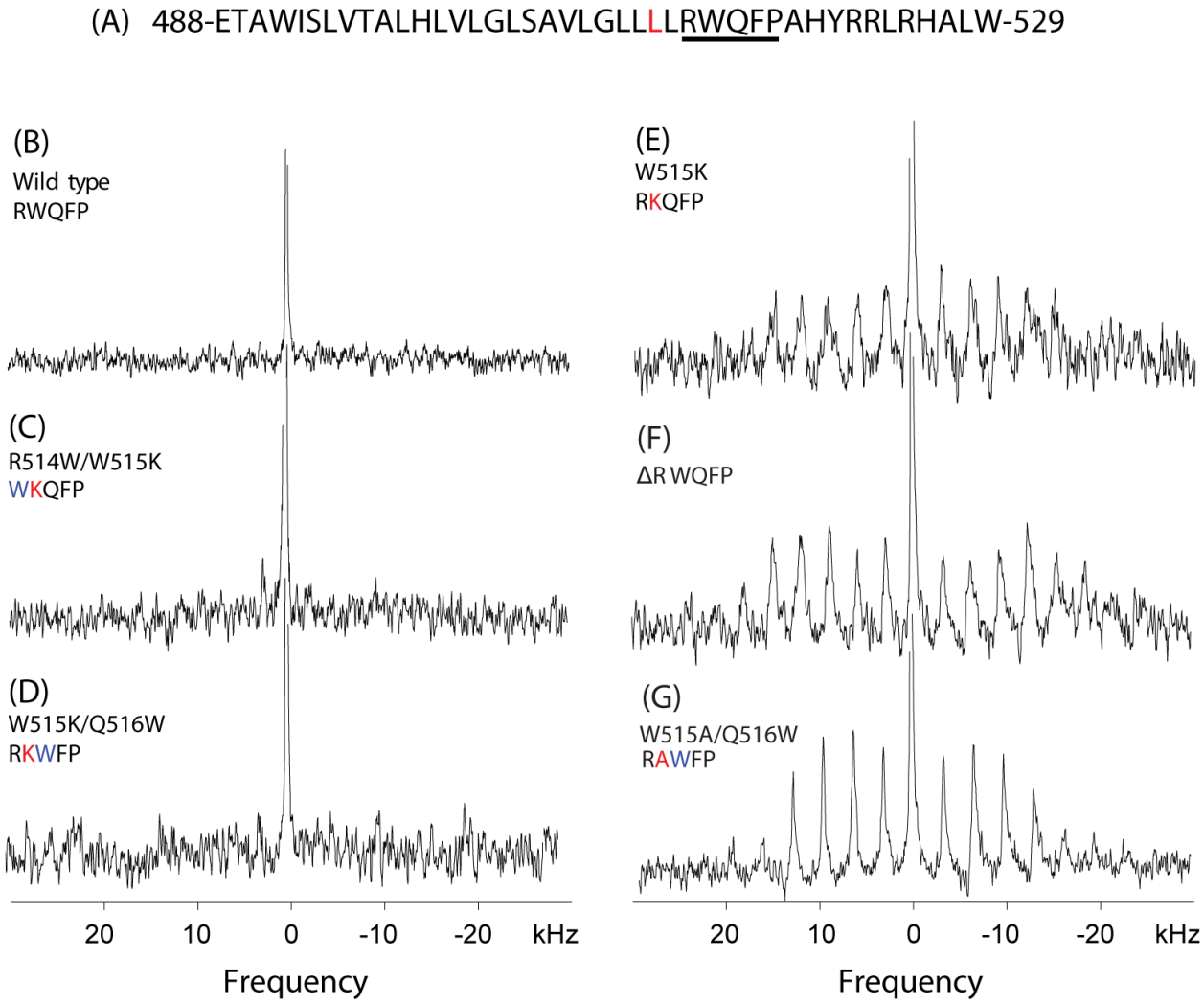

Figure 5.5: Deuterium MAS NMR of the W515K, R514W/W515K and W515K/Q516W mutants. (A) The TpoR TM-JM peptide used in deuterium MAS NMR spectroscopy. The RWQFP motif, in which various mutations were created, is underlined. Leu512, the deuterated residue, is highlighted in red. The wild-type (B) and mutant peptides (C-G) were reconstituted in DMPC:DMPG lipid bilayer membranes. The NMR spectra were obtained using single pulse excitation at a deuterium frequency of 55.26 MHz with a spinning speed of 3 kHz. Each spectrum represents the average of the 600,000-1,500,000 transients. Spectra were obtained at 25 °C. The sharp peak at 0 frequency is residual deuterated water in the sample. Characteristic *d3*-methyl rotational spinning bands were observed in the NMR spectra of W515K (E), ΔRWQFP (F), and W515A/Q516W (G), but not in those of R514W/W515K (C) and W515K/Q516W (D).

5.2.7 Tryptophan controls the TpoR TM-JM tilt angle

Our data suggest that the tryptophan residue in the RWQFP region modulates the TpoR activation and dimerization. However, it remains unclear how this residue affects TM-TM interaction within a TpoR dimer. Considering the data obtained from the dual luciferase reporter assay using W515Y and W515F TpoR, not only the aromaticity, but also the chemical property specific to a tryptophan is critical for regulating the JAK2-STAT signaling transduction. Tryptophan possesses the largest nonpolar side chain as well as a moiety that functions as a hydrogen bond donor. Due to this amphipathic nature, tryptophan residues in a transmembrane protein tend to be located at the membrane proximal region. Such tryptophan residues have been suggested to control the tilt angle of the TM helix, thereby stabilizing a specific membrane protein structure (*147*). Similarly, the tryptophan in the RWQFP motif may regulate the TM-TM interaction in the TpoR dimer by adjusting the TM helix tilt angle. To validate this model, we utilized a polarized attenuated total reflection-Fourier transform infrared (ATR-FTIR) analysis and measured the TM helix tilt angle of four different recombinant TM-JM peptides: the wild-type, W515K, W515K/Q516W, and R514W/W515K (**Figure 2.2**).

A polarized ATR-FTIR spectroscopy is a powerful method to obtain the secondary structure and orientation of a TM peptide in membranes (*106*). The orientation of a TM helix relative to the bilayer normal can be calculated by a dichroic ratio ($A_{\parallel}/A_{\perp}$), the ratio of the absorbance of light polarized parallel to the axis of an α-helix sample ($A_{\parallel}$) to the absorbance of light polarized perpendicularly to the sample axis ($A_{\perp}$) (*107*). Then, a dichroic ratio can be

correlated to the orientation of a TM helix peptide (for details, see Chapter 2: ATR-FTIR, **Figure 2.4**).

In our ATR-FTIR spectroscopy experiments, each sample (the wild-type, W515K, W515K/Q516W, or R514W/W515K) was reconstituted into DMPC:DMPG lipid bilayers at a lipid/peptide molar ratio of 50:1. As shown in **Figure 5.6**, all of the samples gave rise to a signal peak at 1657 cm^{-1}, which is a characteristic frequency of α-helix. This is an expected result because a TM domain of a single-pass transmembrane protein possesses an α-helix structure. Compared with the wild-type peptide, the constitutively active receptor mutant W515K showed a smaller TM helix tilt angle with respect to the membrane normal (**Figure 5.6** and **Table 5.2**). However, the tilt angle of the W515A/Q516W was almost the same as that of the wild-type peptide. Interestingly, the revertant mutant W515K/Q516W showed the largest tilt angle. These results suggest that a tryptophan residue in the IC-JM region regulates the TM helix tilt angle of TpoR. It is plausible that the narrower tilt angle observed in W515K may contribute to enhanced TM-TM interaction, leading to constitutive receptor activation.

Table 5.2: Dichroic ratio and TM helix tilt angle

	Dichroic ratio ($A_{\parallel}/A_{\perp}$)		Angle (°)	
	AVE	SE	AVE	SE
wild-type: RWQFP	2.84	0.11	29	3.1
W515K (RKQFP)	2.99	0.06	24	1.7
W515K/Q516W (RKWFP)	2.5	0.10	38	2.9
W515A/Q516W (RAWFP)	2.86	0.03	28	0.9

AVE: average; SE: standard error (n = 3 for the wild-type and W515K peptide, n = 2 for W515K/Q516W and W515A/Q516W).

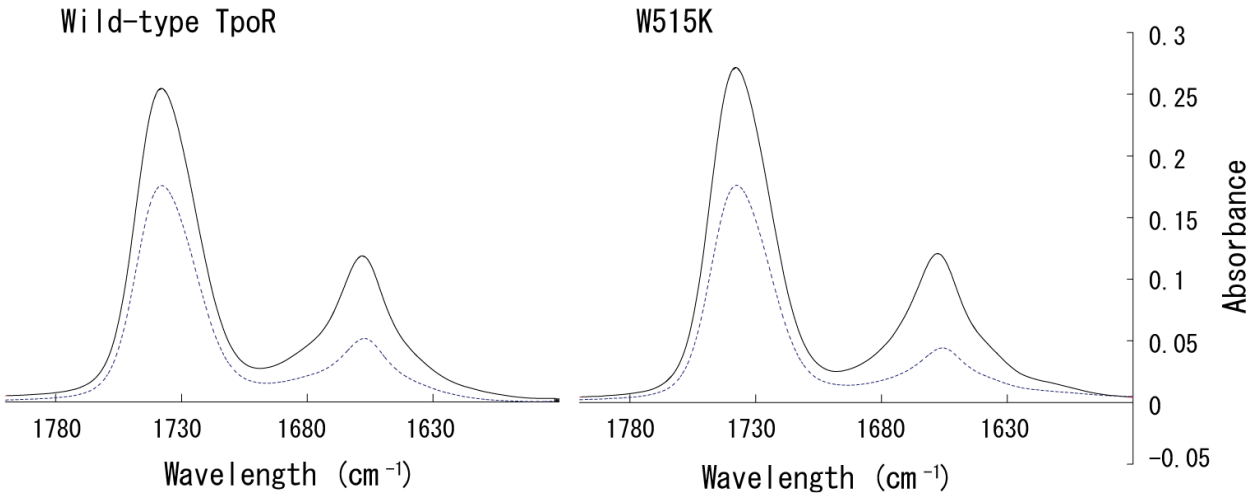

Figure 5.6: Polarized ATR-FTIR spectra of the wild-type and the W515K TpoR TM-JM peptides. The spectra were measured using parallel (solid line) and perpendicular (dashed line) polarized lights to the bilayers normal. The frequencies between 1600 to 1790 cm^{-1} are selected to focus on the IR bands at 1745 cm^{-1} (the lipid carbonyl vibration) and the bands at ~1657cm^{-1} (the protein amide I vibration).

5.3 Discussion

The dual luciferase reporter assay revealed that all of the clinically related mutations at W515 of TpoR (W515K, W515L, W515A, W515R, W515G, and W515S) constitutively activate the JAK2-STAT signaling pathway (**Figure 5.1**), indicating that the W515 plays an important role for regulating the TpoR activity. The role of W515 could not be fully replaced by tyrosine or phenylalanine (**Figure 5.2**), suggesting that tryptophan, rather than just an aromatic residue, is required for stabilization of the inactive receptor conformation.

Interestingly, the second mutation, R514W or Q516W, reverted the constitutively active phenotype caused by a mutation at W515 (W515K, W515L, and W515A), although only the W515A/Q516W mutant still exhibited constitutive receptor activation (**Figure 5.3**). Like the wild-type TpoR, these revertant mutants activated the JAK2-STAT signaling in a ligand-responsive manner. Consistent with this, one of the revertant mutations, Q516W, restored the high dimerization frequency of the W515K receptor to the basal level (**Figure 5.4**). These

observations suggest that a tryptophan residue in the JM region controls the activity of TpoR by modulating the dimerization strength of the receptor.

To further investigate how mutations in the RWQFP motif affect the dimerization of TpoR, the SE-AUC and deuterium MAS NMR analyses were conducted using the TpoR-derived TM-JM peptides. Both assays revealed that the TM domains containing a constitutively active mutation (W515K, ΔRWQFP, and W515A/Q516W) possess a strong tendency to self-interact in detergent micelles as well as lipid bilayer membranes (**Table 5.1**, **Figure 5.5**). In contrast, the TM domain containing a revertant mutation (R514W/W515K and W515K/Q516W) did not interact with each other strongly. Thus, our data suggest that the receptor activation is mediated by a TM-TM interaction.

Our ATR-FTIR using the wild-type and mutant TpoR TM-JM peptides demonstrated that a TM-TM interaction preferentially occurs when the TM helix tilt angle with respect to the membrane plane is relatively small (**Table 5.2**). For example, the W515K peptide, which possesses a strong propensity for self-interaction, resulted in a smaller TM helix tilt angle than the wild-type peptide or the W515K/Q516W revertant mutant. Thus, it is possible that the W515 residue maintains the inactive receptor state by keeping a specific TM helix tilt angle and that the TM-TM interaction and the resultant receptor activation may take place when the tilt angle is reduced by ligand binding. This notion is further supported by a recent molecular dynamic simulation, in which mutations in the TpoR JM region, including W515K, were shown to affect the TM helix tilt angle (*148*).

Based on the studies on W515 of TpoR, we propose two models for the TpoR activation mechanism: one involving ligand-independent receptor dimerization and another involving

ligand-induced receptor dimerization (**Figure 5.7**). In the former model (**Figure 5.7A**), TpoR most likely exists as a pre-formed dimer although the interaction may be weak in the native state. Within the pre-formed dimer, the TM domain does not interact with each other due to a relatively large TM helix tilt angle set by the RWQFP motif. However, binding of Tpo to the pre-formed dimer overrides the inhibitory function of the RWQFP region, leading to a decrease in the TM helix tilt angle. This tilt angle change allows the TM domain to interact with each other, thereby repositioning the TpoR-associated JAK2 kinase in a proper place for its trans-phosphorylation. In the ligand-induced dimerization model (**Figure 5.7B**), TpoR exists as a monomer. A specific TM helix tilt angle induced by the RWQFP motif inhibits dimerization of the TpoR monomer, but ligand binding changes the TM helix tilt angle, resulting in the TpoR dimerization. This allows JAK2 to rearrange its structure/position, leading to activation of the JAK2-STAT signaling pathway.

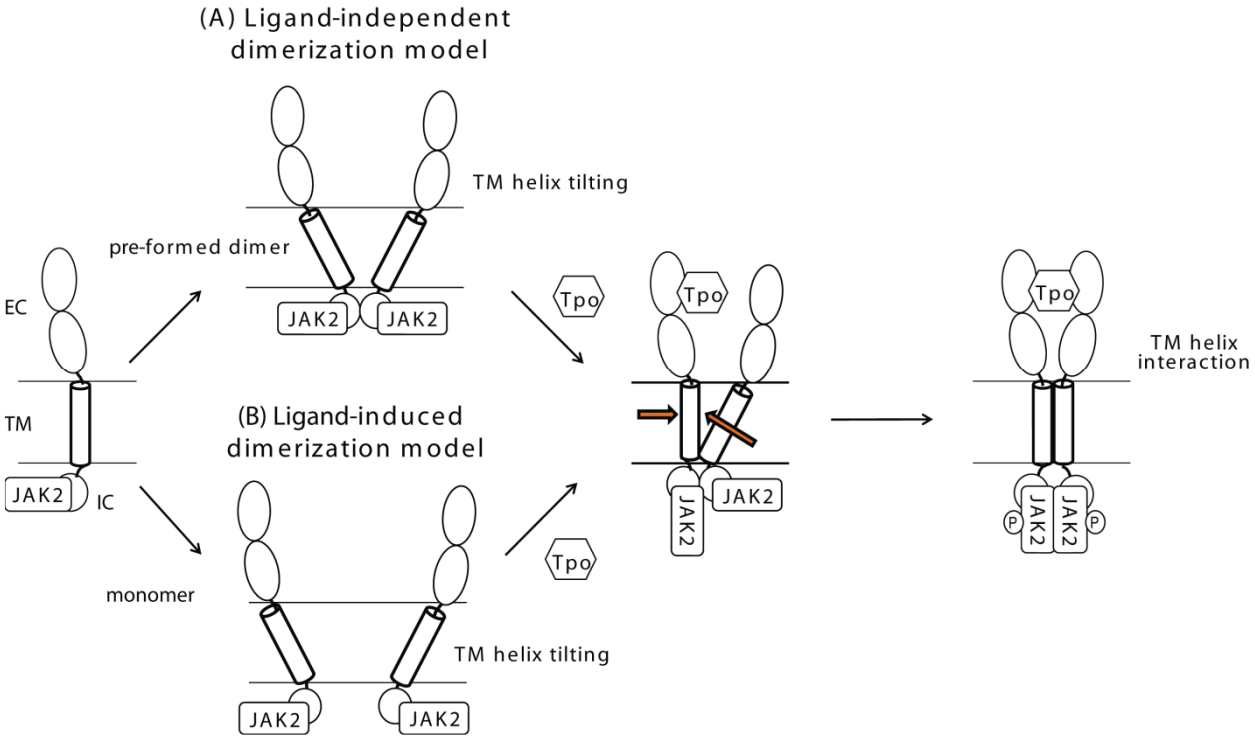

Figure 5.7: Refined models for the TpoR activation mechanism. (A) At least some fraction of TpoR can undergo ligand-independent dimerization, as presented in the previous model (**Figure 3.8**). A specific TM helix tilt angle, which is defined by the RWQFP motif, inhibits a TM-TM interaction (left). Ligand binding to the extracellular (EC) domain reduces the TM helix tilt angle (middle), allowing a TM-TM interaction (right). This receptor conformation in turn reorients JAK2 into an active position (right), resulting in activation of the JAK2-STAT signaling pathway. (B) Alternatively, TpoR may exist as a monomer, as presented in the previous model (**Figure 1.10B**). The inactive monomer state is maintained by a specific TM helix tilt angle. Ligand binding modulates the TM helix tilt angle, allowing the receptor to dimerize, leading to activation of the JAK2-STAT signaling pathway. An ellipse in the EC domain represents one cytokine receptor module (CRM).

It remains elusive how exactly tryptophan in the JM region of a transmembrane protein regulates a TM helix angle. The key to understanding the molecular role of such a tryptophan may lie in its chemical properties. Tryptophan is unique among all amino acids in that it has an indole ring as a side chain. With the help of this side chain, tryptophan can form a hydrogen bond as well as cation-π interactions with adjacent molecules. Thus, W515 may control the TM helix tilt angle by forming stable, non-covalent interactions with its neighboring molecules, such as membrane lipids. We will further discuss the molecular basis of the tryptophan-mediated TM helix tilt angle control in Chapter 6.

5.4 Conclusions

- Clinically relevant mutations at W515 of TpoR constitutively activate the JAK2-STAT signaling pathway.
- The constitutively active mutations at W515 enhance ligand-independent dimerization of TpoR.
- Incorporation of a tryptophan residue at position 514 or 516 reverts the constitutively active phenotype of W515K, W515L, and W515A.
- The TM-JM peptide containing W515K has a strong propensity for dimerization.
- The TM-JM peptide containing a revertant mutation, R514W/W515K or W515K/Q516W does not dimerize.
- Compared with the wild-type and revertant TM-JM peptides, the W515K mutant peptide produces a smaller TM helix tilt angle in the lipid bilayer membrane.
- These observations suggest that W515 regulates the dimerization and activity of TpoR by modulating the TM helix tilt angle in the cell membrane.

Chapter 6. General Discussion

6.1 Introduction

The thrombopoietin receptor (TpoR) regulates megakaryocytopoiesis and platelet development (*12-16*). Despite the importance of TpoR for vertebrates including humans, at the molecular level its activation mechanism remains elusive. To better understand the detailed activation mechanism, we compared the wild-type TpoR with several clinically related mutants of TpoR in terms of their dimerization and receptor activity. Specifically, we analyzed the role of the TM-JM region of TpoR in receptor activation using a combination of five different methods: sedimentation equilibrium analytical ultracentrifugation (SE-AUC), deuterium magic angle spinning (MAS) NMR spectroscopy, polarized attenuated total reflection Fourier transform infrared (ATR-FTIR), a dual luciferase reporter assay, and a split *Gaussia princeps* luciferase complementation assay.

6.2 Summary of results

6.2.1 The TM domain of TpoR does not interact with each other

Previous studies have shown that the other Type I-Group 1 cytokine receptors, namely the erythropoietin receptor (EpoR), the growth hormone receptor (GHR), and the prolactin receptor (PRLR), form dimers even in the absence of ligand (*76-78, 80*). EpoR, the closest relative of TpoR, is known to undergo dimerization via its TM domain (*76*). The EpoR TM domain is thought to stabilize the receptor dimer by forming a TM-TM interaction (*76, 82*). On the other hand, our SE-AUC and deuterium MAS NMR analyses showed that the TM domain of TpoR does not possess a strong propensity to undergo self-interaction (**Figure 3.3**, **Figure 3.4**, **Figure 3.5**). Our split *G. princeps* luciferase complementation assay demonstrated that the full-length TpoR can dimerize in a ligand-independent manner (**Figure 3.7**). However, this ligand-independent dimerization was relatively weak compared with that of EpoR, presumably due to the lack of a TM-TM interaction in the TpoR dimer. These results suggest that two different forms of the inactive TpoR (i.e., monomer and dimer) may co-exist in the cells. As for TpoR molecules that exist as pre-formed dimers, such dimerization may be stabilized by the extracellular (EC) or intracellular (IC) domain.

6.2.2 The S505N mutation enhances ligand-independent receptor dimerization

Although TpoR and EpoR share high sequence similarity, their TM domains play different roles in receptor activation. To further analyze the importance of the TpoR TM domain, we focused on a clinically relevant mutation, S505N, which causes excessive proliferation of megakaryocytes

and platelets in the bone marrow (*22, 35*). The S505N mutation is located in the middle of the TM domain; thus, we reasoned that a close examination of this mutant should enable us to understand the importance of the TM domain in the regulation of TpoR activity. As expected, our dual luciferase reporter assay showed that the S505N mutation increased the activity of the JAK2-STAT signaling pathway in living cells independently of ligand binding (**Figure 4.3**). This enhanced JAK2-STAT activation seems to be due to enhanced dimerization of the mutant TpoR. Indeed, the split *G. princeps* luciferase complementation assay revealed that the S505N mutant receptor undergoes dimerization more frequently than wild-type TpoR (**Figure 4.4**). Moreover, our SE-AUC and deuterium MAS NMR spectroscopy analyses demonstrated that the synthetic TM-JM peptide containing the S505N mutation has a stronger propensity for self-interaction compared with the wild-type TM-JM domain (**Figure 4.1**, **Figure 4.2**). Together, these observations suggest that the S505N mutation stabilizes a pre-formed TpoR dimer by enhancing an interaction between two TM helices. Considering that asparagine can be a potential hydrogen bond acceptor/donor, the TM-TM interaction within the receptor dimer may be mediated by a hydrogen bond between two asparagine residues.

6.2.3 The tryptophan in the RWQFP region of TpoR maintains the receptor inactive state by inhibiting the TM-TM interaction

Another clinically relevant residue of TpoR is W515, the mutation of which causes constitutive activation of TpoR. To date, several mutations at this residue (e.g., W515K, W515L, and W515A) have been isolated from myeloproliferative neoplasm (MPN) patients (*29*). To elucidate the effect of these mutations on TpoR activity, we first examined the JAK2-STAT signaling

activity in living cells transiently expressing the mutant TpoR by the dual luciferase reporter assay. As expected, all of the clinically related mutations at W515 (W515K, W515L, W515A, W515G, W515S, and W515R) upregulated the JAK2-STAT signaling pathway in the absence of Tpo (**Figure 5.1**). Furthermore, we detected the ligand-independent dimerization of W515K, one of the constitutively active TpoR mutants, by the split *G. princeps* luciferase complementation assay. Like S505N, the W515K mutant receptor dimerized more frequently than the wild-type TpoR (**Figure 5.4**). Moreover, the SE-AUC and the deuterium MAS NMR experiments clearly demonstrated that the TM region containing W515K possesses high affinity for self-interaction (**Figure 5.5E**, **Table 5.1**). Thus, we propose that W515K renders TpoR active by enhancing a TM-TM interaction. The same scenario may apply to the other clinically relevant mutations at W515 (W515L, W515A, W515G, W515S, and W515R), all of which are known to cause constitutive activation of TpoR.

How do these mutations at W515 constitutively activate TpoR? The six known amino acid substitutions (i.e., K, L, A, G, S, and R) at W515 do not share a common chemical property in their amino acid side chains. Thus, unlike S505N, the mutations at W515 may be loss-of-function mutations, rather than gain-of-function mutations that forcibly stabilize the active receptor conformation. In other words, W515 itself is important and this residue may play a critical role in inhibition of the TM-TM interaction. To examine this possibility, we first asked whether other aromatic residues, such as tyrosine and phenylalanine, can replace the function of W515. Although both W515Y and W515F enhanced the JAK2-STAT signaling activity even in the absence of Tpo (**Figure 5.2**), these ligand-independent activations were not as exaggerated as those of, for example, W515K and W515A (**Figure 5.1**). In addition, W515Y and W515F were

responsive to addition of Tpo (**Figure 5.2**), suggesting that, to some extent, both mutant receptors can still control the transition between the active and inactive receptor states. Thus, an aromatic residue can at least partly replace the function of W515 in the receptor activity control. Together, our data suggest that the aromaticity of the W515 side chain is important but not sufficient to maintain the inactive TpoR conformation.

To further investigate the role of W515 in regulation of the TpoR activity, we next asked whether the constitutively active phenotype of the W515-related mutant receptors can be reverted by incorporation of a tryptophan residue in the ^{514}RWQFP region. To this end, we replaced R514 or Q516 with tryptophan in the W515K, W515L, and W515A mutant receptors, resulting in six different double mutants: R514W/W515K, W515K/Q516W, R514W/W515L, W515L/Q516W, R514W/W515A, and W515A/Q516W. The dual luciferase reporter assay showed that the normal TpoR activity was restored in all of the double mutants except W515A/Q516W. These double mutants properly activated the JAK2-STAT signaling pathway in a Tpo-dependent manner (**Figure 5.3**). It is plausible that introduction of tryptophan at position 514 or 516 can compromise the high dimerization propensity of the constitutively active receptors (W515K, W515L, and W515A). Consistent with this notion, the split *G. princeps* luciferase complementation assay showed that one of the double mutants, W515K/Q516W, reduced its dimerization affinity almost to the same level as wild-type TpoR (**Figure 5.4**). Furthermore, our SE-AUC and deuterium MAS NMR analyses revealed that the synthetic TM-JM peptide containing a double mutation (R514W/W515K or W515K/Q516W) does not interact with each other as strongly as the W515K TM-JM peptide (**Figure 5.5**, **Table 5.1**). These findings suggest that a tryptophan residue in the TpoR JM region plays a critical role in

stabilization of the inactive receptor conformation via inhibition of a TM-TM interaction within the receptor dimer.

However, it remains unclear how the tryptophan residue in the RWQFP region affects TM-TM interactions within a TpoR dimer. We hypothesized that the tryptophan inhibits a TM-TM interaction by inducing a specific TM helix tilt angle. It has been suggested that tryptophan in a JM region of a single-pass transmembrane protein controls the tilt angle of the TM helix (*147*). To examine this possibility in TpoR, we utilized ATR-FTIR spectroscopy and calculated the helix tilt angle of the TM domains of the wild-type, W515K, R514W/W515K, and W515K/Q516W receptors in the lipid bilayers. As shown in the **Table 5.2** and **Figure 5.6**, the helix tilt angle with respect to the membrane normal was the smallest (24° ± 1.7) in the W515K mutant TM helix, and it progressively became greater as the position of the tryptophan moved toward the C terminus (RKQFP: 24° ± 1.7, RWQFP: 29° ± 3.1, RKWFP: 38° ± 2.9). These observations suggest that the position of the tryptophan in the TpoR JM region may control the helix tilt angle.

6.3 Discussion

6.3.1 Models for the TpoR activation mechanism

On the basis of our data, we propose two models for the TpoR activation mechanism: the ligand-independent receptor dimerization model and the ligand-induced receptor dimerization model (**Figure 5.7**). In the former model (**Figure 5.7A**), TpoR exists as a ligand-independent dimer, the formation of which does not involve TM-TM interactions. Next, ligand binding to the EC domains of the receptor dimer changes the tilt angle of each TM helix, which then induces a TM-

TM interaction within the pre-formed dimer. Finally, the interaction between the two TM domains triggers a specific structural rearrangement of the IC domains, leading to activation of the TpoR-bound JAK2 kinase. Alternatively, the ligand-induced dimerization model is on the assumption that TpoR exists as a monomer in its inactive state (**Figure 5.7B**). In this model, a specific TM helix tilt angle prevents dimerization of the TpoR monomer. Upon ligand binding to the receptor, the TM helix tilt angle alters, leading to the receptor dimerization. As a result, the TpoR-bound JAK2 kinase and its downstream signaling become activated. It should be noted that these two models are not necessarily exclusive to each other; the inactive TpoR molecules may exist as both monomers and dimers.

6.3.2 Importance of ligand-independent receptor dimerization

Traditionally, it has long been believed that single-pass transmembrane receptors are activated by ligand-induced receptor dimerization (*134*). However, this concept has been challenged by the discovery of ligand-independent dimerization of several receptors, including the Type I-Group 1 cytokine receptors. The activity of such receptors is likely to be regulated by a more complex conformational change within the receptor dimers rather than just a change in their oligomeric states. However, a previous study using receptor cross-linking analyses failed to detect the pre-formed TpoR dimers (*38*). In this study, the two EC domains of the potential TpoR dimers were covalently linked together and the oligomeric states were analyzed by SDS-PAGE (*38*). This approach found no TpoR dimer in the absence of Tpo (*38*). Contrary to this result, we found that at least some fraction of TpoR can dimerize in a ligand-independent manner, although this interaction was relatively weak compared with that of EpoR (unpublished data). We speculate

that this discrepancy between our study and the previous study stems from the relatively low detection efficiency of the receptor cross-linking assay. Indeed, the same study showed that only ~10% of total TpoR molecules undergo dimerization even in the presence of Tpo (*38*). This technical limitation, which is inherent with receptor cross-linking approaches, may be the reason why ligand-independent dimerization of TpoR had not been experimentally proven until our present study.

To examine how widespread ligand-independent receptor dimerization is among single-pass transmembrane receptors, highly sensitive assays for protein-protein interactions, such as split luciferase complementation and single-molecule imaging, are required. This notion is not trivial because the presence of a pre-formed receptor dimer may not be detectable by conventional approaches as was the case for TpoR. Similarly, ligand-independent dimerization of the epidermal growth factor receptor (EGFR) had not been clearly demonstrated until single-molecule imaging of fluorescently labeled EGFR was conducted (*149*). Thus, it would be worthwhile to re-examine other single-pass transmembrane receptors for their oligomeric states using a highly sensitive detection system. Such studies should elucidate whether ligand-independent dimerization is a common phenomenon among the majority of receptors.

6.3.3 Comparison between TpoR and EpoR

Activation mechanisms of pre-formed receptor dimers have been intensively studied in EpoR, which shares the highest sequence similarity with TpoR among the Type I-Group 1 cytokine receptors. In the absence of its ligand, EpoR most likely exists as a dimer, which is mediated by a TM-TM interaction (*76, 82, 83*). The current model for EpoR activation is that upon ligand

binding, each TM helix in the pre-formed EpoR dimer rotates on its helical axis, thereby switching the TM-TM interaction surface (**Figure 1.7**, **Figure 1.8**). Such a structural rearrangement within the receptor dimer may be critical to activate the EpoR-bound JAK2 kinase (*86*).

On the other hand, the TM helix rotation model is not likely to be the case for TpoR. Our results suggest that the TM domains of the wild-type TpoR do not interact with each other. On the other hand, the TM domains derived from the constitutively active TpoR mutants were found to possess a high affinity for self-interaction. Thus, TM-TM association/dissociation, rather than switching of TM-TM interaction interface, may control the activity of TpoR.

6.3.4 A possible mechanism of the ligand-induced TM-TM interaction in the TpoR dimer

Our studies shed light on a striking difference between TpoR and EpoR. While the two TM domains of the EpoR dimer are always associated with each other, the TM-TM interaction of TpoR is likely to occur in a ligand-dependent manner. Such ligand-induced TM-TM interaction had never been documented until the present study, and requires a novel mechanistic explanation. We hypothesize that Tpo induces the TM-TM interaction by altering the TM helix tilt angle. The importance of the TM helix tilt angle has been suggested by a recent computational simulation (*148*). In this study, the TpoR TM domain was built by using homology modeling based on a single-pass transmembrane protein segment (PDB ID: 2JPX), while the IC domain structure was predicted by the Rosetta *ab initio* calculation method. The merged structure of the TM and IC domains of TpoR were then inserted into the lipid bilayers composed of palmitoyloleoyl

phosphatidylcholine (POPC). Based on the molecular dynamics simulations on this reconstituted TM-IC domains of TpoR (residues 481 to 635), the TM helix tilt angles of the wild-type and W515K (constitutively active) TpoR receptors were determined to be 27.6° ± 7 and 25.1° ± 6.4, respectively. This study suggests that the TM domains of the active and inactive receptors are associated with the cell membrane at different tilt angles (*148*).

Furthermore, a recent study on an integrin receptor underscored the critical role of a TM helix tilt angle in receptor activation. An integrin receptor exists as a heterodimer composed of α- and β-subunits. This dimerization is mediated by a TM-TM interaction, as is the case for EpoR. Interestingly, binding of a cytoplasmic protein, called talin, to the membrane-proximal region of the β-subunit was shown to change the TM helix tilt angle (*150*). As a result, the TM domains of the α- and β-subunits become dissociated within the integrin heterodimer, promoting structural rearrangement of the EC domains (*150*). Thus, the TM helix tilt angle change may be a common mechanism for regulation of receptor activation.

6.3.5 Maintenance of the inactive state of TpoR

Our data demonstrated that the chemical property and/or position of tryptophan in the RWQFP region play a substantial role in inhibition of a TpoR TM-TM interaction. The side chain of tryptophan not only possesses the largest nonpolar surface among all amino acids, but also serves as a hydrogen bond donor via its NH group. Due to this amphipathic nature, tryptophan residues in a transmembrane protein are preferentially located at the lipid-water boundary (*151*). Similarly, W515 of TpoR most likely resides at the boundary between the cell membrane and the cytoplasm, thereby locking TpoR in a specific conformation/orientation. However, the precise

molecular mechanism by which W515 affects the inactive receptor conformation remains to be investigated. A fascinating hypothesis is that W515 positions the TpoR TM helix at a specific tilt angle via a non-covalent interaction with the cell membrane components (**Figure 6.1**). Tryptophan at the lipid-water boundary is known to possess a strong propensity to interact with the lipid head group (*152*). Consistent with this notion, a computational simulation using a TM peptide predicted that tryptophan located at the lipid-water interface forms a hydrogen bond between its NH group and the ester oxygen of a lipid head group (*153*). In addition to hydrogen bonding, an interfacial tryptophan residue also has the ability to form a cation-π interaction with the lipid head group (*154, 155*). Such a non-covalent interaction is possible between the π-electron cloud of the tryptophan indole ring and the quaternary amine of the phosphocholine (PC) head group (*155*). Considering these unique chemical properties of tryptophan, it will be interesting to examine the possibility that W515 contributes to similar non-covalent interactions with lipids.

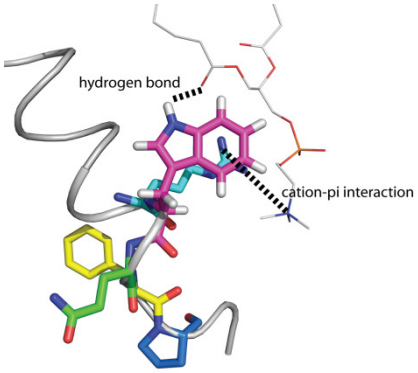

Figure 6.1: Possible interactions between W515 and a lipid head group. A hydrogen bond may be formed between the NH group of the tryptophan and the carbonyl group of a lipid head. Alternatively, a cation-π interaction may be formed between the tryptophan indole ring and the cationic nitrogen of a lipid head. As an example of phospholipids, DMPC is shown. The R514, W515, Q516, F517, and P518 residues are highlighted in cyan, magenta, yellow, green, and blue, respectively. The hydrogen, nitrogen, and oxygen atoms of the amino acids are shown in white, blue, and red, respectively. The phosphorus and hydrocarbon atoms of a DMPC molecule are shown in orange and light gray, respectively.

Another possibility is that W515 offsets the overall hydrophilic nature of the RWQFP region via a cation-π interaction with R514 and squeezes this motif into the cell membrane (**Figure 6.2**). In general, positively charged amino acids, such as arginine, do not penetrate into the hydrophobic core of the cell membrane. Thus, the guanidinium side chain of R514 is most likely located in the aqueous phase just adjacent to the bilayer surface. However, once a cation-π interaction between W515 and R514 occurs, the positive charge of the R514 side chain is compensated by the negatively charged surface of the tryptophan indole ring, leading to an increased "hydrophobicity" of the RWQFP motif. The creation of this additional hydrophobic region in TpoR should alter the length of the TM domain as well as the resultant TM helix tilt angle (**Figure 6.2**).

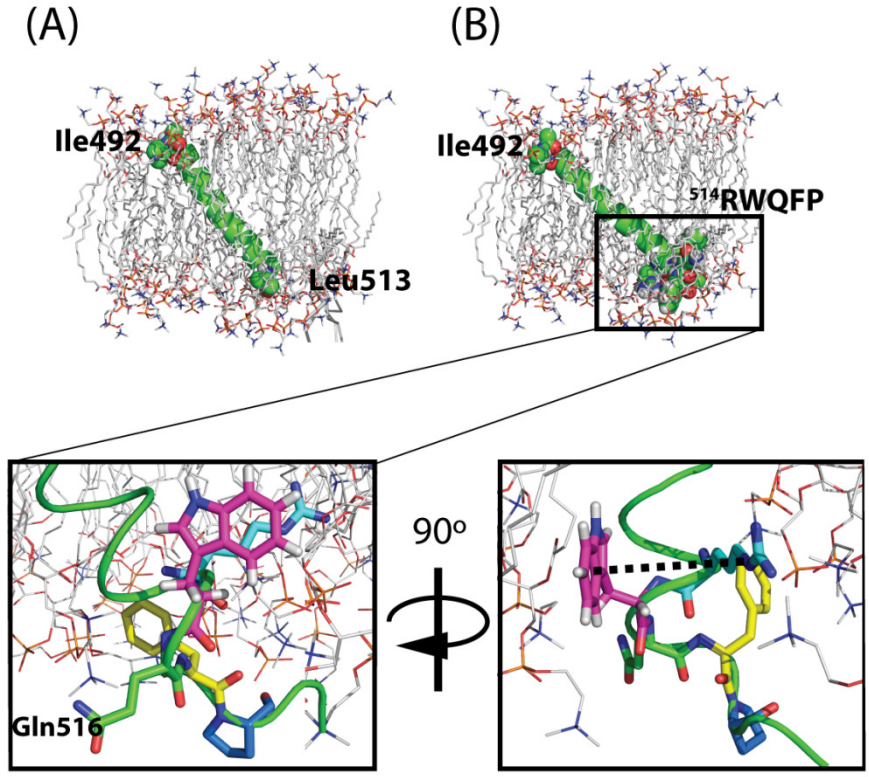

Figure 6.2: Effect of W515 on the TpoR TM helix orientation in the lipid bilayer. Schematic representation of the wild-type TpoR TM domain inserted into a DMPC bilayer. (A) The predicted TM domain of TpoR (I492 to L513) is embedded in the DMPC bilayer. The I492 and L513 residues are presented as spheres. (B) The predicted TM-JM region of TpoR (I492 to P518) is embedded in the DMPC bilayer. The I492 and R514 to P518 residues are presented as spheres. A cation-π interaction (shown in dotted line) between the indole ring of W515 and the cationic group of R514 increases the hydrophobicity of the RWQFP motif. As a result, a longer region, including the RWQFP motif, can be incorporated into the lipid bilayer, altering the TM helix tilt angle. The TM helix is shown in green. The R514, W515, Q516, F517, and P518 residues are highlighted in cyan, magenta, green, yellow, and blue, respectively. The hydrogen, nitrogen, and oxygen atoms of the amino acids are shown in white, blue, and red, respectively. The phosphorus and hydrocarbon atoms of a DMPC molecule are shown in orange and light gray, respectively.

In the case of the constitutively active W515K mutant, R514 should be placed outside of the cell membrane due to the lack of the W515-mediated cation-π interaction. Furthermore, the presence of the W515K residue, a hydrophilic amino acid, decreases the net hydrophobicity of the TpoR JM region. As a result, W515K may produce a shorter TM domain with a smaller TM helix tilt angle (**Figure 6.3A**). This effect of the W515K mutation on the TM helix may be

reversed by the Q516W mutation, which restores the hydrophobicity of the TM-JM region back to the wild-type level through a cation-π interaction with the lysine residue (**Figure 6.3B**).

Contrary to our model involving the TM helix tilt angle change, it has been proposed that long, hydrophilic amino acids, such as lysine and arginine, at the lipid-water boundary affect the length of a TM helix, but do not alter the helix orientation (*156*). Based on this model, the long and flexible side chain of R514 can stretch out its charged amino group towards water (i.e., cytoplasm) while keeping its hydrocarbon part embedded in the lipid bilayer. This phenomenon, termed "snorkeling", might change the length of the TpoR TM helix without affecting the helix tilt angle. Thus, it can be argued that the W515K mutation should not affect the overall tilt angle of the TM helix. However, such snorkeling of R514 at the cytoplasmic side of the cell membrane is energetically unfavorable because the Cα-Cβ bond of R514, which connects the charged group and the TM helix backbone, is oriented towards the extracellular side, rather than the cytoplasmic side of the membrane.

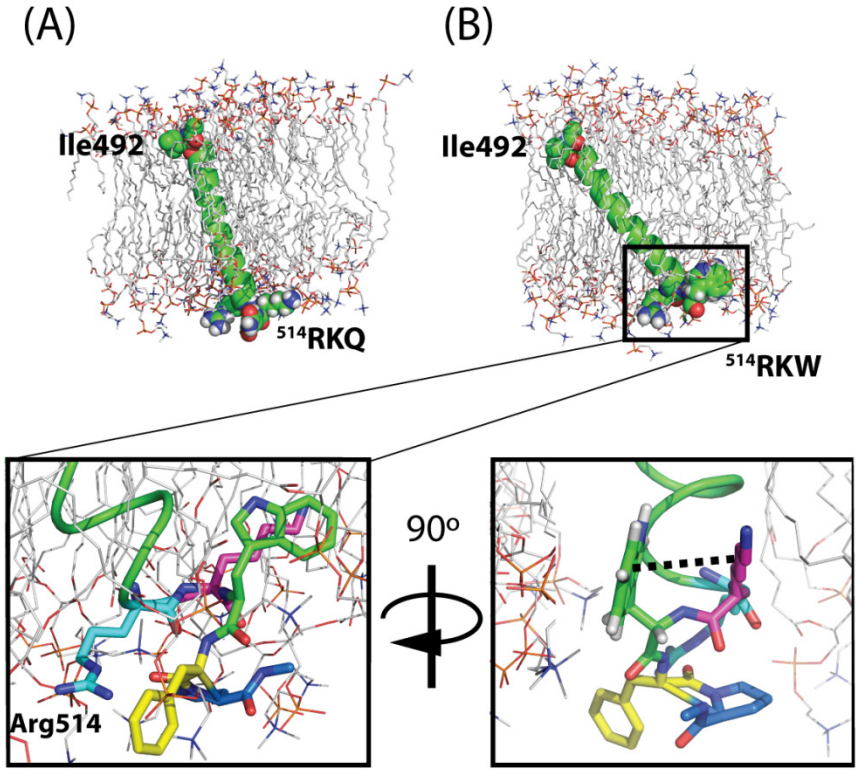

Figure 6.3: Effect of W515K and W515K/Q516W on the TpoR TM helix orientation in the lipid bilayer. Schematic representation of the mutant TpoR TM domains inserted into a DMPC bilayer. (A) The TpoR TM-JM region (I492-Q516) containing the W515K mutation is embedded in a DMPC bilayer. The ^{514}RKQ residues are shown as spheres. The W515K mutation creates a cluster of hydrophilic residues (^{514}RKQ), which tends to move outside of the lipid bilayer. This hydrophilic nature of the JM region and the lack of the cation-π interaction between W515 and R514 give rise to a relatively smaller TM helix tilt angle. The I492 and R514 to Q516 residues are presented as spheres. (B) The TpoR TM-JM region (I492-Q516) containing the W515K/Q516W revertant mutation is placed in a DMPC bilayer. The ^{514}RKW residues are shown as spheres. A cation-π interaction (shown in dotted line) between the indole ring of Q516W and the cationic group of W515K restores the hydrophobicity of the JM region to the normal level. As a result, a longer region, including the RKWFP motif, can be once again embedded in the lipid bilayer, fixing a proper TM helix tilt angle. The I492 and R514 to Q516W residues are presented as spheres. The TM helix is shown in green. The R514, W515K, Q516W, F517, and P518 residues are highlighted in cyan, magenta, green, yellow, and blue, respectively. The hydrogen, nitrogen, and oxygen atoms of the amino acids are shown in white, blue, and red, respectively. The phosphorus and hydrocarbon atoms of a DMPC molecule are shown in orange and light gray, respectively.

The aromatic amino acids (i.e., tryptophan, phenylalanine and tyrosine) share similar chemical properties, such as the ability to form cation-π interactions. Thus, theoretically, phenylalanine and tyrosine should functionally replace the role of W515 in controlling the TM helix tilt angle and receptor activity. However, these aromatic residues could not fully substitute

the function of W515 in TpoR-mediated JAK2-STAT signaling (**Figure 5.2**). A possible explanation for this result may be that neither the phenylalanine side chain (benzene) nor the tyrosine side chain (phenol) can form as strong a cation-π interaction as the tryptophan side chain (indole). Indeed, a computational study revealed that indole has the highest (most negative) electrostatic potential surface among three aromatic amino acid side chains (*157*). Furthermore, the Wimley-White interfacial hydrophobicity scale showed that a pentapeptide (W-L-*X*-L-L) has the highest (most negative) free energy of transfer from water to a lipid bilayer interface when tryptophan is placed at position "*X*" (*152*). This indicates that tryptophan at the lipid-water boundary has the strongest propensity to position itself towards the lipid head group, presumably via a cation-π interaction. On the other hand, phenylalanine and tyrosine give rise to the second and third highest transfer free energies, respectively, when they were incorporated into the peptide at position "*X*" (*152*). However, these free energies were lower than that of the peptide containing tryptophan at the same position (*152*). This difference in the thermodynamic property among those three aromatic residues may be the reason why the W515F and W515Y TpoR mutants could only partially maintain the inactive receptor state in the absence of Tpo (**Figure 5.2**).

6.3.6 Alternative models for the control of TpoR activity

In contrast to our model, a recent study using a dimerization-dependent transcription factor showed that the TpoR TM domain undergoes self-interaction in *E. coli* cell membranes, suggesting that two TM helices within a pre-formed TpoR dimer are associated with each other independently of ligand binding (*133*). Based on this result, it was proposed that the activation of

TpoR is regulated by rotation of the TM helices and the resultant switching of the TM-TM interaction interface. However, caution must be taken in interpreting the data obtained from this study as the TpoR TM peptide used for their analyses does not contain a complete RWQFP motif (includes only R514 and W515). It has been demonstrated that the RWQFP motif plays an essential role in maintaining the inactive TpoR state. Indeed, the insertion-deletion mutation in this motif (RWQFP to RKT) has been shown to cause MNP disorders (*34, 55*) (**Table 1.1**). Furthermore, the murine TpoR is known to be constitutively activated by deletion of the KWQFP motif, which corresponds to the human RWQFP motif (*96*). Moreover, our SE-AUC and deuterium MAS NMR data showed that the TpoR TM domain lacking the RWQFP motif, but not the wild-type TM domain, has a strong propensity to undergo self-interaction (**Figure 5.5**, **Table 5.1**). Thus, the TM helix rotation model, which presupposes a constant TM-TM interaction within a receptor dimer, may not be applied to the native TpoR.

Our study offered convincing evidence that W515 stabilizes the inactive receptor dimer state. However, W515 may not be the exclusive residue that contributes to this function. Indeed, the W515A/Q516W double mutant of TpoR still constitutively activates JAK2-STAT signaling even with the substitution of Q516 for tryptophan (**Figure 5.3**). Consistent with this constitutive receptor activity, the TM domain of the W515A/Q516W mutant strongly interacted with each other (**Figure 5.5**, **Table 5.1**). Thus, we cannot exclude the possibility that some other residues, in concert with W515, also play an indispensable role in the regulation of TpoR activity.

Furthermore, it should be noted that the helix tilt angle of the W515A/Q516W mutant TM domain was similar to that of the wild-type TM domain even though this mutant causes constitutive activation of TpoR. This observation suggests that the tryptophan at position 516 is

still functional for adjusting a proper TM helix orientation in the cell membrane, but cannot stabilize the inactive receptor state presumably due to the W515A mutation. Thus, the two processes, the control of the TM helix tilt angle and the resultant TM-TM association, may be uncoupled. A tryptophan residue in the JM region is sufficient for the former process, while the latter process may require other unknown conditions. To further investigate the TpoR activation mechanism, the W515A/Q516W double mutant will continue to be a great experimental tool.

6.4 Future experiments

We proposed that a tryptophan residue in the TpoR JM region regulates the transition between the active and inactive receptor states by modulating the TM helix tilt angle as well as the TM-TM interaction. However, the W515A/Q516W mutant did not fit this model; this double mutation causes constitutive receptor activation despite the presence of tryptophan in the JM region. We hypothesize that not only the presence of tryptophan, but also the size of the amino acid adjacent to the tryptophan, plays a critical role in inhibition of TM association. In the case of the W515A/Q516W double mutant, the alanine residue at position 515 may be small enough to allow formation of an aromatic stacking or a cation-π interaction between the two tryptophan residues at position 515, which then mediate TM association (**Figure 6.4**). On the other hand, neither W515L/Q516W nor W515K/Q516W constitutively activates TpoR because the presence of a relatively large residue at position 515 (leucine or lysine) does not allow enough space for such an aromatic stacking interaction. To test this hypothesis, we will generate a series of double mutants, such as W515G/Q516W, W515S/Q516W, and W515C/Q516W, and analyze the activity of each mutant TpoR by the dual luciferase reporter assay. In addition, we will examine

the effect of each double mutation on the TM helix tilt angle as well as a TM-TM interaction by ATR-FTIR and the split *G. princeps* luciferase reporter assay. We believe that such analyses will further advance our understanding on the TpoR activation mechanism.

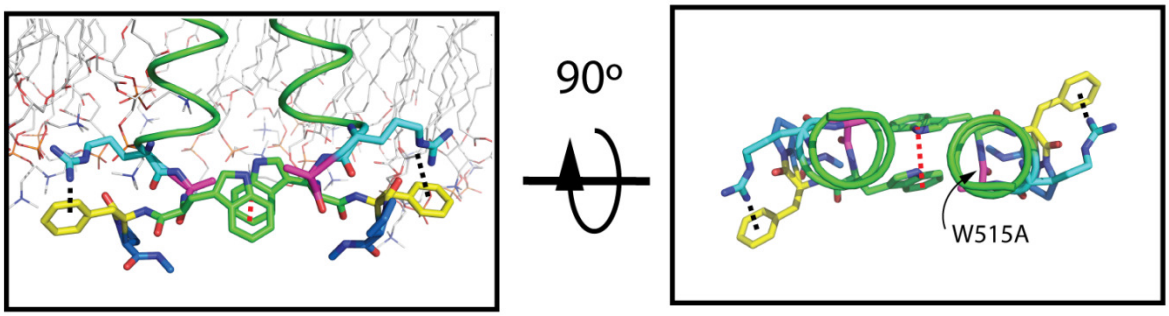

Figure 6.4: A possible mechanism by which the W515A/Q516W still allows constitutive activation of TpoR. Schematic representation of the W515A/Q516W TpoR TM domain inserted into a DMPC bilayer. The W515A/Q516W mutation may allow the Q516W to form a new aromatic stacking interaction (red dotted line). This interaction may facilitate TM association leading to constitutive activation of the JAK2-STAT signaling pathway. In addition, a cation- π interaction between R514 and F517 (black dotted line) may help to locate R514 into the lipid head group region of the bilayer. The R514, W515A, Q516W, F517, and P518 residues are highlighted in cyan, magenta, green, yellow, and blue, respectively. The hydrogen, nitrogen, and oxygen atoms of the amino acids are shown in white, blue, and red, respectively. The phosphorus and hydrocarbon atoms of a DMPC molecule are shown in orange and light gray, respectively. The lipid molecules are removed in the right panel for clarity.

6.5 Conclusions

Our study on TpoR revealed a novel activation mechanism for a single-pass transmembrane receptor. Furthermore, the data underscored the critical role of the TM-JM region, more specifically W515, in maintenance of the inactive receptor state. We propose that ligand binding to a TpoR monomer and/or a pre-formed TpoR dimer induces a TM helix tilt change, which in turn stabilizes an active receptor conformation via TM-TM interactions within the dimer. Is this model applicable to other single-pass transmembrane receptors? If so, how widespread is such an activation mechanism? Can we design new drugs against TpoR mutants based on our model? Is our model also useful for mutants of other single-pass transmembrane receptors? Future studies will likely answer these questions and pave the way to improvement in human health.

Bibliography

1. Bazan, J. F. (1990) Structural design and moleculara evolution of a cytokine receptor superfamily, *Proc. Natl. Acad. Sci. U. S. A. 87*, 6934-6938.

2. Vigon, I., Mornon, J. P., Cocault, L., Mitjavila, M. T., Tambourin, P., Gisselbrecht, S., and Souyri, M. (1992) Molecular-cloning and characterization of mpl, the human homolog of the v-mpl oncogene - identification of a member of the hematopoietic growth-factor receptor superfamily, *Proc. Natl. Acad. Sci. U. S. A. 89*, 5640-5644.

3. Liongue, C., and Ward, A. C. (2007) Evolution of class I cytokine receptors, *BMC Evol. Biol. 7*.

4. Pelletier, S., Gingras, S., Funakoshi-Tago, M., Howell, S., and Ihle, J. N. (2006) Two domains of the erythropoietin receptor are sufficient for Jak2 binding/activation and function, *Mol. Cell. Biol. 26*, 8527-8538.

5. Tong, W., Sulahian, R., Gross, A. W., Hendon, N., Lodish, H. F., and Huang, L. J. S. (2006) The membrane-proximal region of the thrombopoietin receptor confers its high surface expression by JAK2-dependent and -independent mechanisms, *J. Biol. Chem. 281*, 38930-38940.

6. Hintzen, C., Evers, C., Lippok, B. E., Volkmer, R., Heinrich, P. C., Radtke, S., and Hermanns, H. M. (2008) Box 2 region of the oncostatin M receptor determines specificity for recruitment of Janus kinases and STAT5 activation, *J. Biol. Chem. 283*, 19465-19477.

7. Miller, C. P., Liu, Z. Y., Noguchi, C. T., and Wojchowski, D. M. (1999) A minimal cytoplasmic subdomain of the erythropoietin receptor mediates erythroid and megakaryocytic cell development, *Blood 94*, 3381-3387.

8. Livnah, O., Stura, E. A., Johnson, D. L., Middleton, S. A., Mulcahy, L. S., Wrighton, N. C., Dower, W. J., Jolliffe, L. K., and Wilson, I. A. (1996) Functional mimicry of a protein hormone by a peptide agonist: The EPO receptor complex at 2.8 angstrom, *Science 273*, 464-471.

9. Wendling, F., Varlet, P., Charon, M., and Tambourin, P. (1986) MPLV: a retrovirus complex inducing an acute myeloproliferative leukemic disorder in adult mice, *Virology 149*, 242-246.

10. Souyri, M., Vigon, I., Penciolelli, J. F., Heard, J. M., Tambourin, P., and Wendling, F. (1990) A putative truncated cytokine receptor gene trasduced by the myeloproliferative leukemia-virus immortalizes hematopoietic progenitors, *Cell 63*, 1137-1147.

11. Bartley, T. D., Bogenberger, J., Hunt, P., Li, Y. S., Lu, H. S., Martin, F., Chang, M. S., Samal, B., Nichol, J. L., Swift, S., Johnson, M. J., Hsu, R. Y., Parker, V. P., Suggs, S., Skrine, J. D., Merewether, L. A., Clogston, C., Hsu, E., Hokom, M. M., Hornkohl, A., Choi, E., Pangelinan, M., Sun, Y., Mar, V., McNinch, J., Simonet, L., Jacobsen, F., Xie, C., Shutter, J., Chute, H., Basu, R., Selander, L., Trollinger, D., Sieu, L., Padilla, D., Trail, G., Elliott, G., Izumi, R., Covey, T., Crouse, J., Garcia, A., Xu, W., Delcastillo, J., Biron, J., Cole, S., Hu, M. C. T., Pacifici, R., Ponting, I., Saris, C., Wen, D., Yung, Y. P., Lin, H., and Bosselman, R. A. (1994) Identification and cloning of a megakaryocyte growth and development factor that is a ligand for the cytokine receptor Mpl, *Cell 77*, 1117-1124.

12. Methia, N., Louache, F., Vainchenker, W., and Wendling, F. (1993) Oligodeoxynucleotides antisense to the protooncogene c-mpl specifically inhibit in-vitro megakaryocytopoiesis, *Blood 82*, 1395-1401.

13. Kaushansky, K., Lok, S., Holly, R. D., Broudy, V. C., Lin, N., Bailey, M. C., Forstrom, J. W., Buddle, M. M., Oort, P. J., Hagen, F. S., Roth, G. J., Papayannopoulou, T., and Foster, D. C. (1994) Promotion of megakaryocyte progenitor expansion and differentiation by the c-Mpl ligand thrombopoietin, *Nature 369*, 568-571.

14. Kaushansky, K. (1994) The mpl ligand - molecular and cellular biology of the critical regulator of megakaryocyte development, *Stem Cells 12*, 91-97.

15. Debili, N., Wendling, F., Cosman, D., Titeux, M., Florindo, C., Dusanterfourt, I., Schooley, K., Methia, N., Charon, M., Nador, R., Bettaieb, A., and Vainchenker, W. (1995) The Mpi receptor is expressed in the megakaryocytic lineage from late progenitors to platelets, *Blood 85*, 391-401.

16. Kaushansky, K., Broudy, V. C., Lin, N., Jorgensen, M. J., McCarty, J., Fox, N., Zuckerfranklin, D., and Loftonday, C. (1995) Thrombopoietin, the Mpl ligand, is essential for full megakaryocyte development, *Proc. Natl. Acad. Sci. U. S. A. 92*, 3234-3238.

17. Jackson, C. W., Steward, S. A., Hutson, N. K., and McDonald, T. P. (1990) Genetic and physiological variations in megakaryocyte dna content distributions, *Int. J. Cell Cloning 8*, 260-266.

18. Stiff, P. J. (1990) Platelets, In *Clinical methods: the history, physical, and laboratory examinations* (Walker, H. K., Hall, W. D., and Hurst, J. W., Eds.) 3rd ed., pp 728-731, Butterworths, Boston.

19. Pang, L. Y., Weiss, M. J., and Poncz, M. (2005) Megakaryocyte biology and related disorders, *J. Clin. Invest. 115*, 3332-3338.

20. Cooper, B. (2005) Osler's role in defining the third corpuscle, or “blood plates”, *Proc. (Bayl. Univ. Med. Cent.) 18*, 376-378.

21. Kaushansky, K. (2008) Historical review: megakaryopoiesis and thrombopoiesis, *Blood 111*, 981-986.

22. Kaushansky, K., Lichtman, M. A., Beutler, E., Kipps, T. J., Seligsohn, U., and Prchal, J. T. (2010) *Williams hematology*, 8th ed., McGraw-Hill Professional.

23. Ihara, K., Ishii, E., Eguchi, M., Takada, H., Suminoe, A., Good, R. A., and Hara, T. (1999) Identification of mutations in the c-mpl gene in congenital amegakaryocytic thrombocytopenia, *Proc. Natl. Acad. Sci. U. S. A. 96*, 3132-3136.

24. van den Oudenrijn, S., Bruin, M., Folman, C. C., Peters, M., Faulkner, L. B., de Haas, M., and von dem Borne, A. (2000) Mutations in the thrombopoietin receptor, Mpl, in children with congenital amegakaryocytic thrombocytopenia, *Br. J. Haematol. 110*, 441-448.

25. Ballmaier, M., Germeshausen, M., Schulze, H., Cherkaoui, K., Lang, S., Gaudig, A., Krukemeier, S., Eilers, M., Strauss, G., and Welte, K. (2001) c-mpl mutations are the cause of congenital amegakaryocytic thrombocytopenia, *Blood 97*, 139-146.

26. Fox, N. E., Chen, R., Hitchcock, I., Keates-Baleeiro, J., Frangoul, H., and Geddis, A. E. (2009) Compound heterozygous c-Mpl mutations in a child with congenital amegakaryocytic thrombocytopenia: Functional characterization and a review of the literature, *Exp. Hematol. 37*, 495-503.

27. Muraoka, K., Ishii, E., Tsuji, K., Yamamoto, S., Yamaguchi, H., Hara, T., Koga, H., Nakahata, T., and Miyazaki, S. (1997) Defective response to thrombopoietin and impaired expression of c-mpl mRNA of bone marrow cells in congenital amegakaryocytic thrombocytopenia, *Br. J. Haematol. 96*, 287-292.

28. Walne, A. J., Dokal, A., Plagnol, V., Beswick, R., Kirwan, M., de la Fuente, J., Vulliamy, T., and Dokal, I. (2012) Exome sequencing identifies MPL as a causative gene in familial aplastic anemia, *Haematol-Hematol. J. 97*, 524-528.

29. Beer, P. A., Campbell, P. J., Scott, L. M., Bench, A. J., Erber, W. N., Bareford, D., Wilkins, B. S., Reilly, J. T., Hasselbalch, H. C., Bowman, R., Wheatley, K., Buck, G., Harrison, C. N., and Green, A. R. (2008) MPL mutations in myeloproliferative disorders: analysis of the PT-1 cohort, *Blood 112*, 141-149.

30. Pardanani, A. D., Levine, R. L., Lasho, T., Pikman, Y., Mesa, R. A., Wadleigh, M., Steensma, D. P., Elliott, M. A., Wolanskyj, A. R., Hogan, W. J., McClure, R. F., Litzow, M. R., Gilliland, D. G., and Tefferi, A. (2006) MPL515 mutations in myeloproliferative and other myeloid disorders: a study of 1182 patients, *Blood 108*, 3472-3476.

31. Tefferi, A., and Vardiman, J. W. (2008) Classification and diagnosis of myeloproliferative neoplasms: the 2008 World Health Organization criteria and point-of-care diagnostic algorithms, *Leukemia 22*, 14-22.

32. Pikman, Y., Lee, B. H., Mercher, T., McDowell, E., Ebert, B. L., Gozo, M., Cuker, A., Wernig, G., Moore, S., Galinsky, I., DeAngelo, D. J., Clark, J. J., Lee, S. J., Golub, T. R., Wadleigh, M., Gilliland, D. G., and Levine, R. L. (2006) MPLW515L is anovel somatic activating mutation in myelofibrosis with myeloid metaplasia, *PLoS Medicine 3*, 1140-1151.

33. Chaligne, R., Tonetti, C., Besancenot, R., Roy, L., Marty, C., Mossuz, P., Kiladjian, J. J., Socie, G., Bordessoule, D., Le Bousse-Kerdiles, M. C., Vainchenker, W., and Giraudier, S. (2008) New mutations of MPL in primitive myelofibrosis: only the MPL W515 mutations promote a G(1)/S-phase transition, *Leukemia 22*, 1557-1566.

34. Ma, W., Zhang, X., Wang, X., Zhang, Z., Yeh, C.-H., Uyeji, J., and Albitar, M. (2011) MPL mutation profile in JAK2 mutation-negative patients with myeloproliferative disorders, *Diagn. Mol. Pathol. 20*, 34-39.

35. Ding, F., Komatsu, H., Wakita, A., Kato-Uranishi, M., Ito, M., Satoh, A., Tsuboi, K., Nitta, M., Miyazaki, H., Lida, S., and Ueda, R. (2004) Familial essential thrombocythemia associated with a dominant-positive activating mutation of the c-MPL gene, which encodes for the receptor for thrombopoietin, *Blood 103*, 4198-4200.

36. Liu, K., Martini, M., Rocca, B., Amos, C. I., Teofili, L., Giona, F., Ding, J., Komatsu, H., Larocca, L. M., and Skoda, R. C. (2009) Evidence for a founder effect of the MPL-S505N mutation in eight Italian pedigrees with hereditary thrombocythemia, *Haematol-Hematol. J. 94*, 1368-1374.

37. Teofili, L., Giona, F., Torti, L., Cenci, T., Ricerca, B. M., Rumi, C., Nunes, V., Foa, R., Leone, G., Martini, M., and Larocca, L. M. (2010) Hereditary thrombocytosis caused by MPL Ser505Asn is associated with a high thrombotic risk, splenomegaly and progression to bone marrow fibrosis, *Haematol-Hematol. J. 95*, 65-70.

38. Ding, J., Komatsu, H., Iida, S., Yano, H., Kusumoto, S., Inagaki, A., Mori, F., Ri, M., Ito, A., Wakita, A., Ishida, T., Nitta, M., and Ueda, R. (2009) The Asn505 mutation of the c-MPL gene, which causes familial essential thrombocythemia, induces autonomous homodimerization of the c-Mpl protein due to strong amino acid polarity, *Blood 114*, 3325-3328.

39. Fox, C. B., Wayment, J. R., Myers, G. A., Endicott, S. K., and Harris, J. M. (2009) Single-molecule fuorescence imaging of peptide binding to supported lipid bilayers, *Anal. Chem. 81*, 5130-5138.

40. Germeshausen, M., Ballmaier, M., and Welte, K. (2006) MPL mutations in 23 patients suffering from congenital amegakaryocytic thrombocytopenia: the type of mutation predicts the course of the disease, *Hum. Mutat. 27*, 296-301.

41. Savoia, A., Dufour, C., Locatelli, F., Noris, P., Ambaglio, C., Rosti, V., Zecca, M., Ferrari, S., di Bari, F., Corcione, A., Di Stazio, M., Seri, M., and Balduini, C. L. (2007) Congenital amegakavyocytic thrombocytopenia: clinical and biological consequences of five novel mutations, *Haematol-Hematol. J. 92*, 1186-1193.

42. Steinberg, O., Gilad, G., Dgany, O., Krasnov, T., Zoldan, M., Laor, R., Kapelushnik, J., Gabriel, H., Churi, C., Stein, J., Yaniv, I., and Tamary, H. (2007) Congenital amegakaryocytic thrombocytopenia - 3 novel c-MPL mutations and their phenotypic correlations, *J. Pediatr. Hematol. Oncol. 29*, 822-825.

43. Passos-Coelho, J. L., Sebastiao, M., Gameiro, P., Reichert, A., Vieira, L., Ferreira, I., Miranda, N., Guimaraes, A., Leal-da-Costa, F., and Abecasis, M. M. (2007) Congenital amegakaryocytic thrombocytopenia - report of a new c-mpl gene missense mutation, *Am. J. Hematol. 82*, 240-241.

44. Kawamata, N., Ogawa, S., Yamamoto, G., Lehmann, S., Levine, R. L., Pikman, Y., Nannya, Y., Sanada, M., Miller, C. W., Gilliland, D. G., and Koeffler, H. P. (2008) Genetic profiling of myeloproliferative disorders by single-nucleotide polymorphism oligonucleotide microarray, *Exp. Hematol. 36*, 1471-1479.

45. Williams, D. M., Kim, A. H., Rogers, O., Spivak, J. L., and Molitemo, A. R. (2007) Phenotypic variations and new mutations in JAK2 V617F-neagative polycythemia vera, erythrocytosis, and idiopathic myelofibrosis, *Exp. Hematol. 35*, 1641-1646.

46. Lambert, M. P., Jiang, J., Batra, V., Wu, C., and Tong, W. (2012) A novel mutation in MPL (Y252H) results in increased thrombopoietin sensitivity in essential thrombocythemia, *Am. J. Hematol. 87*, 532-534.

47. Malinge, S., Ragu, C., Della-Valle, V., Pisani, D., Constantinescu, S. N., Perez, C., Villeval, J. L., Reinhardt, D., Landman-Parker, J., Michaux, L., Dastugue, N., Baruchel, A., Vainchenker, W., Bourquin, J. P., Penard-Lacronique, V., and Bernard, O. A. (2008) Activating mutations in human acute megakaryoblastic leukemia, *Blood 112*, 4220-4226.

48. Siemiatkowska, A., Bieniaszewska, M., Hellmann, A., and Limon, J. (2010) JAK2 and MPL gene mutations in V617F-negative myeloproliferative neoplasms, *Leukemia Res. 34*, 387-389.

49. Pietra, D., Brisci, A., Rumi, E., Boggi, S., Elena, C., Pietrelli, A., Bordoni, R., Ferrari, M., Passamonti, F., De Bellis, G., Cremonesi, L., and Cazzola, M. (2011) Deep sequencing

reveals double mutations in cis of MPL exon 10 in myelloproliferative neoplasm's, *Haematol-Hematol. J. 96*, 607-611.

50. Boyd, E. M., Bench, A. J., Goday-Fernandez, A., Anand, S., Vaghela, K. J., Beer, P., Scott, M. A., Bareford, D., Green, A. R., Huntly, B., and Erber, W. N. (2010) Clinical utility of routine MPL exon 10 analysis in the diagnosis of essential thrombocythaemia and primary myelofibrosis, *Br. J. Haematol. 149*, 250-257.

51. Schnittger, S., Bacher, U., Haferlach, C., Beelen, D., Bojko, P., Buerkle, D., Dengler, R., Distelrath, A., Eckart, M., Eckert, R., Fries, S., Knoblich, J., Koechling, G., Laubenstein, H.-P., Petrides, P., Planker, M., Pihusch, R., Weide, R., Kern, W., and Haferlach, T. (2009) Characterization of 35 new cases with four different MPLW515 mutations and essential thrombocytosis or primary myelofibrosis, *Haematol-Hematol. J. 94*, 141-144.

52. Millecker, L., Lennon, P. A., Verstovsek, S., Barkoh, B., Galbincea, J., Hu, P., Chen, S. S., and Jones, D. (2010) Distinct patterns of cytogenetic and clinical progression in chronic myeloproliferative neoplasms with or without JAK2 or MPL mutations, *Cancer Genet. Cytogenet. 197*, 1-7.

53. Ruan, G.-R., Jiang, B., Li, L.-D., Niu, J.-H., Li, J.-L., Xie, M., Qin, Y.-Z., Liu, Y.-R., Huang, X.-J., and Chen, S.-S. (2010) MPL W515L/K mutations in 343 Chinese adults with JAK2V617F mutation-negative chronic myeloproliferative disorders detected by a newly developed RQ-PCR based on Taq Man MGB probes, *Hematol. Oncol. 28*, 33-39.

54. Vannucchi, A. M., Antonioli, E., Guglielmelli, P., Pancrazzi, A., Guerini, V., Barosi, G., Ruggeri, M., Specchia, G., Lo-Coco, F., Delaini, F., Villani, L., Finotto, S., Ammatuna, E., Alterini, R., Carrai, V., Capaccioli, G., Di Lollo, S., Liso, V., Rambaldi, A., Bosi, A., and Barbui, T. (2008) Characteristics and clinical correlates of MPL 515W > L/K mutation in essential thrombocythemia, *Blood 112*, 844-847.

55. Ohashi, H., Arita, K., Fukami, S., Oguri, K., Nagai, H., Yokozawa, T., Hotta, T., and Hanada, S. (2009) Two rare MPL gene mutations in patients with essential thrombocythemia, *Int. J. Hematol. 90*, 431-432.

56. Kisseleva, T., Bhattacharya, S., Braunstein, J., and Schindler, C. W. (2002) Signaling through the JAK/STAT pathway, recent advances and future challenges, *Gene 285*, 1-24.

57. Shuai, K., and Liu, B. (2003) Regulation of JAK-STAT signalling in the immune system, *Nature Reviews Immunology 3*, 900-911.

58. Ezumi, Y., Takayama, H., and Okuma, M. (1995) Thrombopoietin, c-Mpl ligand, induces tyrosine phosphorylation of Tyk2, JAK2, and STAT3, and enhances agonists-induced aggregation in platelets in-vitro, *FEBS Lett. 374*, 48-52.

59. Feng, J., Witthuhn, B. A., Matsuda, T., Kohlhuber, F., Kerr, I. M., and Ihle, J. N. (1997) Activation of Jak2 catalytic activity requires phosphorylation of Y-1007 in the kinase activation loop, *Mol. Cell. Biol. 17*, 2497-2501.

60. Drachman, J. G., and Kaushansky, K. (1997) Dissecting the thrombopoietin receptor: Functional elements of the Mpl cytoplasmic domain, *Proc. Natl. Acad. Sci. U. S. A. 94*, 2350-2355.

61. Gaur, M., Murphy, G. J., deSauvage, F. J., and Leavitt, A. D. (2001) Characterization of MPl mutants using primary megakaryocyte-lineage cells from mpl(-/-) mice: a new system for Mpl structure-function studies, *Blood 97*, 1653-1661.

62. Shuai, K., Horvath, C. M., Huang, L. H. T., Qureshi, S. A., Cowburn, D., and Darnell, J. E. (1994) Interferon activation of the transcription factor Stat91 involves dimerization through SH2-phosphotyrosyl peptide interactions, *Cell 76*, 821-828.

63. Yamaoka, K., Saharinen, P., Pesu, M., Holt, V. E. T., Silvennoinen, O., and O'Shea, J. J. (2004) The Janus kinases (Jaks), *Genome Biol. 5*, 253.

64. Manning, G., Whyte, D. B., Martinez, R., Hunter, T., and Sudarsanam, S. (2002) The protein kinase complement of the human genome, *Science 298*, 1912-1934.

65. Rane, S. G., and Reddy, E. P. (2000) Janus kinases: components of multiple signaling pathways, *Oncogene 19*, 5662-5679.

66. Feener, E. P., Rosario, F., Dunn, S. L., Stancheva, Z., and Myers, M. G. (2004) Tyrosine phosphorylation of Jak2 in the JH2 domain inhibits cytokine signaling, *Mol. Cell. Biol. 24*, 4968-4978.

67. Argetsinger, L. S., Kouadio, J. L. K., Steen, H., Stensballe, A., Jensen, O. N., and Carter-Su, C. (2004) Autophosphorylation of JAK2 on tyrosines 221 and 570 regulates its activity, *Mol. Cell. Biol. 24*, 4955-4967.

68. Geddis, A. E., Linden, H. M., and Kaushansky, K. (2002) Thrombopoietin: a pan-hematopoietic cytokine, *Cytokine Growth Factor Rev. 13*, 61-73.

69. Kaushansky, K. (2003) Thrombopoietin: a tool for understanding thrombopoiesis, *J. Thromb. Haemost. 1*, 1587-1592.

70. Hitchcock, I. S., Chen, M. M., King, J. R., and Kaushansky, K. (2008) YRRL motifs in the cytoplasmic domain of the thrombopoietin receptor regulate receptor internalization and degradation, *Blood 112*, 2222-2231.

71. Carter-Su, C., Rui, L. Y., and Stofega, M. R. (2000) SH2-B and SIRP: JAK2 binding proteins that modulate the actions of growth hormone, In *Recent Progress in Hormone Research, Vol 55: Proceedings of the 1999 Conference* (Conn, P. M., Ed.), pp 293-311, Endocrine Soc, Bethesda.

72. Greenhalgh, C. J., and Hilton, D. J. (2001) Negative regulation of cytokine signaling, *J. Leukocyte Biol. 70*, 348-356.

73. Endo, T. A., Masuhara, M., Yokouchi, M., Suzuki, R., Sakamoto, H., Mitsui, K., Matsumoto, A., Tanimura, S., Ohtsubo, M., Misawa, H., Miyazaki, T., Leonor, N., Taniguchi, T., Fujita, T., Kanakura, Y., Komiya, S., and Yoshimura, A. (1997) A new protein containing an SH2 domain that inhibits JAK kinases, *Nature 387*, 921-924.

74. Chung, C. D., Liao, J. Y., Liu, B., Rao, X. P., Jay, P., Berta, P., and Shuai, K. (1997) Specific inhibition of Stat3 signal transduction by PIAS3, *Science 278*, 1803-1805.

75. Heldin, C.-H. (1995) Dimerization of cell surface receptors in signal transduction, *Cell 80*, 213-223.

76. Constantinescu, S. N., Keren, T., Socolovsky, M., Nam, H. S., Henis, Y. I., and Lodish, H. F. (2001) Ligand-independent oligomerization of cell-surface erythropoietin receptor is mediated by the transmembrane domain, *Proc. Natl. Acad. Sci. U. S. A. 98*, 4379-4384.

77. Livnah, O., Stura, E. A., Middleton, S. A., Johnson, D. L., Jolliffe, L. K., and Wilson, I. A. (1999) Crystallographic evidence for preformed dimers of erythropoietin receptor before ligand activation, *Science 283*, 987-990.

78. Brown, R. J., Adams, J. J., Pelekanos, R. A., Wan, Y., McKinstry, W. J., Palethorpe, K., Seeber, R. M., Monks, T. A., Eidne, K. A., Parker, M. W., and Waters, M. J. (2005) Model for growth hormone receptor activation based on subunit rotation within a receptor dimer, *Nat. Struct. Mol. Biol. 12*, 814-821.

79. Yang, N., Wang, X., Jiang, J., and Frank, S. J. (2007) Role of the growth hormone (GH) receptor transmembrane domain in receptor predimerization and GH-induced activation, *Mol. Endocrinol. 21*, 1642-1655.

80. Gadd, S. L., and Clevenger, C. V. (2006) Ligand-independent dimerization of the human prolactin receptor isoforms: Functional implications, *Mol. Endocrinol. 20*, 2734-2746.

81. Qazi, A. M., Tsai-Morris, C. H., and Dufau, M. L. (2006) Ligand-independent homo- and heterodimerization of human prolactin receptor variants: inhibitory action of the short forms by heterodimerization, *Mol. Endocrinol. 20*, 1912-1923.

82. Ebie, A. Z., and Fleming, K. G. (2007) Dimerization of the erythropoietin receptor transmembrane domain in micelles, *J. Mol. Biol. 366*, 517-524.

83. Kubatzky, K. F., Ruan, W. M., Gurezka, R., Cohen, J., Ketteler, R., Watowich, S. S., Neumann, D., Langosch, D., and Klingmüller, U. (2001) Self assembly of the transmembrane domain promotes signal transduction through the erythropoietin receptor, *Curr. Biol. 11*, 110-115.

84. Waters, M. J., and Brooks, A. J. (2011) Growth hormone receptor: structure function relationships, *Horm. Res. Paediatr. 76*, 12-16.

85. Syed, R. S., Reid, S. W., Li, C. W., Cheetham, J. C., Aoki, K. H., Liu, B. S., Zhan, H. J., Osslund, T. D., Chirino, A. J., Zhang, J. D., Finer-Moore, J., Elliott, S., Sitney, K., Katz, B. A., Matthews, D. J., Wendoloski, J. J., Egrie, J., and Stroud, R. M. (1998) Efficiency of signalling through cytokine receptors depends critically on receptor orientation, *Nature 395*, 511-516.

86. Seubert, N., Royer, Y., Staerk, J., Kubatzky, K. F., Moucadel, V., Krishnakumar, S., Smith, S. O., and Constantinescu, S. N. (2003) Active and inactive orientations of the transmembrane and cytosolic domains of the erythropoietin receptor dimer, *Mol. Cell 12*, 1239-1250.

87. Constantinescu, S. N., Huang, L. J. S., Nam, H. S., and Lodish, H. F. (2001) The erythropoietin receptor cytosolic juxtamembrane domain contains an essential, precisely oriented, hydrophobic motif, *Mol. Cell 7*, 377-385.

88. Kubatzky, K. F., Liu, W., Goldgraben, K., Simmerling, C., Smith, S. O., and Constantinescu, S. N. (2005) Structural requirements of the extracellular to transmembrane domain junction for erythropoietin receptor function, *J. Biol. Chem. 280*, 14844-14854.

89. Lu, X. H., Gross, A. W., and Lodish, H. F. (2006) Active conformation of the erythropoietin receptor: Random and cysteine-scanning mutagenesis of the extracellular juxtamembrane and transmembrane domains, *J. Biol. Chem. 281*, 7002-7011.

90. Walters, K. J., Dayie, K. T., Reece, R. J., Ptashne, M., and Wagner, G. (1997) Structure and mobility of the PUT3 dimer, *Nat. Struct. Biol. 4*, 744-750.

91. Staerk, J., Defour, J.-P., Pecquet, C., Leroy, E., Antoine-Poirel, H., Brett, I., Itaya, M., Smith, S. O., Vainchenker, W., and Constantinescu, S. N. (2011) Orientation-specific signalling by thrombopoietin receptor dimers, *EMBO J. 30*, 4398-4413.

92. Glembotsky, A. C., Korin, L., Lev, P. R., Chazarreta, C. D., Marta, R. F., Molinas, F. C., and Heller, P. G. (2010) Screening for MPL mutations in essential thrombocythemia and

primary myelofibrosis: normal Mpl expression and absence of constitutive STAT3 and STAT5 activation in MPLW515L-positive platelets, *Eur. J. Haematol. 84*, 398-405.

93. Bargmann, C. I., Hung, M. C., and Weinberg, R. A. (1986) Multiple independent activations of the neu oncogene by a point mutation altering the transmembrane domain of p185, *Cell 45*, 649-657.

94. Smith, S. O., Smith, C., Shekar, S., Peersen, O., Ziliox, M., and Aimoto, S. (2002) Transmembrane interactions in the activation of the Neu receptor tyrosine kinase, *Biochemistry 41*, 9321-9332.

95. Li, E., You, M., and Hristova, K. (2006) FGFR3 dimer stabilization due to a single amino acid pathogenic mutation, *J. Mol. Biol. 356*, 600-612.

96. Staerk, J., Lacout, C., Sato, T., Smith, S. O., Vainchenker, W., and Constantinescu, S. N. (2006) An amphipathic motif at the transmembrane-cytoplasmic junction prevents autonomous activation of the thrombopoietin receptor, *Blood 107*, 1864-1871.

97. Fisher, L. E., and Engelman, D. M. (2001) High-yield synthesis and purification of an α-helical transmembrane domain, *Anal. Biochem. 293*, 102-108.

98. Kent, S. B. H. (1988) Chemical Synthesis of Peptides and Proteins, *Annu. Rev. Biochem. 57*, 957-989.

99. Lew, S., and London, E. (1997) Simple procedure for reversed-phase high-performance liquid chromatographic purification of long hydrophobic peptides that form transmembrane helices, *Anal. Biochem. 251*, 113-116.

100. Nallamsetty, S., and Waugh, D. S. (2007) A generic protocol for the expression and purification of recombinant proteins in *Escherichia coli* using a combinatorial His6-maltose binding protein fusion tag, *Nat. Protoc. 2*, 383-391.

101. Hu, J., Qin, H., Li, C., Sharma, M., Cross, T. A., and Gao, F. P. (2007) Structural biology of transmembrane domains: Efficient production and characterization of transmembrane peptides by NMR, *Protein Sci. 16*, 2153-2165.

102. Sulistijo, E. S., and MacKenzie, K. R. (2009) Structural basis for dimerization of the BNIP3 transmembrane domain, *Biochemistry 48*, 5106-5120.

103. Kochendoerfer, G. G., Salom, D., Lear, J. D., Wilk-Orescan, R., Kent, S. B. H., and DeGrado, W. F. (1999) Total chemical synthesis of the integral membrane protein influenza A virus M2: Role of its C-terminal domain in tetramer, *Biochemistry 38*, 11905-11913.

104. Mimms, L. T., Zampighi, G., Nozaki, Y., Tanford, C., and Reynolds, J. A. (1981) Phospholipid vesicle formation and transmembrane protein incorporation using octyl glucoside, *Biochemistry 20*, 833-840.

105. Laue, T. M., Shah, B., Ridgeway, T. M., and Pelletier, S. L. (1992) Computer-aided interpretation of analytical sedimentation data for proteins, In *Analytical Ultracentrifugation in Biochemistry and Polymer Science* (Harding, S. E., Rowe, A. J., and Horton, J. C., Eds.), pp 90-125, Royal Society of Chemistry, Cambridge, UK.

106. Smith, S. O., Eilers, M., Song, D., Crocker, E., Ying, W. W., Groesbeek, M., Metz, G., Ziliox, M., and Aimoto, S. (2002) Implications of threonine hydrogen bonding in the glycophorin A transmembrane helix dimer, *Biophys. J. 82*, 2476-2486.

107. Tamm, L. K., and Tatulian, S. A. (1997) Infrared spectroscopy of proteins and peptides in lipid bilayers, *Q. Rev. Biophys. 30*, 365-429.

108. Arkin, I. T., MacKenzie, K. R., and Brünger, A. T. (1997) Site-directed dichroism as a method for obtaining rotational and orientational constraints for oriented polymers, *J. Am. Chem. Soc. 119*, 8973-8980.

109. Harrick, N. J. (1967) *Internal Reflection Spectroscopy*, Interscience Publishers, New York.

110. Bechinger, B., Ruysschaert, J. M., and Goormaghtigh, E. (1999) Membrane helix orientation from linear dichroism of infrared attenuated total reflection spectra, *Biophys. J. 76*, 552-563.

111. Siminovitch, D. J., Ruocco, M. J., Olejniczak, E. T., Das Gupta, S. K., and Griffin, R. G. (1988) Anisotropic ^{2}H-nuclear magnetic resonance spin-lattice relaxation in cerebroside- and phospholipid-cholesterol bilayer membranes, *Biophys. J. 54*, 373-381.

112. Bloom, M., and Smith, I. C. P. (1985) Manifestations of lipid-protein interactions in deuterium NMR, In *Progress in Protein-Lipid Interactions* (Watts, A., and De Pont, J. J. H. H. M., Eds.), pp 61-88, Elsevier, Amsterdam.

113. Ying, W. W., Irvine, S. E., Beekman, R. A., Siminovitch, D. J., and Smith, S. O. (2000) Deuterium NMR reveals helix packing interactions in phospholamban, *J. Am. Chem. Soc. 122*, 11125-11128.

114. Liu, W., Crocker, E., Constantinescu, S. N., and Smith, S. O. (2005) Helix packing and orientation in the transmembrane dimer of gp55-P of the spleen focus forming virus, *Biophys. J. 89*, 1194-1202.

115. Adams, P. D., Engelman, D. M., and Brünger, A. T. (1996) Improved prediction for the structure of the dimeric transmembrane domain of glycophorin A obtained through global searching, *Proteins. 26*, 257-261.

116. Royer, Y., Staerk, J., Costuleanu, M., Courtoy, P. J., and Constantinescu, S. N. (2005) Janus kinases affect thrombopoietin receptor cell surface localization and stability, *J. Biol. Chem. 280*, 27251-27261.

117. Dumoutier, L., Van Roost, E., Colau, D., and Renauld, J. C. (2000) Human interleukin-10-related T cell-derived inducible factor: molecular cloning and functional characterization as an hepatocyte-stimulating factor, *Proc. Natl. Acad. Sci. U. S. A. 97*, 10144-10149.

118. Remy, I., and Michnick, S. W. (2006) A highly sensitive protein-protein interaction assay based on Gaussia luciferase, *Nat. Methods 3*, 977-979.

119. Pear, W. S., Nolan, G. P., Scott, M. L., and Baltimore, D. (1993) Production of high-titer helper-free retroviruses by transient transfection, *Proc. Natl. Acad. Sci. U. S. A. 90*, 8392-8396.

120. Kohlhuber, F., Rogers, N. C., Watling, D., Feng, J., Guschin, D., Briscoe, J., Witthuhn, B. A., Kotenko, S. V., Pestka, S., Stark, G. R., Ihle, J. N., and Kerr, I. M. (1997) A JAK1/JAK2 chimera can sustain alpha and gamma interferon responses, *Mol. Cell. Biol. 17*, 695-706.

121. MacKenzie, K. R. (1996) Structure determination of the dimeric membrane spanning domain of glycophorin A in detergent micelles by triple resonance nuclear magnetic resonance (Ph.D. thesis), In *Molecular Biophysics and Biochemistry*, Yale University, New Haven, CT.

122. Lemmon, M. A., Flanagan, J. M., Hunt, J. F., Adair, B. D., Bormann, B. J., Dempsey, C. E., and Engelman, D. M. (1992) Glycophorin A dimerization is driven by specific interactions between transmembrane α-helices, *J. Biol. Chem. 267*, 7683-7689.

123. Adair, B. D., and Engelman, D. M. (1994) Glycophorin A helical transmembrane domains dimerize in phospholipid bilayers: a resonance energy transfer study, *Biochemistry 33*, 5539-5544.

124. Yu, X. C., Sharma, K. D., Takahashi, T., Iwamoto, R., and Mekada, E. (2002) Ligand-independent dimer formation of epidermal growth factor receptor (EGFR) is a step separable from ligand-induced EGFR signaling, *Mol. Biol. Cell 13*, 2547-2557.

125. Chantry, A. (1995) The kinase domain and membrane localization determine intracellular interactions between epidermal growth-factor receptors, *J. Biol. Chem. 270*, 3068-3073.

126. Jura, N., Endres, N. F., Engel, K., Deindl, S., Das, R., Lamers, M. H., Wemmer, D. E., Zhang, X. W., and Kuriyan, J. (2009) Mechanism for activation of the EGF receptor catalytic domain by the juxtamembrane segment, *Cell 137*, 1293-1307.

127. Barleon, B., Totzke, F., Herzog, C., Blanke, S., Kremmer, E., Siemeister, G., Marme, D., and MartinyBaron, G. (1997) Mapping of the sites for ligand binding and receptor dimerization at the extracellular domain of the vascular endothelial growth factor receptor FLT-1, *J. Biol. Chem. 272*, 10382-10388.

128. Gurezka, R., Laage, R., Brosig, B., and Langosch, D. (1999) A heptad motif of leucine residues found in membrane proteins can drive self-assembly of artificial transmembrane segments, *J. Biol. Chem. 274*, 9265-9270.

129. Ruan, W. M., Becker, V., Klingmüller, U., and Langosch, D. (2004) The interface between self-assembling erythropoietin receptor transmembrane segments corresponds to a membrane-spanning leucine zipper, *J. Biol. Chem. 279*, 3273-3279.

130. Brett, I. C. (2012) Transmembrane domain structure and function in the erythropoietin receptor (Ph.D. thesis), In *Department of Biochemistry and Cell Biology*, Stony Brook University, Stony Brook, NY.

131. Landschulz, W. H., Johnson, P. F., and McKnight, S. L. (1988) The leucine zipper: A hypothetical structure common to a new class of DNA binding proteins, *Science 240*, 1759-1764.

132. Eilers, M., Patel, A. B., Liu, W., and Smith, S. O. (2002) Comparison of helix interactions in membrane and soluble α-bundle proteins, *Biophys. J. 82*, 2720-2736.

133. Matthews, E. E., Thevenin, D., Rogers, J. M., Gotow, L., Lira, P. D., Reiter, L. A., Brissette, W. H., and Engelman, D. M. (2011) Thrombopoietin receptor activation: transmembrane helix dimerization, rotation, and allosteric modulation, *FASEB J. 25*, 2234-2244.

134. Fuh, G., Cunningham, B. C., Fukunaga, R., Nagata, S., Goeddel, D. V., and Wells, J. A. (1992) rational design of potent antagonists to the human growth-hormone receptor, *Science 256*, 1677-1680.

135. Lemmon, M. A., and Schlessinger, J. (2010) Cell signaling by receptor tyrosine kinases, *Cell 141*, 1117-1134.

136. Meyers, G. A., Orlow, S. J., Munro, I. R., Przylepa, K. A., and Jabs, E. W. (1995) Fibroblast-growth-factor-receptor-3 (FGFR3) transmembrane mutation in Crouzon-syndrome with Acanthosis nigricans, *Nat. Genet. 11*, 462-464.

137. Demeler, B. (2005) UltraScan - a comprehensive data analysis software package for analytical ultracentrifugation experiments, In *Modern analytical ultracentrifugation: techniques and methods* (Scott, D. J., Harding, S. E., and Rowe, A. J., Eds.), pp 210-229, Royal society of chemistry, UK.

138. Onishi, M., Mui, A. L., Morikawa, Y., Cho, L., Kinoshita, S., Nolan, G. P., Gorman, D. M., Miyajima, A., and Kitamura, T. (1996) Identification of an oncogenic form of the thrombopoietin receptor MPL using retrovirus-mediated gene transfer, *Blood 88*, 1399-1406.

139. Gratkowski, H., Lear, J. D., and DeGrado, W. F. (2001) Polar side chains drive the association of model transmembrane peptides, *Proc. Natl. Acad. Sci. U. S. A. 98*, 880-885.

140. Stockner, T., Ash, W. L., MacCallum, J. L., and Tieleman, D. P. (2004) Direct simulation of transmembrane helix association: Role of asparagines, *Biophys. J. 87*, 1650-1656.

141. Choma, C., Gratkowski, H., Lear, J. D., and DeGrado, W. F. (2000) Asparagine-mediated self-association of a model transmembrane helix, *Nat. Struct. Biol. 7*, 161-166.

142. Lear, J. D., Gratkowski, H., Adamian, L., Liang, J., and DeGrado, W. F. (2003) Position-dependence of stabilizing polar interactions of asparagine in transmembrane helical bundles, *Biochemistry 42*, 6400-6407.

143. Bargmann, C. I., Hung, M. C., and Weinberg, R. A. (1986) The neu oncogene encodes an epidermal growth factor receptor-related protein, *Nature 319*, 226-230.

144. Chen, F., Degnin, C., Laederich, M., Horton, W. A., and Hristova, K. (2011) The A391E mutation enhances FGFR3 activation in the absence of ligand, *Biochim. Biophys. Acta 1808*, 2045-2050.

145. Tefferi, A. (1998) The Philadelphia chromosome negative chronic myeloproliferative disorders: A practical overview, *Mayo Clin. Proc. 73*, 1177-1184.

146. Liu, W., Crocker, E., Siminovitch, D. J., and Smith, S. O. (2003) Role of side-chain conformational entropy in transmembrane helix dimerization of glycophorin A, *Biophys. J. 84*, 1263-1271.

147. Holt, A., and Killian, J. A. (2010) Orientation and dynamics of transmembrane peptides: the power of simple models, *Eur. Biophys. J. Biophys. Lett. 39*, 609-621.

148. Lee, T.-S., Kantarjian, H., Ma, W., Yeh, C.-H., Giles, F., and Albitar, M. (2011) Effects of clinically relevant MPL mutations in the transmembrane domain revealed at the atomic level through computational modeling, *PLoS One 6*, e23396.

149. Sako, Y., Minoguchi, S., and Yanagida, T. (2000) Single-molecule imaging of EGFR signalling on the surface of living cells, *Nat Cell Biol. 2*, 168-172.

150. Kim, C., Ye, F., Hu, X., and Ginsberg, M. H. (2012) Talin activates integrins by altering the topology of the beta transmembrane domain, *J. Cell Biol. 197*, 605-611.

151. Landolt-Marticorena, C., Williams, K. A., Deber, C. M., and Reithmeier, R. A. (1993) Non-random distribution of amino acids in the transmembrane segments of human type I single span membrane proteins, *J. Mol. Biol. 229*, 602-608.

152. Wimley, W. C., and White, S. H. (1996) Experimentally determined hydrophobicity scale for proteins at membrane interfaces, *Nat. Struct. Biol. 3*, 842-848.

153. Shrivastava, I. H., Capener, C. E., Forrest, L. R., and Sansom, M. S. P. (2000) Structure and dynamics of K channel pore-lining helices: a comparative simulation study, *Biophys. J. 78*, 79-92.

154. Gaede, H. C., Yau, W. M., and Gawrisch, K. (2005) Electrostatic contributions to indole-lipid interactions, *J. Phys. Chem. B 109*, 13014-13023.

155. Petersen, F. N. R., Jensen, M. O., and Nielsen, C. H. (2005) Interfacial tryptophan residues: A role for the cation-π effect?, *Biophys. J. 89*, 3985-3996.

156. Strandberg, E., and Killian, J. A. (2003) Snorkeling of lysine side chains in transmembrane helices: how easy can it get?, *FEBS Lett. 544*, 69-73.

157. Mecozzi, S., West, A. P., and Dougherty, D. A. (1996) Cation-pi interactions in aromatics of biological and medicinal interest: electrostatic potential surfaces as a useful qualitative guide, *Proc. Natl. Acad. Sci. U. S. A. 93*, 10566-10571.